DISSECTING THE MECHANISMS OF CELL MOVEMENTS DURING MORPHOGENESIS

Minna Roh

A dissertation submitted to the faculty of the University of North Carolina at Chapel Hill in partial fulfillment of the requirements for the degree of Doctor of Philosophy in the Department of Biology.

Chapel Hill
2009

Approved by:

Bob Goldstein

Victoria Bautch

Steven Rogers

David Reiner

Mark Peifer

ABSTRACT

MINNA ROH: Dissecting the Mechanisms of Cell Movements During Morphogenesis
(Under the direction of Bob Goldstein)

How embryonic cells transition from spatial patterning to morphogenesis is a fascinating and incompletely understood topic. In *C. elegans*, the first morphogenetic movement is the internalization of two endodermal precursor cells (E cells). The current model for how these cells become internalized is that an apically-enriched population of activated non-muscle myosin II motors drives apical constriction, and this may pull a ring of six neighboring cells together to cover the free surfaces of the E cells. Depleting Arp2/3 complex in *C. elegans* results in gastrulation defects (Severson et al., 2002). Although Arp2/3 is known to function in morphogenesis in various developmental systems, its specific roles in motile cells during morphogenesis are not well understood. We have found that in Arp2/3 depleted *C. elegans* embryos, although the E cells do not fully internalize, the E cells have normal fate and apicobasal polarity. Non-muscle myosin II still accumulates and becomes activated in the apical region of the E cells. When analyzing actin dynamics, we found that half of the ring of six neighboring cells (three of the six cells) extends Arp2/3-dependent, short, dynamic, F-actin-rich structures near their apical borders with the E cells. These results suggest that in addition to apical constriction, E cell internalization may also involve migration of the neighboring cells. We also examined non-muscle myosin II dynamics to follow movements of myosin foci with respect to the zones where E cells contact their neighboring cells in wild-type embryos. We expected to observe narrowing of the contact zones in concert with contraction of the actomyosin network. We were surprised

to find instead that centripetal myosin movements preceded narrowing of contact zones, contracting the apical actomyosin network multiple times over before significant neighboring cell movements. Later, myosin foci continued to coalesce centripetally and contact zones narrowed in concert. This suggests that a regulatable link (a clutch) may connect cortical actomyosin contraction to neighboring cell movements. To test this hypothesis, first, we tracked cell surface movements using fluorescent quantum dots. Our results suggest that free surfaces of E cells move together with cortical actomyosin contraction before neighboring cells move in concert, suggesting that the regulatable link lies between the E cell apical cytoskeleton and neighboring cells, and hence may be comprised of cell-cell adhesion complex proteins or proteins that link these complexes to the cytoskeleton. Second, we analyzed adhesion-defective embryos and found that coupling of myosin and contact zone dynamics fails. Together with the finding that similar centripetal myosin movements move polarity proteins toward the center of the apical surface at earlier embryonic stages (Munro et al., 2004), our results suggest that the transition from apicobasal cell polarization to cell internalization is governed by a molecular clutch.

ACKNOWLEDGEMENTS

Deciding to come to UNC for graduate school was one of the best decisions I ever made. Not only did it allow me to do the kind of science that I am passionate about, but it let me be in a wonderfully collaborative atmosphere with intelligent and generous people. I am appreciative to be a part of the community here at UNC and I will miss it when I have to leave. The fact that I am writing my dissertation and will defend in just a few weeks is very surreal. I know that I didn't do it alone and the only reason why I have come this far is because of the people who have helped me along the way. I believe that I will not make it through these acknowledgements without drenching my keyboard with tears, but I will do my best.

I am in research because someone gave me the opportunity to work in her lab. I'm not sure what made her choose me, but because of her decision, I was able to discover what I really wanted to do for the rest of my life. So, I thank Dr. Esther Verheyen at Simon Fraser University for that opportunity. I also thank Dr. Nancy Hawkins for taking the time to teach me so much during my Masters program. When I started the program, I had no idea what I was doing, but Nancy walked me through so many things and was a wonderful mentor.

During my time at UNC, I have been truly lucky to have an amazing thesis committee. This group of faculty members goes above and beyond their role as committee members and has also been there to give advice outside of committee meetings. I feel that

each member played a special role in my graduate career. Dr. Victoria Bautch always managed to ask questions that were directly relevant to my project and made me think "outside the box". She was there not only as a committee member, but as a graduate advisor when I came to her with questions and concerns. Dr. David Reiner is a walking encyclopedia of *C. elegans* knowledge. He is "wormbase" with arms and legs. He is also very kind and encouraging and made me feel that I could accomplish anything. Dr. Steven Rogers kindly let me work in his tissue culture room when I first started working with S2 cells. When I was applying for postdocs, I turned to him for advice. He is also great fun and awesome to drink with at ASCB meetings. Dr. Mark Peifer has played a large role during my graduate training. Mark was one of the main reasons I came to UNC, and I will always be grateful for that. My brief foray into *Drosophila* imaging during the last few months has partially fulfilled my desire to work in his lab. Mark is tough, but supportive, and he always looks out for graduate students. I never saw Mark miss a training grant-sponsored symposium or any graduate student run function. He challenged me throughout my time here, and I appreciate it so much.

Dr. Bob Goldstein is a super-awesome mentor. I'm not sure if I could describe it in any other way. Bob is one of the most generous people I have ever met. I was allowed to attend a conference that was tangentially related to what I was studying now because I was interested in that field for my postdoc. He has never told me that I could not purchase a reagent or piece of equipment that would help me propel my project forward. I think Bob is truly interested in seeing us succeed, in the manner that we feel is successful, and I think that this is the hallmark of a wonderful mentor. I appreciate all of the freedom he has given me to explore whatever avenues I am interested in, and I appreciate his enthusiasm for all types of science (even the kind that involves taking pictures of night creatures). Bob has always

treated me like a colleague and when we disagree, I have never felt that he dismisses my argument because I am a mere graduate student. He has taught me a lot scientifically (and grammatically! – Have you read Strunk and White?). I have thoroughly enjoyed my time in his lab, and I am grateful for the opportunity to work with such a brilliant person.

The Goldstein lab has been a family when I didn't have my family around. It is such an amazing environment, with supportive and intelligent people who are also very fun to be around! I laugh every day. I am grateful for the time I had with Drs. Nathaniel Dudley, Daniel Marston, and Willow Gabriel. I am especially thankful for Dr. Erin McCarthy Campbell's wonderful friendship during my first few years in the lab.

Dr. Jenny Tenlen is an excellent resource and the most gifted writing editor I have ever met. I am still amazed that she knows everything about everything! Dr. Jessica Sullivan-Brown, a new(er) addition to our group, has an enthusiasm for science that is unrivalled. It is also very contagious, which is just wonderful to have in the lab. Dr. Gidi Shemer (Professor Shemer!) is a wonderful friend and mentor. He was always there for advice, science related and unrelated, and I treasure the time we spent together in the lab. Jacob Sawyer is a graduate student who entered the same year as me, and he is an excellent story-teller (ask him about the brown scarf). Adam Werts can think up (good) experiments at the drop of a hat (he can also do the same with one-liners), and is all-around a great person. Jessica Harrell and I have been bench-mates twice during my time at UNC. I missed her when I left her lab, but was graced with her presence a couple of years later! She is a great friend and a cheerleader, and she has always been there to listen.

Our lab has been lucky enough to have amazing undergraduate students, both as technicians and as researchers. Their work makes our work a little easier, and I am thankful

for that. I'd especially like to thank Joe McCllelan for his amazing work, his enthusiasm, and his optimism.

It's easy to get sucked up in experiments and think that the results of a PCR reaction just ruined everything, but I've been fortunate enough to have people that take me out of the lab and make me enjoy my life. My friends in the IBMS 2004 class are absolutely wonderful. I can't believe I was lucky enough to be a part of such an amazing group of people. They are all so intelligent and successful, and extraordinarily fun! I thank them for all for the wonderful memories that are too numerous to mention. I'm also thankful for my friends back home who have been very supportive and have cheered me on the whole time. I am very lucky to have friends like you.

Most importantly, I'd like to thank my family – Mom, Dad and Eugene. I've met many people here and many of them have been hard workers, but I have yet to meet people who work as hard as my parents and my brother. They are the most dedicated and determined people I know and I thank them for showing me that if you want it bad enough, just put your head down and go get it. My brother has also always been very supportive and big brotherly, and I am grateful for always knowing that I have him to turn to.

And lastly, I want to thank my one and only special someone and his 4-legged side-kick. I thank my puppy Miles for helping me through rough times without even knowing it. I thank Jarrod for always being supportive and for sharing in this whole experience with me. He is a brilliant scientist, a genuine friend, and a loving husband (-to-be). He has made my time here more enjoyable than I could have ever imagined, and I love him very much.

PREFACE

I started my university career at Simon Fraser University in British Columbia, Canada, intending to become a teacher. The only unknown I had was whether I wanted to teach at the elementary school level or at the high school level. I had always loved science, and it was clear that I was going to major in Biology, but I also minored in Education with a concentration in Early Childhood Psychology. In the beginning of my 4th year, I had a scheduling conflict with my courses. As a result, I decided to register for a course that had a flexible schedule, and I started my 3 credits of "undergraduate research". I was pretty much hooked right away.

I spent the rest of my final year peering at flies and trying to understand more about signal transduction pathways. I fell in love with asking questions and designing experiments to answer them. I loved the bench and could spend hours at the microscope. Needless to say, I never entered a teaching program after I finished my Bachelor's degree. Much to my parents' surprise, I decided to apply for a Masters program in the Molecular Biology and Biochemistry Department at Simon Fraser University. A new faculty member, Dr. Nancy Hawkins, had just joined the department. I met with her to discuss project ideas and talked about my interests in molecular biology and genetics. In the Fall of 2002, I started my Masters degree in her lab trying to understand asymmetric neuroblast divisions in *C. elegans*.

In the summer of 2003, I attended my first international *C. elegans* meeting. At the meeting, I was fortunate enough to catch what I thought was the best talk of the meeting. This was the title of the talk: Polarization of a single cell by asymmetric Wnt signaling in the presence of Src signaling. Bob Goldstein. Biology Dept, UNC Chapel Hill. In the talk, Bob showed that Wnt and Src can function together to polarize cells; however, Src does not provide positional information. Wnt can dictate the axis of polarity. I'm not sure if it was the scientific result that intrigued me, or the elegant method that he used to address it. I just thought it was so cool.

When I started my Ph.D. program at UNC, I was delighted to see that my rotation project in Bob's lab would be working on the project that he had presented at the worm meeting the year prior. I had an amazing time working on the Wnt project during my rotation, and when I decided to stay, I continued to work on it. Although this project is not written in my dissertation, I feel that it would be disingenuous to not mention it at all. After all, this project had a large part to do with me wanting to join the lab.

Graduate school has not been easy, and for awhile, the Wnt project wasn't going anywhere. When I thought the Wnt project would flop, I started on a completely unrelated project: Understanding the role of the Arp2/3 complex during gastrulation. The Arp2/3 project became my straightforward, bread and butter project, while my Wnt project was risky and exciting. I kept both projects moving forward over several years. While I was trying to wrap up the Arp2/3 project for publication, I stumbled upon an exciting result. In the E cells, myosin was already moving centripetally prior to constriction of the apical surface. This result launched a whole new and exciting avenue of study for me and allowed me to start a collaboration with a fellow lab member and dear friend of mine, Dr. Gidi Shemer.

My time in the Goldstein lab has been wonderful and exciting. I have learned that you never know where your research will lead you. Just when you think you have it figured out, there is a surprise waiting around the corner to take you in new and beautiful directions. How can you not love that?

This dissertation is written solely on the gastrulation projects, although I am certain that the Wnt paper will also find a nice home. The first chapter is an introduction to actin dynamics during morphogenesis. This chapter was written as an invited chapter on actin in morphogenesis that will be published in a new actin book. I have thoroughly enjoyed writing this chapter as it allowed me to write about two things I love very much: actin and cell migration. I enjoyed writing it even more when I was lucky enough to write this chapter with our newest postdoc, Dr. Jessica Sullivan-Brown. The second chapter is a published Arp2/3 paper which has been accepted to the Journal of Cell Science (Roh-Johnson and Goldstein, 2009). While I spent most of my graduate career despising this project because of its lack of novelty, this project taught me that persistence (and a little luck) will yield reward. The third chapter of my dissertation is my reward. I dove into a very unfamiliar territory when we identified a molecular clutch that might regulate developmental processes. The Wnt project will always be near and dear to me since it was the project that brought me to this wonderful lab, but I have immensely enjoyed working on the clutch project and am excited for where the story will lead. I am grateful for these experiences and for the people who I have been lucky enough to share them with, and I look forward to what the future will bring.

TABLE OF CONTENTS

LIST OF FIGURES

ABBREVIATIONS

aPKC	Atypical Protein Kinase C
ApCAM	Aplysia Cell Adhesion Molecule
Arp2/3	Actin Related Protein 2/3
ARX	Arp2/3 Related Complex
cDNA	Complementary Deoxyribonucleic Acid
CED	Cell Death
DIC	Differential Interference Contrast
Dock	Dedicator of Cytokineses
E	Endoderm
EGM	Edgar's Growth Medium
END	Endoderm
EMS	Endomesoderm
GATA	Guanine Adenine Thymine Adenine
GEF	Guanine nucleotide exchange factor
GFP	Green Fluorescent Protein
HIV	Human Immunodeficiency Virus
HMR	Hammerhead
MS	Mesoderm

MOE	Moesin
NEF	Negative Factor
NCAM	Neuronal Cell Adhesion Molecule
NMY-2	Non-muscle Myosin – 2
PAR	Partitioning Defective
PCP	Planar Cell Polarity
PCR	Polymerase Chain Reaction
PH	Plextrin Homology
PLC	Phospholipase C
POP	Posterior Pharynx Defective
rMLC	Regulatory Myosin Light Chain
RNAi	Ribonucleic Acid Interference
SD	Standard Deviation
UNC	Uncoordinated
WASp	Wiskott-Aldrich Syndrome Protein
ZF1	Zinc Finger 1

CHAPTER 1

INTRODUCTION

This chapter is written to be included as a chapter on actin in morphogenesis in a book on actin published by Springer-London, Biomedical Sciences/Biotechnology Division. This chapter was written in collaboration with Dr. Jessica Sullivan-Brown. Jessica Sullivan-Brown wrote the section on neural crest migration, and I have written the remainder of the chapter.

Actin is integral to the dynamic cellular movements and rearrangements that occur during morphogenesis. Actin filaments have both a structural role and a role in producing force for cell movements. There are many types of cell movements that occur during morphogenesis, including ingression (single cell migration out of an epithelium, often from the surface to the interior of the embryo), epiboly (spreading and thinning of an epithelial sheet, often to enclose the interior layers of an embryo), invagination (inward folding of a cell sheet into an embryo), involution (inward rolling of an epithelial sheet across an opening), and delamination (separation of two sheets of cells or separation of a cell from a sheet). All of these cell movements involve remodeling of the actin cytoskeleton.

Studies *in vitro* have contributed much to the knowledge of actin biology, from the discovery of actin in muscle extracts to the observation of the delicate architecture of actin networks at the leading edge of a cell (Szent-Gyorgi, 1945; Svitkina and Borisy, 1999). During

development, there are significant differences in the extracellular milieu, for example a variety of intercellular signals as well as forces exerted by cells in moving tissues, that can differentially regulate actin dynamics and organization. In this chapter, we will highlight several examples of actin-based cell migrations in morphogenesis during development. These models of cell migration are commonly used as paradigms for understanding actin dynamics while taking into the account the microenvironment of the cell. Morphogenetic processes often require multiple, redundant actin-based mechanisms. Dissecting the respective contribution of each mechanism is essential to understanding the forces that drive a morphogenetic process.

Cell movements require cell shape changes that are dependent on remodeling of the cytoskeleton. One example of a simple change in cell shape is apical constriction, a process in which cells narrow their apical surfaces, generally by contraction of an apical actomyosin network (Sawyer et al., 2009). Apical constriction can drive cell movements during the processes of ingression or invagination (Harris et al., 2009; Lee and Harland, 2007). For example, in *C. elegans*, the endodermal precursor cells Ea and Ep (referred to collectively here as Ea/p), are born on the surface of the embryo. The Ea/p cells apically constrict, driving their movement to the embryonic interior, and this movement marks the initiation of gastrulation (Lee and Goldstein, 2003; Lee et al., 2006) (Figure 1A-F). Pharmacological inhibition of actin polymerization or depletion of actin regulators, such as the Arp2/3 complex, results in cell internalization defects, supporting a role for actin architecture and/or dynamics in gastrulation (Lee and Goldstein, 2003; Severson et al., 2002). As Ea/p cells internalize, neighboring cells fill in a gap that is left behind. Observations of F-actin dynamics in vivo, using an F-actin-binding

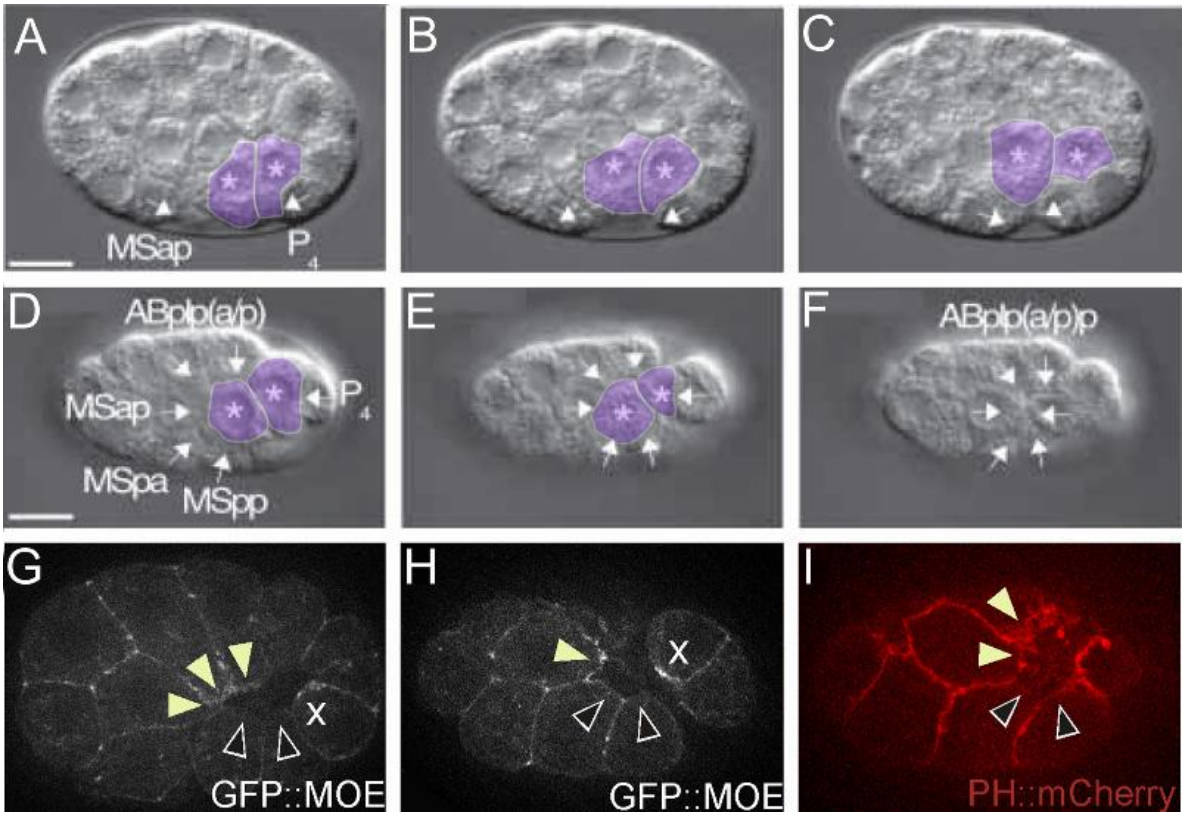
A
MSap
P4
B
C
D
ABplp(a/p)
MSap
P4
MSpa
MSpp
E
F
ABplp(a/p)p
G
x
GFP::MOE
H
x
GFP::MOE
I
PH::mCherry

Figure 1: *C. elegans* may internalize endodermal precursor cells by apical constriction and active cell migration. Gastrulation stage embryos with Ea/p cells marked by asterisks, and neighbouring cells labeled. (A-C) A lateral view. Ea/p cells shorten their apical surfaces through actomyosin contraction to move toward the embryonic interior, and neighbouring cells fill in the gap (arrows). (D-F) A ventral view. A ring of six cells fill in the gap (arrows) that is left behind by internalizing Ea/p cells. (G,H) A ventral view of embryos expressing GFP::MOE to visualize F-actin. F-actin is enriched specifically at the border between mesodermal descendants and Ea/p (yellow arrowhead), and not at the other neighbouring cell boundaries (black arrowhead). The germline cell, P4, also has actin accumulation (cross). (I) A ventral view of an embryo expressing PH domain::mCherry to visualize cell membranes. Membrane protrusions form only where mesodermal descendants contact Ea/p cells (yellow arrowhead). (A-F) Adapted with permission from Lee and Goldstein, 2003. (G-I) Adapted with permission from Roh-Johnson and Goldstein, 2009.

domain of moesin fused to GFP (Edwards et al., 1997) have revealed that specific neighboring cells form dynamic, Arp2/3-dependent, F-actin-enriched extensions at their borders with Ea/p cells (Roh-Johnson and Goldstein, 2009). Interestingly, the neighbors that form these extensions comprise one side of a closing ring of cells, or three of the six cells that form the ring. The role that these extensions play in gastrulation is not well understood. It is possible that the extensions are specializations for cell crawling or cell rolling, or that they participate in sealing the ring upon closure (Roh-Johnson and Goldstein, 2009; Figure 1G-I). Endoderm internalization in *C. elegans* involves very few cells, with only two cells internalizing and a ring of just six cells closing the gap left, yet it provides one of many examples in which multiple types of cell movements participate together in morphogenesis. The roles that actin plays in these developmental processes is under active exploration.

We will highlight several selected examples of directed cell migration during morphogenesis, from movement of a sheet and/or groups of cells to single cell migration. We discuss similarities and differences between concerted cell movements and single cell migration during development, and we will compare what has been learned *in vivo* in developmental systems with *in vitro* studies of single cells. We focus on examples in which actin dynamics have been observed directly in live-imaging studies, and we discuss key signaling pathways that regulate actin dynamics in actively migrating cells during morphogenesis.

Movements of cell sheets and groups of cells during morphogenesis

C. elegans ventral enclosure – closing both ends

Cells can move as a sheet in dramatic rearrangements of the germ layers of an animal. In *C. elegans*, epidermal cells are born on the dorsal side of the animal as two rows of cells. These cells intercalate (dorsal intercalation), forming a single row on the dorsal midline. After dorsal intercalation, the epidermal sheet undergoes epiboly, spreading and fully enclosing the animal as the two edges of the sheet meet on the ventral side. Ventral enclosure occurs in two phases (Williams-Masson et al., 1997) (Figure 2). In the first phase, two anterior pairs of cells, termed the "leading cells", extend long, actin-rich protrusions, making contact with each other on the ventral side. In the second phase, the cells posterior to the leading cells, termed the "pocket cells", close the remaining gap. Both the leading cells and the pocket cells are important for ventral enclosure, as perturbing either cell population results in ventral enclosure defects (Williams-Masson et al., 1997). Both the leading cells and the pocket cells form F-actin-based structures. Live imaging of adhesion complexes shows protrusions, similar to filopodia, as well as broad lamellae, from the leading cells (Raich et al., 1999). Phalloidin staining reveals that the protrusions from the leading cells are F-actin rich (Sawa et al., 2003; Williams-Masson et al., 1997). In addition to proposed roles for filopodia in cell motility during ventral enclosure, these actin-rich fingers may play a role in facilitating strong cell-cell adhesion after cell contact is established (Raich et al., 1999). In a process termed "filopodial priming", α-catenin is rapidly recruited at sites where contralateral filopodial tips first make contact. This recruitment is thought to allow for rapid cell-cell adhesion as the epithelium seals on the ventral side. The

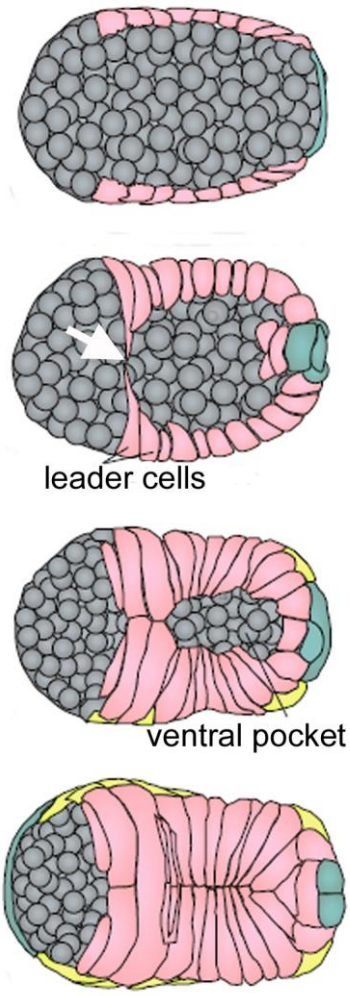
leader cells
ventral pocket

Figure 2: *C. elegans* ventral enclosure. Schematic of ventral enclosure. Ventral cells are shown in pink. The first 2 pairs of cells, the leader cells, extend long protrusions and make contact with their contralateral neighbour (arrow). After the leader cells make contact, the remaining cells termed the pocket cells are pulled around the embryo and meet along the midline. Figure adapted with permission from Chisholm and Hardin, 2009.

ventral pocket cells accumulate a continuous belt of F-actin along the edge of the pocket. The formation of this F-actin belt suggests that a purse-string mechanism may be driving the closure of the ventral pocket, a mechanisms analogous to pulling closed a drawstring bag, except that each cell's portion of the drawstring acts as a contractile unit (Williams-Masson et al., 1997). This observation leads to a model where the leading cells that seal at the midline produce a tension that pulls the ventral pocket cells around the embryo toward the ventral side. Once the pocket cells are pulled close enough to form a ring, ventral enclosure completes by an actin purse-string mechanism (Figure 2B).

Many actin regulators are involved in ventral enclosure. Several components of the Rac signaling pathway have been implicated in the process. These proteins include homologs of the GTPase Rac, a Rac1-associating protein (Sra), and a Nck-associating protein (HEM2/NAP1/Kette) (Lundquist et al., 2001; Patel et al., 2008; Soto et al., 2002). The ventral enclosure defects observed in Rac signaling mutants may be due to disruption of the Arp2/3 complex, a complex that nucleates new actin branches off pre-existing actin filaments. Indeed, the Arp2/3 complex, as well as one of its upstream activators Wasp, have been shown to regulate ventral enclosure (Sawa et al., 2003; Severson et al., 2002). Several of the Rac components, as well as Arp2/3 and Wasp, have been shown to localize to the ventral edge of the leading cells, suggesting a role for these proteins in the protrusive activity (Sawa et al., 2003). Ena/Vasp also regulates ventral enclosure, presumably through its effects on dynamics at the plus end of actin filaments (Sheffield et al., 2007; Withee et al., 2004). Thus, key actin regulators play a role in ventral enclosure and have predictable roles in ventral enclosure. However, little is known about the precise effects of these proteins on actin dynamics during ventral enclosure. Improving

microscopy techniques for visualization of actin architecture and dynamics may allow for a greater understanding of how these key actin regulators function in this system.

Drosophila dorsal closure – combining multiple actin-based forces in a single morphogenetic process

The combination of actin-based cell protrusions and actin purse-string mechanisms to drive morphogenesis is not restricted to *C. elegans*. In *Drosophila*, a process known as dorsal closure also requires both actin-rich protrusions and an actin cable. During the final phases of *Drosophila* embryogenesis, there is a large hole on the dorsal side that is covered by a squamous epithelium, the amnioserosal cells (Figure 3A-E). Forces from the migrating epidermal sheet combine with the forces from the contracting amnioserosal cells to drive closure: Amnioserosal cells apically constrict, pulling the leading edge cells toward the ventral midline, and the leading edge of the migrating epidermal sheet forms a supracellular F-actin purse-string that shortens by more than 25% as the hole closes (Kiehart et al., 2000; Hutson et al., 2003). Additionally, the leading edge cells form long filopodial protrusions, approximately 10 μm long. These protrusions are thought to participate in completing dorsal closure by zipping the two edges of the epidermal sheet (Hutson et al., 2003; Jacinto et al., 2000; Kiehart et al., 2000). Zipping occurs with great precision, with cells of the same segmental position meeting on each side of the opening, and the closed seam eventually matures into a continuous epithelium. The process of dorsal closure provides an excellent model for teasing apart the forces contributed by multiple tissue types to drive a single morphogenetic process,

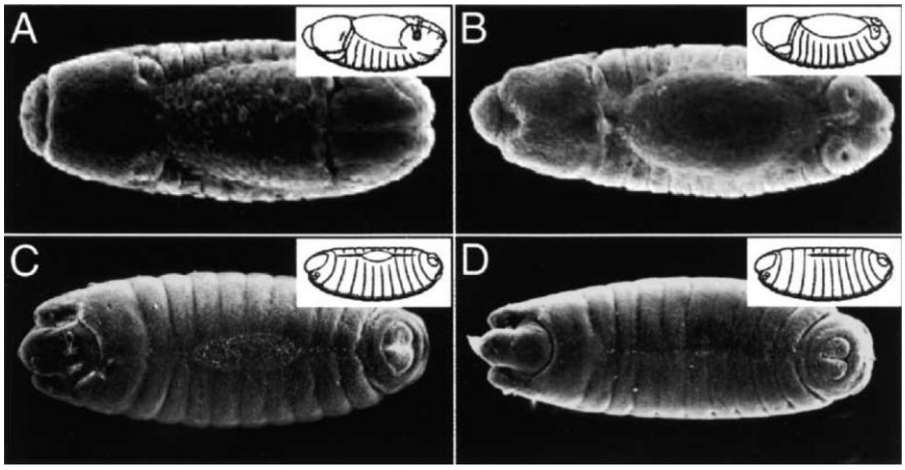
A
B
C
D

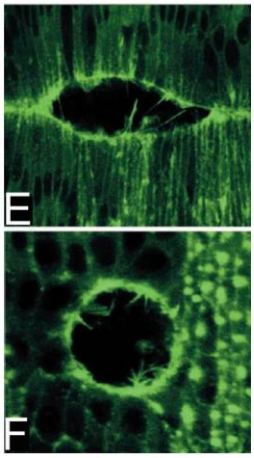
E
F

Figure 3: *Drosophila* dorsal closure occurs through actin-based contributions from multiple tissues. (A-D) SEM of dorsal closure. The epidermal sheet migrates by actin-based movements to cover the hole that is filled with amnioserosal cells. (E) GFP-actin expressing embryo during dorsal closure. Actin-rich cable and filopodia form at the leading edge. (F) GFP-actin expressing embryo that has been wounded with a laser. As in the embryo in (E), an actin-rich cable and filopodia form along the epithelial front. (A-D) Images adapted with permission from Jacinto et al., 2002. (E,F) Images adapted with permission from Martin and Parkhurst, 2004.

combining tools of genetics, live microscopic imaging of fluorescently-labeled proteins, and precise laser cuts to assess relative forces.

Both the actin cable and the filopodia contribute to the migration and sealing of the epidermal sheet during dorsal closure. GFP labeled moesin or actin show enrichment continuously along the leading edge of the epidermal sheet (Hutson et al., 2003; Jacinto et al., 2000; Kiehart et al., 2000; Reed et al., 2004). Myosin II also colocalizes with actin along the leading edge and is thought to provide the force necessary for the contractile purse string mechanism (Franke et al., 2005). When a laser is used to cut the supracellular actin purse-string, the leading edge recoils from the site of injury, revealing that this cable is under tension (Kiehart et al., 2000). In Rho or myosin II mutants, the F-actin cable disassembles part way through dorsal closure. Observing GFP-labelled actin in these mutants reveals that the leading edge is less taut, and there is an increase in the number of filopodia, which can often coalesce into broad lamellipodia (Jacinto et al., 2002). Excessive filopodial protrusions were also observed when Rac signaling was depleted (Woolner et al., 2005). Thus, in addition to the role of actin as a purse string, the cable may also have a structural role to maintain epithelial integrity and restrain the formation of excess protrusions.

F-actin rich filopodia can act as sensory processes used to investigate the environment (Mattila and Lappalainen, 2008). During dorsal closure, filopodia actively sense for their contralateral partners. This phenomenon is best visualized when GFP-actin is expressed only in 4 cell wide stripes across the embryo (Jacinto et al., 2000). GFP expressing filopodia on one epithelial front will contact filopodial on the other epithelial front, and seem to “sample” along the non-GFP expressing filopodia until the filopodia reaches GFP-expressing filopodia. Once filopodia find their contralateral partner, they appear to draw the epithelial sheets together and

align the GFP-expressing stripes (Jacinto et al., 2000). There are two pieces of evidence that suggest that filopodia tug towards one another (Jacinto et al., 2000). First, the rate of movement of the epithelial front is slower prior to filopodial engagement. The initial rate is 0.11 ± 0.02 μm/min (average ± SD), but upon filopodial contact, the rate increases to 0.24 ± 0.07 μm/min (average ± SD). Secondly, at the sites of filopodial tugging, the actin cable appears kinked toward the site, thus suggesting that a force toward the opposite epithelial sheet is being exerted on the actin cable. These filopodial tethers also pull the epithelial sheet into proper alignment with their correct neighbours (Millard and Martin, 2008). Depleting filopodial formation by dominant-negative Cdc42 expression, by blocking Jun N-terminal kinase signaling, or by depleting Ena function reveals that dorsal closure can still proceed, but the epithelial sheet is misaligned during sealing (Jacinto et al., 2000; Gates et al., 2007). Similar to what is observed during *C. elegans* ventral enclosure, the filopodia during dorsal closure are speculated to participate in filopodial priming, possibly mediated through α-catenin (Jacinto et al., 2000). It is thought that during *Drosophila* dorsal closure, rather than forming nascent adhesion complexes when the two tips of filopodia meet as in ventral enclosure, filopodia interdigitate during dorsal closure and fuse along the two epithelial fronts.

The regulation of F-actin dynamics in this system has been investigated by dissecting the phenotypes of mutants of several actin regulators. Filopodia in tissue culture cells are known to be regulated by WASP and Scar proteins through activation of the Arp2/3 complex (Pollard and Borisy, 2003; Zallen et al., 2002). In *Drosophila*, SCAR is the primary activator of Arp2/3 in morphogenesis (Zallen et al., 2002); however, it is unknown whether SCAR plays a role in dorsal closure. There are several upstream activators that do play roles in dorsal closure. Four small GTPases have been shown to be involved in the enrichment of cytoskeletal machinery at

the leading edge: Rho1, Rac1, Cdc42 and Ras1. Dominant negative studies suggest that these proteins have overlapping roles in regulating myosin and actin localization to form the actin cable (Harden et al., 1999). Expressing a dominant negative Rac specifically in the epidermis results in defects in myosin and actin localization along the leading edge, whereas dominant negative Cdc42 results in subtle actin and myosin localization defects (Harden et al., 1999). Cdc42 also plays a role in the formation of filopodia (Jacinto et al., 2000). Mutations in Cdc42 abolish filopodial formation, affecting the ability of the leading edge cells to sense their neighbors. Mutations in Abelson kinase (Abl) also exhibit defects in dorsal closure. In embryos expressing a constitutively active Abl kinase, filopodia are absent and replaced with broad lamellae, the actin cable is disorganized, and the cells in the two sheets do not precisely align with one another (Stevens et al., 2008). A known target of Abl is the anti-capper Ena (Gertler et al., 1990). Overexpression of Ena can rescue defects caused by Abl mutations, suggesting that the roles of Abl in dorsal closure are mediated by Ena (Gates et al., 2007; Stevens et al., 2008). Furthermore, Ena localizes to filopodial tips and affects filopodial dynamics, thus Ena mutants slow dorsal closure timing and interfere with the ability of cells to match correctly with their neighbors (Gates et al., 2007).

Neural crest cell migration – delamination and then cell contact-dependent migratory behaviors position cells

Neural crest cells are highly migratory, traveling long distances through the embryo, and they are multipotent, giving rise to many tissue types, including peripheral neurons, glia, connective tissue, bone, melanocytes, and the outflow tract of the heart (Gammill and Bronner-

Fraser, 2003). These “explorers of the embryo” are unique to vertebrates, arising at the border between the neural and non-neural ectoderm during closure of the neural tube (Figure 4A) (Gammill and Bronner-Fraser, 2003). Although the induction and migration patterns of the neural crest have been well studied, the cues that guide cytoskeletal rearrangements that are important for neural crest cell migration are only beginning to be revealed.

Before neural crest cells begin their migration, they segregate from the neuroepithelium by an epithelial to mesenchymal transition (EMT). During EMT, neural crest cells display a sequence of protrusive activities, forming blebs and then filopodial protrusions. Blebbing occurs as delamination begins, followed by the translocation of the cell soma in the direction of the bleb (Berndt et al., 2008). Actin-rich filopodia and lamellopodia then form as neural crest cells exit the neuroepithelium. *In vivo* imaging of actin dynamics confirms that the blebs observed on the neural crest cells are similar to blebs of other cell types, with bleb formation initiated by separation of the F-actin network from the membrane, and with actin filaments accumulating beneath the membrane as the bleb retracts (Figure 5A, Berndt et al., 2008). Similar bleb dynamics are seen, for example, in mammalian tumour cells (Sahai, 2005; Wolf et al., 2003). When the myosin inhibitor blebbistatin is added to zebrafish embryos, actin accumulation to the bleb is delayed and the blebs fail to retract, but interestingly, lamellipodia and filopodia are not affected. Thus, actomyosin contractility may regulate the dynamics of membrane blebbing in neural crest cells (Berndt et al., 2008).

What signals regulate actin dynamics during EMT? Bmp signaling and Wnt signaling have been implicated in neural crest delamination and migration and have been shown to regulate key actin regulators such as the Rho GTPases (Burstyn-Cohen et al., 2004; De

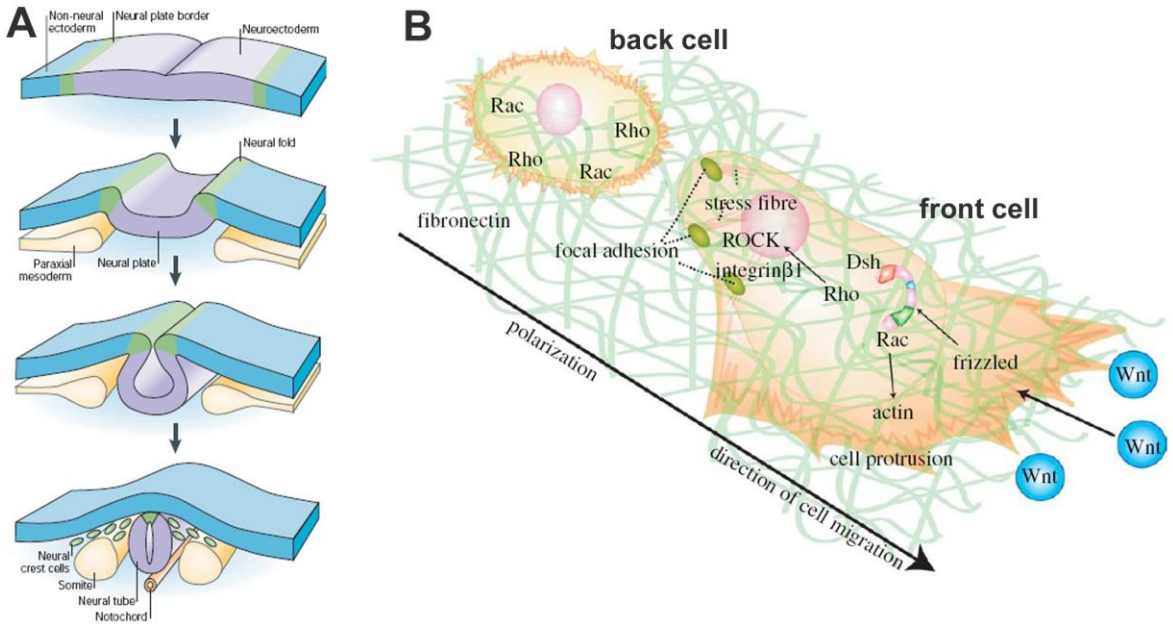
A
Non-neural ectoderm
Neural plate border
Neuroectoderm
Neural fold
Paraxial mesoderm
Neural plate
Neural crest cells
Somite
Neural tube
Notochord
B
back cell
Rac
Rho
Rho
Rac
stress fibre
front cell
fibronectin
focal adhesion
ROCK
integrinβ1
Dsh
Rho
Rac
frizzled
Wnt
Wnt
Wnt
actin
cell protrusion
polarization
direction of cell migration

Figure 4: Neural crest cells delaminate from the neural epithelium and then migrate to their final destination. (A) Neural plate border (green) is specified by two adjacent cell types, the neuroectoderm (purple) and the non-neuroectoderm (blue). During neurulation, the neurofolds elevate as the neural plate apically constricts to form the neural tube. The neural crest cells (green) then delaminate from the neural tube. (B) Neural crest migration: the front cell is polarized by PCP signalling, whereas the back cell is unpolarized. (A) Image adapted with permission from Gammill and Bronner-Fraser, 2003. (B) Image adapted with permission from Kuriyama and Mayor, 2008.

Calisto et al., 2005; Groysman et al., 2008). BMP4 triggers the downregulation of N-cadherin. N-cadherin normally maintains the neural crest in a premigratory state by two mechanisms: by increasing cell adhesion and by repressing canonical Wnt signaling (Shoval et al., 2007). BMP4 also induces expression of RhoB, which is expressed in the dorsal midline of the neural tube in a region where the neural crest forms (Liu and Jessell, 1998). Blocking Rho activity with the C3 exotoxin in chick neural tube explants inhibits neural crest cell delamination and disrupts formation of actin stress fibers (Liu and Jessell, 1998). Pharmacological agents that block Rho kinase (ROCK) or myosin II can also decrease the number of cells undergoing EMT in zebrafish embryos (Berndt et al., 2008). These studies suggest that Rho signaling may positively regulate EMT in the neural crest. However, a recent study has shown that both in explants and *in vivo,* loss of function of Rho signaling enhances emigration of the neural crest rather than preventing EMT (Groysman et al., 2008). Blocking Rho signaling by a membrane-permeable C3 enzyme in chick neural tube explants enhances cell emigration from the explants. The membrane-permeable C3 enzyme is effective at much lower concentrations than the C3 exotoxin used in earlier studies, and it is possible that this could account for the differing results (Groysman et al., 2008; Liu and Jessell, 1998). Consistent with a role for RhoB in preventing migration, disrupting RhoB activity by another means, using a dominant negative RhoB GTPase construct, results in fewer stress fibers and increased emigration from the neural epithelium (Groysman et al., 2008). Inhibiting ROCK activity with the Y27632 compound also results in a similar effect: more cells emigrate, and vinculin-containing focal contacts are reduced, suggesting that Rho/ROCK is required to maintain F-actin stress fibers in neural crest progenitors before EMT (Groysman et al., 2008). Interestingly, blocking Rho or ROCK activity by either pharmacological experiments or dominant negative constructs also results in the downregulation of N-cadherin *in ovo,*

suggesting the Rho/ROCK is also involved in maintaining neural cell adhesion (Groysman et al., 2008). These studies indicate that Rho and ROCK activity has important roles in neural crest cell emigration, but directly conflicting results leave unsettled the issue of whether Rho and ROCK promote or inhibit emigration (Berndt et al., 2008; Groysman et al., 2008).

After the neural crest cells undergo EMT, they follow specific migratory patterns to multiple destinations. In general, neural crest cells from the cranial region migrate in three streams from the rhombomeres to the branchial arches. Neural crest cells from the trunk regions migrate along a medial route, through the somites, or a dorsolateral route, between the ectoderm and somites (Kuriyama and Mayor, 2008). Several cytoskeletal regulators, including N-cofilin, Nedd9, Syndecan-4, and Myosin-X, affect the migratory behavior of neural crest cells (Aquino et al., 2009; Gurniak et al., 2005; Hwang et al., 2009; Matthews et al., 2008; Nie et al., 2009). *In vivo* imaging of migratory patterns from various populations of the neural crest reveal that these cells can arrange in chain-like formations, with cells contacting each other through filopodia-like processes (Figure 5C) (Kasemeier-Kulesa et al., 2005; Teddy and Kulesa, 2004; Young et al., 2004). Contacts made by these processes to neighboring cells can vary from short-range contacts (10-20μm) to long-range contacts (up to 100μm) (Teddy and Kulesa, 2004). When a neural crest cell becomes separated from a filopodial contact in the stream, the cell appears to move in an undirected manner (Kasemeier-Kulesa et al., 2005). Although direct observation alone cannot resolve the functions of these contacts, it raises the possibility that filopodial extensions may play roles in the collective and directional migration of the neural crest.

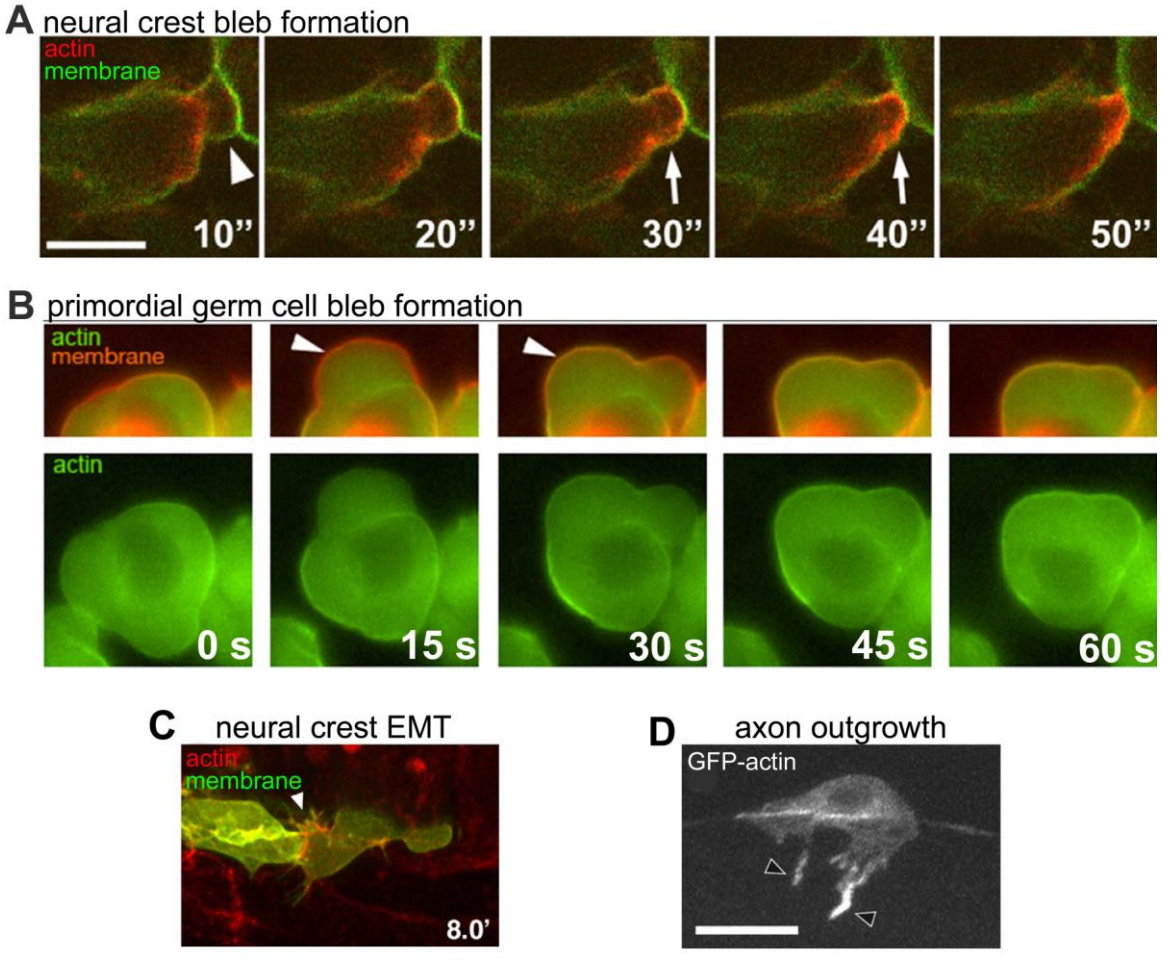
A neural crest bleb formation
actin
membrane
10”
20”
30”
40”
50”
B primordial germ cell bleb formation
actin
membrane
actin
0 s
15 s
30 s
45 s
60 s
C neural crest EMT
actin
membrane
8.0’
D axon outgrowth
GFP-actin

Figure 5: Cells can migrate by membrane blebs and by actin-dependent protrusions at the leading edge. (A) Neural crest bleb formation. The membrane bleb expands past the actin cortex. Then actin accumulates beneath the bleb as the bleb retracts. (B) Primordial germ cell bleb formation. The upper panel is the merge of actin in green and membrane in red. The bottom panel is actin only. Much like neural crest bleb formation, the PGC bleb is actin free. Actin then accumulates beneath the bleb during retraction. (C) Neural crest EMT. Actin-rich protrusions (white arrowhead) form at the leading edge of migrating neural crest cells. (D) A *C. elegans* HSN neuron expressing GFP:actin. HSN neurons form actin-rich filopodia (black arrowheads) on the growth cone. (A,C) Images adapted with permission from Berndt et al., 2008. (B) Image adapted with permission from Blaser et al., 2005. (D) Image adapted with permission from Adler et al., 2006.

Neural crest cells have been shown to display contact inhibition of locomotion *in vivo* (Figure 4B) (Carmona-Fontaine et al., 2008). Contact inhibition of locomotion is a long standing hypothesis in which cell contacts influence the direction of cell movements: at sites where a cell contacts another cell, protrusions involved in cell migration cease formation, and protrusions form at other sites instead. Contact inhibition of locomotion was first observed in fibroblasts *in vitro* (Abercrombie and Heaysman, 1954; Abercrombie et al., 1957). When two neural crest cells come in contact *in vivo*, their protrusions collapse, and they can change their direction of migration. This behavior appears to be regulated by a planar cell polarity (PCP) signaling pathway, as inhibition of Dishevelled (Dsh) or classic PCP genes (Wnt11, *strabismus* or *prickle1*) prevents the collapse of lamellipodia, and these cells fail to significantly change the direction of migration upon contact (Carmona-Fontaine et al., 2008). Furthermore, Dsh is enriched at sites of cell-cell contact (Carmona-Fontaine et al., 2008). Signaling appears to work through RhoA, as RhoA is required for filopodia retraction (Rupp and Kulesa, 2007), and RhoA is active at sites of cell-cell contact (Carmona-Fontaine et al., 2008). Interestingly, PCP signaling has been shown to activate RhoA , and this activation has an inhibitory effect on Rac activity in neural crest cells (Matthews et al., 2008). It has been proposed the contact inhibition may account for the directional migration of a stream of neural crest cells, as only the exposed end of a cell at the leading edge can extend protrusions when other sides are in contact with other cells. Other studies have shown neural crest cells with extensions at both the leading and trailing end, making simultaneous contacts in lines of cells (Rupp and Kulesa, 2007; Teddy and Kulesa, 2004). Filopodia-like extensions at the trailing ends of cells may be retraction fibers -- contacts left behind that are progressively retracted -- rather than filopodia extended in this direction.

Differences in neural crest cells migratory mechanisms between frog, mouse and chick are also possible. Further studies examining the formation of filopodial-like protrusions at specific times and domains during the migratory path and comparing experimental systems may shed more light on this issue.

Single cell migration during morphogenesis

Zebrafish primordial germ cell migration – single cells come together to form cell clusters and migrate together to their final destination

Studies *in vitro* predominantly examine the migration of single cells. In development, although cells tend to migrate as sheets or groups of cells (Friedl and Gilmour, 2009), there are also examples of individual cell migration. Primordial germ cell (PGC) migration takes advantage of both single and collective cell migration.

In zebrafish, PGCs are specified at four different regions in the embryo. These four populations migrate to the site of gonad formation within the first day of development. The fidelity of the process is highlighted when ectopic PGCs are transplanted randomly in the embryo, and these transplanted cells can still efficiently migrate to the appropriate location (Ciruna et al., 2002). PGCs transition to migration in three stages (Blaser et al., 2005; Reichman-Fried et al., 2004). First, the PGCs are rounded and morphologically indistinguishable from their somatic neighbors. During the next stage, PGCs extend protrusions in all directions, but do not actively migrate. Approximately 1 hour later, the PGCs become sensitive to directional cues provided by somatic cells secreting the chemokine, SDF-1a. The PGCs begin sending out

polarized protrusions (Doitsidou et al., 2002; Raz, 2004; Weidinger et al., 2002), and transition into a migratory phase that requires the downregulation of E-cadherin. PGCs migrate as individual cells until they form two clusters on each side of the body axis. At these sites, the PGCs send out small protrusions and remain at the same location for approximately 3 hours (Reichman-Fried et al., 2004). They then migrate as a cluster to the site where the gonad will develop. High resolution imaging of GFP expressed specifically in the PGCs reveals that the clusters move by individual cell migrations, with a lack of coordinated movement within the cluster, each cell exhibits variably-directed short-range migrations. Furthermore, close cell-cell contacts are not observed. Consistent with cells in the cluster moving independently, each cell spends a portion of its time at the front of the cluster. The cells at the front, which may be exposed to the highest levels of SDF-1a, then exhibit directed migration toward the cue.

During PGC migration, PGCs cycle between two phases: A "run" phase, when they actively migrate, and a "tumble" phase, when they lose their polarity and stay stationary (Reichman-Fried et al., 2004). The tumble phase has been interpreted as a pause, in which cells may resample the environment and reorient their polarity, which may allow cells to more readily and precisely reach their target. Phalloidin staining of fixed PGCs shows F-actin enriched in the cell cortex (Blaser et al., 2005). Live imaging of EGFP-actin fusion protein reveals that there is an enrichment of actin at the cell front during directed cell migration. However, when the cells form protrusions, the protrusion extends past the belt of actin and is not itself enriched for actin. Thus, PGCs also form membrane blebs during their migration. During the tumbling phase, the cells lose their polarity yet still continue to form membrane blebs (Figure 5B). Similar to blebs observed on neural crest cells, once the bleb is in its expanded state, F-actin accumulates beneath the bleb, and the bleb retracts. Experimentally disrupting actomyosin contractility by treating

embryos with the myosin inhibitor blebbistatin, or expressing dominant negative constructs to prevent the phosphorylation and activation of myosin light chain, leads to loss of membrane bleb formation, and PGC migration is impaired (Blaser et al., 2005). These results are consistent with the hypothesis that a process dependent on actomyosin contraction, perhaps cytoplasmic flow, is required for bleb formation. PGCs differ from neural crest cells in that neural crest cells form blebs only during delamination from the neural epithelium and not during long distance migration.

Interestingly, among the proteins that have been found to modulate PGC migration is a viral protein. Nef is a myristoylated HIV-1 protein abundant at early stages of infection, and Nef is known to disrupt cell migration when expressed in fibroblasts. Nef functions by interacting with the P21-activated kinase Pak2 and down-regulating the actin filament severing activity of cofilin. Fibroblast cells expressing Nef have disorganized F-actin. Nef can also inhibit SDF-1-induced chemotaxis of T-lymphocytes (Stolp et al., 2009). PGCs expressing Nef also have altered migration patterns (Stolp et al., 2009). Whether Nef blocks the migration of PGCs by similar mechanisms as in other cell types is currently unknown. However, expression of Nef without the Pak2 interacting domain in zebrafish has no effect on PGC migration, suggesting that Nef's interaction with Pak2 is critical in inhibiting PGC migration.

A central player in many migrating cells is the phosphoinositide 3-kinase (PI_3K) family of proteins. In *Dictyostelium*, phosphoinositol (3,4,5)-triphosphase (PIP_3) accumulates at the leading edge in response to receptor activation (Kolsch et al., 2008). This accumulation recruits several other downstream proteins which then act to regulate actin dynamics. During zebrafish PGC migration, loss of PIP_3 results in slower PGC motility and reduced filopodial-like protrusions (Dumstrei et al., 2004). However, in contrast to *Dictyostelium*, PIP_3 is uniformly

localized around the cell periphery in PGCs. Thus, although PIP_3 is required for overall PGC migration, PIP_3 is unlikely play a role in directional PGC migration.

C. elegans axon guidance – using a genetic system to identify proteins required for single cell migration in vivo

A classic example of single cell migration during morphogenesis is axon outgrowth. Axon outgrowth is led by the guidance of the growth cone. Growth cone guidance *in vivo* is an excellent paradigm to study how a cell responds to cues in its extracellular environment, and specifically how the cell remodels its actin cytoskeleton to respond appropriately to this cue. *C. elegans* is an ideal genetic system to tease apart the signaling pathways that regulate the cytoskeleton in axon guidance because *C. elegans* lends itself readily to genetics and RNAi, and loss of many of the worm's 302 neurons can produce phenotypes in viable, reproductive strains of worms.

Growth cone guidance is mediated by filopodial and lamellipodial dynamics that are regulated by actin dynamics. Growth cones produce these protrusions, which make contact with substrates and function in propelling the growth cone forward. There are many actin regulators known to regulate the formation of these actin-based structures, and thus affect growth cone migration (Figure 6). In *C. elegans*, Arp2/3 activation, abLIM/UNC-115, and Ena/UNC-34 directly regulate actin dynamics. Ena/UNC-34 also genetically and biochemically interacts with the single *C. elegans* lamellipodin (Lpd) homolog, MIG-10 (Chang et al., 2006), RhoG/MIG-2, Rac/RAC-2, and Rac/CED-10 act redundantly for axon guidance, and the Nck- interacting

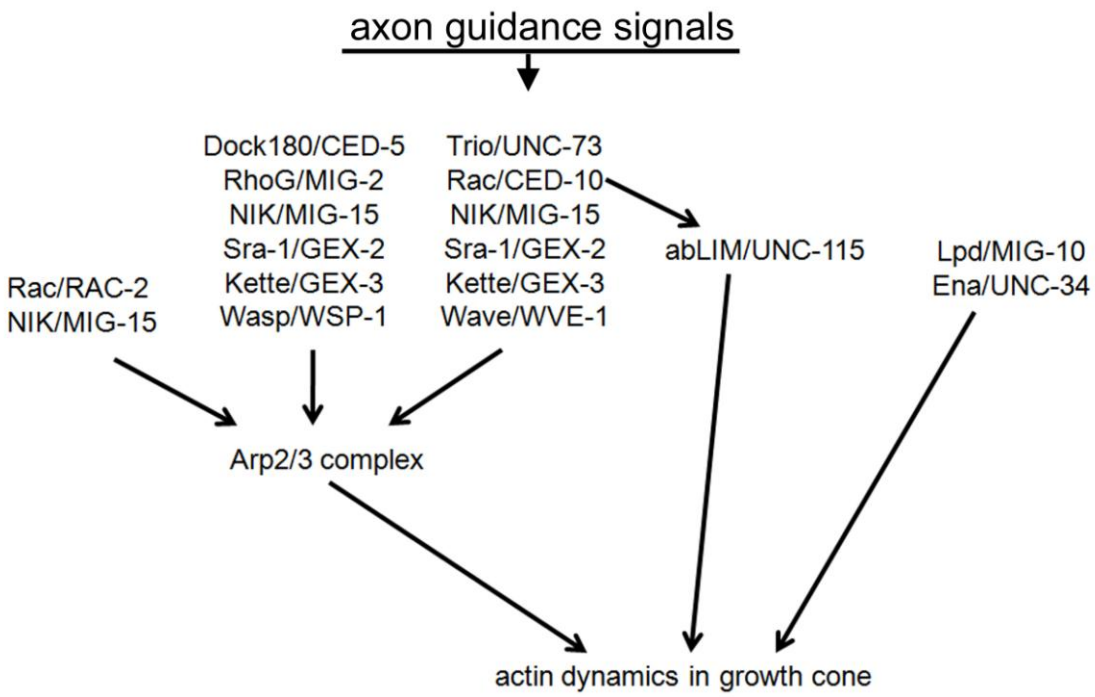

Figure 6: Several pathways regulate actin during *C. elegans* axon outgrowth. Image adapted with permission from Shakir et al., 2008.

kinase (NIK), MIG-15, functions in all three Rac signaling pathways (Shakir et al., 2006). Thus, NIK/MIG-15 is a core component of each signaling pathway. The Rho GTPases and their upstream activators act as modulators for specificity. For example, the Rho GTPases RhoG/MIG-2 and Rac/CED-10 are regulated by the guanine nucleotide exchange factors (GEFs) Trio/UNC-73 and DOCK180/CED-5, respectively (Lundquist et al., 2001; Steven et al., 1998; Wu et al., 2002). Furthermore, genetic analysis indicates that RhoG/MIG-2 is in the same pathway as the upstream activator Wasp/WSP-1, while Rac/CED-10 is in the same pathway as the upstream activator Wave/WVE-1 (Shakir et al., 2008). Both Rac GTPases converge on Sra-1/GEX-2 and Kette/GEX-3 and regulate Arp2/3 function (Shakir et al., 2008). Thus, taken together, there are three pathways that lead to Arp2/3 activation (Figure 6). The components of these pathways again highlight the idea that there are several core components that are used in each pathway to elicit a response (e.g. Sra-1/GEX-2 and Kette/GEX-3), and the specificity of each pathway is then dictated by specific Rho GTPases and upstream regulators. There is also crosstalk between the major pathways, as Rac/CED-10 can function through abLIM/UNC-115 (Struckhoff and Lundquist, 2003). The Arp2/3 complex itself has also been shown to have roles in neuronal migration. Recently it was shown that depleting *C. elegans* of Arp2/3 results in defects in mechanosensory neuron migration (Schmidt et al., 2009).

Growth cones respond to signals in their extracellular environment and alter actin dynamics in response to a signal. One such signal in *C. elegans* is the Netrin homolog UNC-6. Netrin/UNC-6 is a conserved axon guidance cue. A motor neuron, HSN, responds to Netrin/UNC-6 by asymmetrically localizing the receptor DCC/UNC-40 toward the direction of the signal (Adler et al., 2006). Lpd/MIG-10 also localizes asymmetrically in the growth cone through the activity of Rac/CED-10 in response to Netrin/UNC-6 (Chang et al., 2006; Quinn et

al., 2008). This asymmetric Lpd/MIG-10 localization is also coincident with asymmetric F-actin accumulation (Quinn et al., 2008). Plasma membrane markers can reveal projections, or neurites, from the cell body of developing HSN neurons (Figure 5D) (Adler et al., 2006). These neurites are F-actin rich, and form toward the Netrin/UNC-6 cue. The HSN neuron has a clear leading edge, and filopodia and lamellipodia grow and retract in the direction of the signal (Adler et al., 2006). Defects caused by increased Netrin/UNC-6 signaling are suppressed in loss-of-function mutations in Rac/CED-10, Ena/UNC-34, and abLIM/UNC-115, suggesting that growth cone outgrowth and turning by Netrin-UNC-6 signals are mediated by these cytoskeletal regulators (Gitai et al., 2003). Interestingly, although filopodia are present on all growth cones, suggesting that the formation of these F-actin rich structures is critical for axon guidance, lack of filopodia in *ena/unc-34* mutants still leads to proper HSN guidance (Chang et al., 2006). Thus, *in vivo*, it appears that dynamic filopodia form, but are dispensable for guidance, and perhaps other cues in the extracellular milieu stimulate alternative migratory mechanisms.

The growth of an axon is important for guidance, but the inhibition of outgrowth is equally important for precision. Although there are many proteins that function to promote axon outgrowth, there are few proteins known to negatively regulate this process. CRML-1, the CARMIL homolog, was identified in *C. elegans* to inhibit axon outgrowth by affecting Trio/UNC-73 activity, although mammalian CARMIL acts to promote glioblastoma migration (Vanderzalm et al., 2009; Yang et al., 2005). CRML-1 and Trio/UNC-73 physically interact, and together control the direction of growth cone migration by altering the levels of a guidance receptor, Robo/SAX-3. Thus, through the inhibition of Rac signaling, CRML-1 can negatively regulate neuronal migration.

Conclusions

Collective Cell Migration

This chapter discusses three different modes of collective migration: epithelial sheets, cell clusters, and cell streaming. Interestingly, actin-based cell migrations during morphogenesis generally occur through collective cell migration instead of single cell migration (Friedl and Gilmour, 2009). Why do cells tend to prefer to migrate in groups? One hypothesis is that forces generated by cell clusters appear higher than by single cells (Kolega et al., 1982).

C. elegans ventral enclosure and *Drosophila* dorsal closure both require multiple actin-dependent cell movements. Different forces are evident during *Drosophila* dorsal closure including actomyosin contraction of the amnioserosal cells, a supracellular purse string at the leading edge, and dynamic filopodia, are coordinated spatially and temporally to regulate a single morphogenetic process (Hutson et al., 2003). This process is similar to *C. elegans* ventral enclosure, which requires the combination of forces from actively migrating leading cells and an actin purse string like mechanism in the pocket cells. In both *C. elegans* ventral enclosure and in *Drosophila* dorsal closure, filopodia aid in closing a ring. While actin purse-string mechanisms and filopodia formation are both necessary for these epibolic movements, somewhat surprisingly, key molecular components are not conserved. The Arp2/3 complex, a major actin regulator, is required for *C. elegans* ventral enclosure (Sawa et al., 2003), but no role for Arp2/3 has been described for *Drosophila* dorsal closure. Similarly, upstream Arp2/3 activators such as Wave also do not appear to have a role during dorsal closure. It is possible that other actin nucleators, such as formins or Spire, may play a role in dorsal closure, and that Arp2/3 may be

acting redundantly with these players. The differences observed between *C. elegans* ventral enclosure and *Drosophila* dorsal closure suggest that there may be developmental plasticity, with different inputs acting on a common outcome.

Factors that are required to prevent filopodia formation and migration are also important for dorsal closure and possibly ventral enclosure. During the last stages of dorsal closure, the two epithelial leading edges must recognize each other and cease active migration. It is possible that apposition between the two edges of the migrating epithelium during dorsal closure results in contact inhibition, preventing the over-migration of the leading edges. Contact inhibition in neural crest cells is regulated by PCP/non-canonical Wnt signaling. When two neural crest cells contact each other, Dishevelled become localized to the membrane at areas of cell-cell contact and RhoA becomes active (Carmona-Fontaine et al., 2008). RhoA is thought to direct the collapse of filopodia at the cell contact zones and aid in the change of migratory direction. However, during dorsal closure, when filopodial tips touch, the filopodia do not retract immediately (Jacinto et al., 2000). Rather they appear to grasp on to each other to tether the edges of the epithelial sheet and pull them into proper alignment. Thus, it is possible that filopodial protrusions could first be used to promote the epithelial zippering, and then used later to inhibit over-migration. It will be interesting to determine if contact inhibition does occur during dorsal closure and ventral enclosure via a different mechanism than in neural crest cells.

Single cell migration – amoeboid versus mesenchymal migration

The mechanism of bleb formation appears to be different between neural crest cells and PGCs. PGCs require local actomyosin contraction which produces cytoplasmic flow to form a

membrane bleb. When PGCs are treated with blebbistatin, the membrane bleb does not form (Blaser et al., 2005). Neural crest cells, on the other hand, can still form membrane blebs when treated with blebbistatin, suggesting that actomyosin contraction is not required for bleb formation, but is required for bleb retraction (Berndt et al., 2008).

It is possible that this difference in bleb formation may account for the difference in long distance migration mechanisms between neural crest cells and PGCs. Neural crest cells exhibit blebs during delamination from the neural epithelium. Although the neural crest cells translocate their cell body, thus suggesting that they are motile, they then adopt characteristics of a mesenchymal cell with a clear leading edge to actively migrate over longer distances. PGCs, on the other hand, form membrane blebs for long-range active migration. Thus, unlike what is seen in most other systems where actin polymerization produces the force to form a pseudopod for active migration, zebrafish PGCs have adopted a different form of motility.

Why do PGCs actively migrate by membrane bleb formation rather than actin polymerization-induced protrusions? The fact that cells can convert from amoeboid to mesenchymal forms of movement, and vice versa, suggests that a cell can change its migratory behaviour based on its environment. It has been shown that bleb-dependent motility occurs as a result of changes in cell contacts or cell-cell adhesion (Shook and Keller, 2003). Rather than making contacts with the underlying substratum, bleb-dependent motility allows cells to squeeze past obstacles and navigate through matrices without attaching to a substrate (Gadea et al., 2007; Hegerfeldt et al., 2002; Tournaviti et al., 2007). This form of motility is similar to amoeboid motility. Cancer cells have also adopted this amoeboid form of motility to bypass the requirements of matrix metalloproteases (Friedl, 2004; Sahai, 2005; Wyckoff et al., 2006). It is

possible that PGCs have also adopted this form of motility to bypass a requirement for adhesion-based mechanisms.

What can we learn about actin dynamics in a model organism?

Many actin regulators are conserved between cell migrations during morphogenesis and cell migrations *in vitro*. Components of the Rac signaling pathway, as well as key actin regulators such as Ena, are found to be involved in actin dynamics in diverse systems. There are, however, some clear differences. Notably, filopodia in *C. elegans* growth cones are shown to be dispensable for axon outgrowth in vivo. This result is markedly different than the proposed function for filopodia during axon outgrowth in vitro (Drees and Gertler, 2008). It is possible that other factors are present in the extracellular milieu of an animal that could provide a redundant role or providing an alternative mechanism for axon guidance.

The strength of analyzing actin dynamics during morphogenesis is that one can understand the role of actin in its native environment. Morphogenetic processes seldom involve a single actin-based mechanism. More often, a morphogenetic process requires multiple and redundant actin-based mechanisms. Thus, dissecting the contribution of each actin-dependent process can only be accomplished in model organisms. *Drosophila* dorsal closure is a powerful model to measure the contributions of each actin-dependent mechanism for a single morphogenetic process. Specific actin-rich areas are cut with a laser and the recoil of the adjacent areas is analyzed to measure the amount of force produced by that actin-rich area. These experiments revealed that that the supracellular purse-string at the leading edge and contraction of the amnioserosa contribute to most of the forces required for dorsal closure (Hutson et al.,

2003). The forces provided by the filopodia at the leading edge are essential only for the late stages of closure. Thus, analyzing actin-dependent forces during morphogenesis allows for the understanding of how cells and tissues coordinate their forces and how these forces are regulated in space and time.

These types of force studies need not be limited to dorsal closure. *C. elegans* is an attractive model for applying laser microsurgery to analyze the contributions of multiple actin-dependent processes during endodermal internalization and ventral enclosure. Similar cell movements and actin-based structures can also be found during wound healing. When *Drosophila* or *Xenopus* embryos are wounded with a needle, the leading edge cells surrounding the wound form a supracellular actin cable as well as filopodia (Clark et al., 2009; Wood et al., 2002) (Figure 3F). The wound heals in part by an actin purse-string mechanism. When the wound size is sufficiently decreased, filopodia can reach across the wound. The filopodia then form tethers with one another to facilitate wound closure. Teasing apart the forces in these processes is an important step to understanding the cell movements themselves.

Actin dynamics have only recently been analyzed in real time in several model systems. Due to the optical clarity of some model systems like zebrafish and *C. elegans,* actin dynamics can be more readily imaged during different morphogenetic events. Furthermore, with the development of new technology to image cells deep within an animal while minimizing the toxic effects of lasers, actin dynamics in a host of cells can be imaged in their native environment. The future of this research will certainly involve an interdisciplinary approach with both *in vitro* and *in vivo* studies, which will open windows into the variable and dynamic world of actin.

References

Abercrombie, M. and Heaysman, J. E. (1954). Observations on the social behaviour of cells in tissue culture. II. Monolayering of fibroblasts. *Exp Cell Res* 6, 293-306.

Abercrombie, M., Heaysman, J. E. and Karthauser, H. M. (1957). Social behaviour of cells in tissue culture. III. Mutual influence of sarcoma cells and fibroblasts. *Exp Cell Res* 13, 276-91.

Adler, C. E., Fetter, R. D. and Bargmann, C. I. (2006). UNC-6/Netrin induces neuronal asymmetry and defines the site of axon formation. *Nat Neurosci* 9, 511-8.

Aquino, J. B., Lallemend, F., Marmigere, F., Adameyko, II, Golemis, E. A. and Ernfors, P. (2009). The retinoic acid inducible Cas-family signaling protein Nedd9 regulates neural crest cell migration by modulating adhesion and actin dynamics. *Neuroscience* 162, 1106-19.

Berndt, J. D., Clay, M. R., Langenberg, T. and Halloran, M. C. (2008). Rho-kinase and myosin II affect dynamic neural crest cell behaviors during epithelial to mesenchymal transition in vivo. *Dev Biol* 324, 236-44.

Blaser, H., Eisenbeiss, S., Neumann, M., Reichman-Fried, M., Thisse, B., Thisse, C. and Raz, E. (2005). Transition from non-motile behaviour to directed migration during early PGC development in zebrafish. *J Cell Sci* 118, 4027-38.

Bloor, J. W. and Kiehart, D. P. (2002). Drosophila RhoA regulates the cytoskeleton and cell-cell adhesion in the developing epidermis. *Development* 129, 3173-83.

Burstyn-Cohen, T., Stanleigh, J., Sela-Donenfeld, D. and Kalcheim, C. (2004). Canonical Wnt activity regulates trunk neural crest delamination linking BMP/noggin signaling with G1/S transition. *Development* 131, 5327-39.

Carmona-Fontaine, C., Matthews, H. K., Kuriyama, S., Moreno, M., Dunn, G. A., Parsons, M., Stern, C. D. and Mayor, R. (2008). Contact inhibition of locomotion in vivo controls neural crest directional migration. *Nature* 456, 957-61.

Chang, C., Adler, C. E., Krause, M., Clark, S. G., Gertler, F. B., Tessier-Lavigne, M. and Bargmann, C. I. (2006). MIG-10/lamellipodin and AGE-1/PI3K promote axon guidance and outgrowth in response to slit and netrin. *Curr Biol* 16, 854-62.

Chisholm, A. D. and Hardin, J. (2005). Epidermal morphogenesis. *WormBook*, 1-22.

Ciruna, B., Weidinger, G., Knaut, H., Thisse, B., Thisse, C., Raz, E. and Schier, A. F. (2002). Production of maternal-zygotic mutant zebrafish by germ-line replacement. *Proc Natl Acad Sci U S A* 99, 14919-24.

Clark, A. G., Miller, A. L., Vaughan, E., Yu, H. Y., Penkert, R. and Bement, W. M. (2009). Integration of single and multicellular wound responses. *Curr Biol* 19, 1389-95.

Condeelis, J. and Segall, J. E. (2003). Intravital imaging of cell movement in tumours. *Nat Rev Cancer* 3, 921-30.

De Calisto, J., Araya, C., Marchant, L., Riaz, C. F. and Mayor, R. (2005). Essential role of non-canonical Wnt signalling in neural crest migration. *Development* 132, 2587-97.

Doitsidou, M., Reichman-Fried, M., Stebler, J., Koprunner, M., Dorries, J., Meyer, D., Esguerra, C. V., Leung, T. and Raz, E. (2002). Guidance of primordial germ cell migration by the chemokine SDF-1. *Cell* 111, 647-59.

Drees, F. and Gertler, F. B. (2008). Ena/VASP: proteins at the tip of the nervous system. *Curr Opin Neurobiol* 18, 53-9.

Dumstrei, K., Mennecke, R. and Raz, E. (2004). Signaling pathways controlling primordial germ cell migration in zebrafish. *J Cell Sci* 117, 4787-95.

Edwards, K. A., Demsky, M., Montague, R. A., Weymouth, N. and Kiehart, D. P. (1997). GFP-moesin illuminates actin cytoskeleton dynamics in living tissue and demonstrates cell shape changes during morphogenesis in Drosophila. *Dev Biol* 191, 103-17.

Franke, J. D., Montague, R. A. and Kiehart, D. P. (2005). Nonmuscle myosin II generates forces that transmit tension and drive contraction in multiple tissues during dorsal closure. *Curr Biol* 15, 2208-21.

Friedl, P. (2004). Dynamic imaging of cellular interactions with extracellular matrix. *Histochem Cell Biol* 122, 183-90.

Friedl, P. and Gilmour, D. (2009). Collective cell migration in morphogenesis, regeneration and cancer. *Nat Rev Mol Cell Biol* 10, 445-57.

Gadea, G., de Toledo, M., Anguille, C. and Roux, P. (2007). Loss of p53 promotes RhoA-ROCK-dependent cell migration and invasion in 3D matrices. *J Cell Biol* 178, 23-30.

Gammill, L. S. and Bronner-Fraser, M. (2003). Neural crest specification: migrating into genomics. *Nat Rev Neurosci* 4, 795-805.

Gates, J., Mahaffey, J. P., Rogers, S. L., Emerson, M., Rogers, E. M., Sottile, S. L., Van Vactor, D., Gertler, F. B. and Peifer, M. (2007). Enabled plays key roles in embryonic epithelial morphogenesis in Drosophila. *Development* 134, 2027-39.

Gertler, F. B., Doctor, J. S. and Hoffmann, F. M. (1990). Genetic suppression of mutations in the Drosophila abl proto-oncogene homolog. *Science* 248, 857-60.

Gitai, Z., Yu, T. W., Lundquist, E. A., Tessier-Lavigne, M. and Bargmann, C. I. (2003). The netrin receptor UNC-40/DCC stimulates axon attraction and outgrowth through enabled and, in parallel, Rac and UNC-115/AbLIM. *Neuron* 37, 53-65.

Goldstein, B. and Hamada, H. (2009). Shape meets polarity in Japan. *Development* 136, 2487-92.

Groysman, M., Shoval, I. and Kalcheim, C. (2008). A negative modulatory role for rho and rho-associated kinase signaling in delamination of neural crest cells. *Neural Dev* 3, 27.

Gurniak, C. B., Perlas, E. and Witke, W. (2005). The actin depolymerizing factor n-cofilin is essential for neural tube morphogenesis and neural crest cell migration. *Dev Biol* 278, 231-41.

Harden, N., Ricos, M., Ong, Y. M., Chia, W. and Lim, L. (1999). Participation of small GTPases in dorsal closure of the Drosophila embryo: distinct roles for Rho subfamily proteins in epithelial morphogenesis. *J Cell Sci* 112 (Pt 3), 273-84.

Harris, T. J., Sawyer, J. K. and Peifer, M. (2009). How the cytoskeleton helps build the embryonic body plan: models of morphogenesis from Drosophila. *Curr Top Dev Biol* 89, 55-85.

Hegerfeldt, Y., Tusch, M., Brocker, E. B. and Friedl, P. (2002). Collective cell movement in primary melanoma explants: plasticity of cell-cell interaction, beta1-integrin function, and migration strategies. *Cancer Res* 62, 2125-30.

Homem, C. C. and Peifer, M. (2008). Diaphanous regulates myosin and adherens junctions to control cell contractility and protrusive behavior during morphogenesis. *Development* 135, 1005-18.

Hutson, M. S., Tokutake, Y., Chang, M. S., Bloor, J. W., Venakides, S., Kiehart, D. P. and Edwards, G. S. (2003). Forces for morphogenesis investigated with laser microsurgery and quantitative modeling. *Science* 300, 145-9.

Hwang, Y. S., Luo, T., Xu, Y. and Sargent, T. D. (2009). Myosin-X is required for cranial neural crest cell migration in Xenopus laevis. *Dev Dyn* 238, 2522-2529.

Jacinto, A., Wood, W., Balayo, T., Turmaine, M., Martinez-Arias, A. and Martin, P. (2000). Dynamic actin-based epithelial adhesion and cell matching during Drosophila dorsal closure. *Curr Biol* 10, 1420-6.

Jacinto, A., Wood, W., Woolner, S., Hiley, C., Turner, L., Wilson, C., Martinez-Arias, A. and Martin, P. (2002). Dynamic analysis of actin cable function during Drosophila dorsal closure. *Curr Biol* 12, 1245-50.

Kasemeier-Kulesa, J. C., Kulesa, P. M. and Lefcort, F. (2005). Imaging neural crest cell dynamics during formation of dorsal root ganglia and sympathetic ganglia. *Development* 132, 235-45.

Kiehart, D. P., Galbraith, C. G., Edwards, K. A., Rickoll, W. L. and Montague, R. A. (2000). Multiple forces contribute to cell sheet morphogenesis for dorsal closure in Drosophila. *J Cell Biol* 149, 471-90.

Kolega, J., Shure, M. S., Chen, W. T. and Young, N. D. (1982). Rapid cellular translocation is related to close contacts formed between various cultured cells and their substrata. *J Cell Sci* 54, 23-34.

Kolsch, V., Charest, P. G. and Firtel, R. A. (2008). The regulation of cell motility and chemotaxis by phospholipid signaling. *J Cell Sci* 121, 551-9.

Kuriyama, S. and Mayor, R. (2008). Molecular analysis of neural crest migration. *Philos Trans R Soc Lond B Biol Sci* 363, 1349-62.

Lee, J. Y. and Goldstein, B. (2003). Mechanisms of cell positioning during C. elegans gastrulation. *Development* 130, 307-20.

Lee, J. Y. and Harland, R. M. (2007). Actomyosin contractility and microtubules drive apical constriction in Xenopus bottle cells. *Dev Biol* 311, 40-52.

Lee, J. Y., Marston, D. J., Walston, T., Hardin, J., Halberstadt, A. and Goldstein, B. (2006). Wnt/Frizzled signaling controls C. elegans gastrulation by activating actomyosin contractility. *Curr Biol* 16, 1986-97.

Liu, J. P. and Jessell, T. M. (1998). A role for rhoB in the delamination of neural crest cells from the dorsal neural tube. *Development* 125, 5055-67.

Lundquist, E. A., Herman, R. K., Shaw, J. E. and Bargmann, C. I. (1998). UNC-115, a conserved protein with predicted LIM and actin-binding domains, mediates axon guidance in C. elegans. *Neuron* 21, 385-92.

Lundquist, E. A., Reddien, P. W., Hartwieg, E., Horvitz, H. R. and Bargmann, C. I. (2001). Three C. elegans Rac proteins and several alternative Rac regulators control axon guidance, cell migration and apoptotic cell phagocytosis. *Development* 128, 4475-88.

Martin, P. and Parkhurst, S. M. (2004). Parallels between tissue repair and embryo morphogenesis. *Development* 131, 3021-34.

Matthews, H. K., Marchant, L., Carmona-Fontaine, C., Kuriyama, S., Larrain, J., Holt, M. R., Parsons, M. and Mayor, R. (2008). Directional migration of neural crest cells in vivo is regulated by Syndecan-4/Rac1 and non-canonical Wnt signaling/RhoA. *Development* 135, 1771-80.

Mattila, P. K. and Lappalainen, P. (2008). Filopodia: molecular architecture and cellular functions. *Nat Rev Mol Cell Biol* 9, 446-54.

Millard, T. H. and Martin, P. (2008). Dynamic analysis of filopodial interactions during the zippering phase of Drosophila dorsal closure. *Development* 135, 621-6.

Nie, S., Kee, Y. and Bronner-Fraser, M. (2009). Myosin-X is critical for migratory ability of Xenopus cranial neural crest cells. *Dev Biol*.

Norris, A. D., Dyer, J. O. and Lundquist, E. A. (2009). The Arp2/3 complex, UNC-115/abLIM, and UNC-34/Enabled regulate axon guidance and growth cone filopodia formation in Caenorhabditis elegans. *Neural Dev* 4, 38.

Patel, F. B., Bernadskaya, Y. Y., Chen, E., Jobanputra, A., Pooladi, Z., Freeman, K. L., Gally, C., Mohler, W. A. and Soto, M. C. (2008). The WAVE/SCAR complex promotes polarized cell movements and actin enrichment in epithelia during C. elegans embryogenesis. *Dev Biol* 324, 297-309.

Pollard, T. D. and Borisy, G. G. (2003). Cellular motility driven by assembly and disassembly of actin filaments. *Cell* 112, 453-65.

Quinn, C. C., Pfeil, D. S. and Wadsworth, W. G. (2008). CED-10/Rac1 mediates axon guidance by regulating the asymmetric distribution of MIG-10/lamellipodin. *Curr Biol* 18, 808-13.

Raich, W. B., Agbunag, C. and Hardin, J. (1999). Rapid epithelial-sheet sealing in the Caenorhabditis elegans embryo requires cadherin-dependent filopodial priming. *Curr Biol* 9, 1139-46.

Raz, E. (2004). Guidance of primordial germ cell migration. *Curr Opin Cell Biol* 16, 169-73.

Reed, B. H., Wilk, R., Schock, F. and Lipshitz, H. D. (2004). Integrin-dependent apposition of Drosophila extraembryonic membranes promotes morphogenesis and prevents anoikis. *Curr Biol* 14, 372-80.

Reichman-Fried, M., Minina, S. and Raz, E. (2004). Autonomous modes of behavior in primordial germ cell migration. *Dev Cell* 6, 589-96.

Rupp, P. A. and Kulesa, P. M. (2007). A role for RhoA in the two-phase migratory pattern of post-otic neural crest cells. *Dev Biol* 311, 159-71.

Sahai, E. (2005). Mechanisms of cancer cell invasion. *Curr Opin Genet Dev* 15, 87-96.

Sawa, M., Suetsugu, S., Sugimoto, A., Miki, H., Yamamoto, M. and Takenawa, T. (2003). Essential role of the C. elegans Arp2/3 complex in cell migration during ventral enclosure. *J Cell Sci* 116, 1505-18.

Sawyer, J. M., Harrell, J. R., Shemer, G., Sullivan-Brown, J., Roh-Johnson, M. and Goldstein, B. (2009). Apical constriction: A cell shape change that can drive morphogenesis. *Dev Biol*.

Schmidt, K. L., Marcus-Gueret, N., Adeleye, A., Webber, J., Baillie, D. and Stringham, E. G. (2009). The cell migration molecule UNC-53/NAV2 is linked to the ARP2/3 complex by ABI-1. *Development* 136, 563-74.

Severson, A. F., Baillie, D. L. and Bowerman, B. (2002). A Formin Homology protein and a profilin are required for cytokinesis and Arp2/3-independent assembly of cortical microfilaments in C. elegans. *Curr Biol* 12, 2066-75.

Shakir, M. A., Gill, J. S. and Lundquist, E. A. (2006). Interactions of UNC-34 Enabled with Rac GTPases and the NIK kinase MIG-15 in Caenorhabditis elegans axon pathfinding and neuronal migration. *Genetics* 172, 893-913.

Shakir, M. A., Jiang, K., Struckhoff, E. C., Demarco, R. S., Patel, F. B., Soto, M. C. and Lundquist, E. A. (2008). The Arp2/3 activators WAVE and WASP have distinct genetic interactions with Rac GTPases in Caenorhabditis elegans axon guidance. *Genetics* 179, 1957-71.

Sheffield, M., Loveless, T., Hardin, J. and Pettitt, J. (2007). C. elegans Enabled exhibits novel interactions with N-WASP, Abl, and cell-cell junctions. *Curr Biol* 17, 1791-6.

Shook, D. and Keller, R. (2003). Mechanisms, mechanics and function of epithelial-mesenchymal transitions in early development. *Mech Dev* 120, 1351-83.

Shoval, I., Ludwig, A. and Kalcheim, C. (2007). Antagonistic roles of full-length N-cadherin and its soluble BMP cleavage product in neural crest delamination. *Development* 134, 491-501.

Soto, M. C., Qadota, H., Kasuya, K., Inoue, M., Tsuboi, D., Mello, C. C. and Kaibuchi, K. (2002). The GEX-2 and GEX-3 proteins are required for tissue morphogenesis and cell migrations in C. elegans. *Genes Dev* 16, 620-32.

Steven, R., Kubiseski, T. J., Zheng, H., Kulkarni, S., Mancillas, J., Ruiz Morales, A., Hogue, C. W., Pawson, T. and Culotti, J. (1998). UNC-73 activates the Rac GTPase and is required for cell and growth cone migrations in C. elegans. *Cell* 92, 785-95.

Stevens, T. L., Rogers, E. M., Koontz, L. M., Fox, D. T., Homem, C. C., Nowotarski, S. H., Artabazon, N. B. and Peifer, M. (2008). Using Bcr-Abl to examine mechanisms by which abl kinase regulates morphogenesis in Drosophila. *Mol Biol Cell* 19, 378-93.

Stolp, B., Reichman-Fried, M., Abraham, L., Pan, X., Giese, S. I., Hannemann, S., Goulimari, P., Raz, E., Grosse, R. and Fackler, O. T. (2009). HIV-1 Nef interferes with host cell motility by deregulation of Cofilin. *Cell Host Microbe* 6, 174-86.

Struckhoff, E. C. and Lundquist, E. A. (2003). The actin-binding protein UNC-115 is an effector of Rac signaling during axon pathfinding in C. elegans. *Development* 130, 693-704.

Svitkina, T. M. and Borisy, G. G. (1999). Arp2/3 complex and actin depolymerizing factor/cofilin in dendritic organization and treadmilling of actin filament array in lamellipodia. *J Cell Biol* 145, 1009-26.

Teddy, J. M. and Kulesa, P. M. (2004). In vivo evidence for short- and long-range cell communication in cranial neural crest cells. *Development* 131, 6141-51.

Tournaviti, S., Hannemann, S., Terjung, S., Kitzing, T. M., Stegmayer, C., Ritzerfeld, J., Walther, P., Grosse, R., Nickel, W. and Fackler, O. T. (2007). SH4-domain-induced plasma membrane dynamization promotes bleb-associated cell motility. *J Cell Sci* 120, 3820-9.

Vanderzalm, P. J., Pandey, A., Hurwitz, M. E., Bloom, L., Horvitz, H. R. and Garriga, G. (2009). C. elegans CARMIL negatively regulates UNC-73/Trio function during neuronal development. *Development* 136, 1201-10.

Weidinger, G., Wolke, U., Koprunner, M., Thisse, C., Thisse, B. and Raz, E. (2002). Regulation of zebrafish primordial germ cell migration by attraction towards an intermediate target. *Development* 129, 25-36.

Williams-Masson, E. M., Malik, A. N. and Hardin, J. (1997). An actin-mediated two-step mechanism is required for ventral enclosure of the C. elegans hypodermis. *Development* 124, 2889-901.

Withee, J., Galligan, B., Hawkins, N. and Garriga, G. (2004). Caenorhabditis elegans WASP and Ena/VASP proteins play compensatory roles in morphogenesis and neuronal cell migration. *Genetics* 167, 1165-76.

Wolf, K., Mazo, I., Leung, H., Engelke, K., von Andrian, U. H., Deryugina, E. I., Strongin, A. Y., Brocker, E. B. and Friedl, P. (2003). Compensation mechanism in tumor cell migration: mesenchymal-amoeboid transition after blocking of pericellular proteolysis. *J Cell Biol* 160, 267-77.

Wood, W., Jacinto, A., Grose, R., Woolner, S., Gale, J., Wilson, C. and Martin, P. (2002). Wound healing recapitulates morphogenesis in Drosophila embryos. *Nat Cell Biol* 4, 907-12.

Woolner, S., Jacinto, A. and Martin, P. (2005). The small GTPase Rac plays multiple roles in epithelial sheet fusion--dynamic studies of Drosophila dorsal closure. *Dev Biol* 282, 163-73.

Wu, Y. C., Cheng, T. W., Lee, M. C. and Weng, N. Y. (2002). Distinct rac activation pathways control Caenorhabditis elegans cell migration and axon outgrowth. *Dev Biol* 250, 145-55.

Wyckoff, J. B., Pinner, S. E., Gschmeissner, S., Condeelis, J. S. and Sahai, E. (2006). ROCK- and myosin-dependent matrix deformation enables protease-independent tumor-cell invasion in vivo. *Curr Biol* 16, 1515-23.

Yang, C., Pring, M., Wear, M. A., Huang, M., Cooper, J. A., Svitkina, T. M. and Zigmond, S. H. (2005). Mammalian CARMIL inhibits actin filament capping by capping protein. *Dev Cell* 9, 209-21.

Young, H. M., Bergner, A. J., Anderson, R. B., Enomoto, H., Milbrandt, J., Newgreen, D. F. and Whitington, P. M. (2004). Dynamics of neural crest-derived cell migration in the embryonic mouse gut. *Dev Biol* 270, 455-73.

Yu, T. W., Hao, J. C., Lim, W., Tessier-Lavigne, M. and Bargmann, C. I. (2002). Shared receptors in axon guidance: SAX-3/Robo signals via UNC-34/Enabled and a Netrin-independent UNC-40/DCC function. *Nat Neurosci* 5, 1147-54.

Zallen, J. A., Cohen, Y., Hudson, A. M., Cooley, L., Wieschaus, E. and Schejter, E. D. (2002). SCAR is a primary regulator of Arp2/3-dependent morphological events in Drosophila. *J Cell Biol* 156, 689-701.

CHAPTER 2

IN VIVO ROLES FOR ARP2/3 IN CORTICAL ACTIN ORGANIZATION DURING C. ELEGANS GASTRULATION

Summary

The Arp2/3 complex is important for morphogenesis in various developmental systems, but specific in vivo roles for this complex in cells that move during morphogenesis are not well understood. We have examined cellular roles for Arp2/3 in the *C. elegans* embryo. In *C. elegans*, the first morphogenetic movement, gastrulation, is initiated by the internalization of two endodermal precursor cells. These cells undergo a myosin-dependent apical constriction, pulling a ring of six neighboring cells into a gap left behind on the ventral surface of the embryo. In agreement with a previous report (Severson et al., 2002), we found that in Arp2/3-depleted *C. elegans* embryos, membrane blebs form and the endodermal precursor cells fail to fully internalize. We show that these cells are normal with respect to several key requirements for gastrulation: cell cycle timing, cell fate, apicobasal cell polarity, and apical accumulation and activation of myosin II. To further understand Arp2/3's function in gastrulation, we examined F-actin dynamics in wild-type embryos. We found that three of the six neighboring cells extend short, dynamic, F-actin-rich processes at their apical borders with the internalizing cells. These processes failed to form in embryos that were depleted of Arp2/3, or of the apical protein PAR-3.

Our results identify an in vivo role for Arp2/3 in the formation of subcellular structures during morphogenesis. The results also suggest a new layer to the model of *C. elegans* gastrulation: in addition to apical constriction, internalization of the endoderm may involve dynamic, Arp2/3-dependent, F-actin-rich extensions on one side of a ring of cells.

Introduction

Morphogenesis involves the reorganization of cells by cell shape changes and cell movements, both of which require intricate regulation of cytoskeletal dynamics. Some of the central goals of studying morphogenesis are to understand how cytoskeletal dynamics are regulated and how the reorganization of the cytoskeleton drives the movements of cells during development.

Gastrulation is one of the first morphogenetic movements in animal embryos. In most embryos, the three germ layers -- ectoderm, mesoderm and endoderm -- become positioned during gastrulation. Gastrulation in *C. elegans* is a powerful model system for dissecting mechanisms of morphogenesis because it involves a small number of cells and hence can be studied at the level of individual cells. Also, one can readily combine live microscopic imaging with gene function studies. Gastrulation in *C. elegans* is initiated at the 26-cell stage by the internalization of the anterior and posterior endodermal precursor cells, Ea and Ep (referred to collectively as Ea/p). Normal cell fate is required for Ea/p cell internalization: mutations in endoderm-specifying genes, such as the endodermal GATA factor genes *end-1* and *end-3*, result in gastrulation defects (Zhu et al., 1997; Maduro et al., 2005; Lee et al., 2006). Ectopic endodermal cells produced experimentally by cell fate transformation also internalize (Lee et al.,

2006). As the Ea/p cells internalize in wild-type embryos, a ring of six cells fills a gap left behind on the ventral surface of the embryo (Lee and Goldstein, 2003). After the Ea/p cells internalize, they divide in the center of the embryo and eventually form the entire endoderm.

The Ea/p cells move to the embryonic interior in part through apical constriction. The Ea/p cells apically accumulate non-muscle myosin II, NMY-2 (Nance and Priess, 2002). This polarized accumulation requires the PAR proteins (Nance and Priess, 2002), conserved polarity proteins with homologs in *Drosophila* and vertebrates (Goldstein and Macara, 2007). Certain PAR proteins such as PAR-3, PAR-6 and an atypical protein kinase C localize to the apical surfaces of the Ea/p cells, whereas PAR-1 and PAR-2 are basolaterally localized (Etemad-Moghadam et al., 1995; Boyd et al., 1996; Hung and Kemphues, 1999; Nance and Priess, 2002). Myosin II becomes activated in a Wnt-dependent manner by phosphorylation of the regulatory myosin light chains (rMLC) (Lee et al., 2006). This activation results in a contraction of the actomyosin meshwork in the apical cell cortex of each Ea/p cell, which is thought to pull the ring of neighboring cells underneath, driving the Ea/p cells to the interior of the embryo.

The known roles for actin in Ea/p cell movements suggest that actin regulation may be involved in this process. One major regulator of the actin cytoskeleton is the Arp2/3 complex (Vartiainen and Machesky, 2004). This complex is composed of seven subunits that act together to nucleate new actin filaments off of pre-existing actin filaments (Pollard, 2007). Two subunits of the Arp2/3 complex are actin-related proteins that nucleate growth of the new filament, and the other five proteins link the two actin-related proteins to the mother filament (Rouiller et al., 2008). In cultured motile cells, where roles for Arp2/3 are intensively studied, Arp2/3-dependent branching at the leading edge results in a densely interconnected network of F-actin that functions to push the membrane forward, producing a pseudopod (Pollard, 2007). The interaction

of the Arp2/3 complex with nucleation-promoting factors, such as the WASp/Scar family of proteins, stimulates the formation of new branched actin filaments, further pushing the membrane forward for cell migration (Pollard and Borisy, 2003).

Loss of function studies in diverse whole organisms have revealed that Arp2/3 is important for a variety of functions that involve the actin cytoskeleton (Vartiainen and Machesky, 2004). Arp2/3 is important for endocytosis in yeast and phagocytosis in mammals (May et al., 2000; Warren et al., 2002). Given Arp2/3's well established role in regulating actin dynamics, it is perhaps not surprising that Arp2/3 regulates the shaping of specialized actin-based structures in developing systems. Studies in *Drosophila* have shown a role for Arp2/3 in ring canal morphogenesis: Arp2/3 affects the size of the ring canal during oogenesis (Hudson and Cooley, 2002; Somogyi and Rorth, 2004). Myoblast fusion and pseudocleavage furrow formation are also regulated by Arp2/3 (Stevenson et al., 2002; Massarwa et al., 2007). Recently, it has been found that Arp2/3's role in endocytosis affects the remodeling of epithelial adherens junctions (Georgiou et al., 2008). Many studies have also identified roles for Arp2/3 and its upstream regulators in shaping plant cells (Mathur, 2005). These studies from metazoa, fungi, and plants revealed roles for Arp2/3 in non-motile cells. Much less is known about how Arp2/3 functions in the embryonic cells that move during morphogenetic events.

Depleting *C. elegans* of Arp2/3 subunits resulted in bleb-like extensions on cells and gastrulation defects: Ea/p cells fail to move to the embryonic interior and instead divide on the surface of the embryo (Severson et al., 2002). *C. elegans* Arp2/3-encoding genes are named Arp2/3-***r****elated complex*, or *arx* genes (Sawa et al., 2003; Severson et al., 2002). *arx-2* and *arx-1* encode the Arp2 and Arp3 homologues, respectively. Depleting *C. elegans* Arp2/3 subunits by RNAi results in more than 95% embryonic lethality (Severson et al., 2002). Arp2/3 RNAi

embryos also have defects in ventral enclosure, a process in which the embryonic epidermis migrates from the dorsal surface and seals the ventral surface (Severson et al., 2002; Sawa et al., 2003; Patel et al., 2008). In Arp2/3-depleted embryos, the leading edge of the migrating epidermis lacks a normal enrichment of filamentous actin, and finger-like protrusions that normally form are absent (Sawa et al., 2003). Another role for Arp2/3 was found in migrating excretory cells in *C. elegans*, where Arp2/3 was discovered to be involved in longitudinal migration (Schmidt et al., 2009). To our knowledge, no other reports have dissected roles for the Arp2/3 complex in cells that move during morphogenesis in animal embryos. Furthermore, there are very few studies examining the roles of Arp2/3 in the moving cells of intact animals as the movements are taking place. Exploring such roles is an important step toward understanding the breadth of in vivo functions of this complex.

To determine cellular roles for the Arp2/3 complex in the embryonic cells that move during morphogenetic events, we used a combination of live imaging and immunohistochemistry in wild-type and RNAi-treated *C. elegans* embryos. A number of possible roles were suggested by the known direct functions of Arp2/3 in F-actin nucleation and branching, as well as by indirect roles for Arp2/3 in endocytosis, apicobasal protein targeting, adhesion, and cell motility (Kovacs and Yap, 2002; Guerriero et al., 2006; Le Clainche and Carlier, 2008; Galletta and Cooper, 2009). We report that Arp2/3 is enriched at cell cortexes, and that previously observed membrane protrusions (Severson et al., 2002) that form in Arp2/3 RNAi embryos are classical membrane blebs. Despite the blebs observed in Arp2/3-depleted embryos, the cells that would normally participate in gastrulation appeared normal with respect to several key upstream inputs to gastrulation: cell cycle timing, cell fates, apicobasal cell polarity, and apical accumulation and activation of myosin II. To further explore how Arp2/3 might affect gastrulation, we examined

F-actin dynamics in living, wild-type embryos during gastrulation. We found that dynamic, F-actin-rich structures form on specific cells – cells on one side of the ring of cells that fills the gap left by the internalizing Ea/p cells, at their apical boundaries with the Ea/p cells. These F-actin-rich structures failed to form in embryos that were depleted of Arp2/3 or of the apical protein PAR-3. Our results identify an in vivo role for Arp2/3 during morphogenetic cell movements. The results also suggest that internalization of the endoderm in *C. elegans* may involve dynamic, Arp2/3-dependent, F-actin-rich extensions that form on specific cells.

Results

Arp2/3 depletion results in partial shrinking of the Ea/p apical surfaces and incomplete Ea/p cell internalization

Severson et al. (2002) reported that depletion of Arp2/3 complex members by RNAi resulted in dead embryos and found that the Ea and Ep cells failed to internalize. We began by confirming this result. In wild-type embryos, Ea and Ep were born on the surface of the embryo and moved to the interior before dividing (Figure 7A-D). In Arp2/3-depleted embryos, Ea and Ep failed to completely internalize, dividing on the surface of the embryo (Figure 7E-H). The gastrulation defects in embryos depleted of *arx-1*/Arp3 (n=65) or *arx-2*/Arp2 (n=25) by RNAi by injection were both 100% penetrant. Our subsequent experiments on Arp2/3 targeted *arx-1*/Arp3 or *arx-2*/Arp2 by injecting double-stranded RNAs into the parental strain because either resulted in gastrulation defects at high penetrance. For convenience we refer to either treatment as Arp2/3 RNAi.

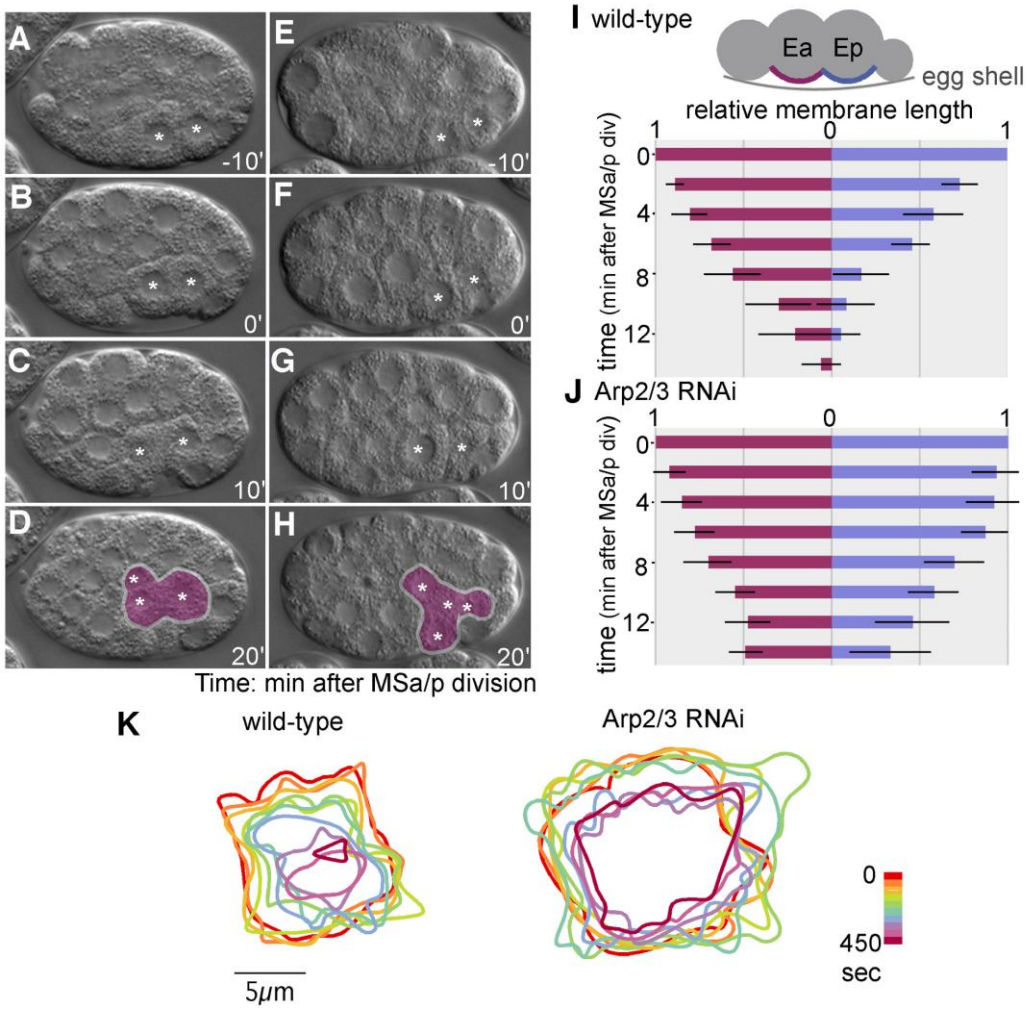
A
E
-10'
B
F
0'
C
G
10'
D
H
20'
Time: min after MSa/p division
I wild-type
Ea Ep
egg shell
relative membrane length
1 0 1
0
4
8
12
time (min after MSa/p div)
J Arp2/3 RNAi
K
wild-type
Arp2/3 RNAi
5μm
0
450
sec

Figure 7: Arp2/3 depletion results in only partial shrinking of the Ea/p cell apical surfaces. (A-D) The Ea/p cells move into the interior of the embryo as surrounding cells fill in the gap left in the ventral (bottom) side. The Ea/p cells subsequently divide (D) in the interior. Only 3 of the 4 Ea/p descendants (shaded in purple) are marked with asterisks because the 4^{th} descendant is not in same imaging plane. (E-H) Ea/p cells in Arp2/3-depleted embryos begin to move to the interior but fail to complete internalization and divide on the surface of the embryo. The progeny of Ea/p did eventually internalize as four cells. In this and subsequent figures, asterisks mark Ea/p cells and/or Ea/p descendants, except where noted. (I) Lengths of exposed Ea/p apical surfaces are shown as ratios of the initial lengths ± 95% confidence intervals. In wild-type embryos (n=6), Ea/p cells internalized by ~14 minutes after MSa/p division. (J) In Arp2/3 RNAi embryos (n=6), the lengths of exposed apical Ea/p cell surfaces failed to completely decrease to zero. (K) Tracings of en face (ventral) views of individual cells. The apical surfaces of Ea/p cells in wild-type and Arp2/3 RNAi embryos were traced at 50 sec intervals from films of the PH:mCherry membrane marker, and individual tracings were color-coded by time and overlain. The legend indicates seconds after MSa/p division.

To understand why endodermal internalization did not complete in Arp2/3-depleted embryos, we further quantified the degree to which cell internalization failed by placing embryos on their lateral sides and measuring the maximum anterior-to-posterior length of the exposed surfaces of Ea and Ep. In wild-type embryos, these exposed apical lengths decreased over time, and by 14 minutes after neighboring MS cells (MSa/p) divided, the apical surfaces of Ea and Ep were covered or almost entirely covered by neighboring cells (Figure 7I). In Arp2/3 RNAi embryos, the lengths of exposed apical Ea/p cell surfaces began to decrease as in wild-type, but this process failed to complete (Figure 7J). To visualize the entire apical surface as Ea/p cell internalization occurred, we imaged the cell-cell boundaries on the ventral surface of embryos using a plasma membrane marker, a fluorescently-tagged plextrin homology domain of phospholipase C gamma (mCherry::PH) (Kachur et al., 2008). We traced the apical edges of an Ep cell as the exposed surface decreased in total area (Figure 7K). Tracing apical edges in an Arp2/3-depleted embryo showed, as with the lateral measurements, that the apical surface failed to fully decrease in size (Fig 7K). We conclude that in Arp2/3-depleted embryos, the Ea/p cells began to internalize, and they failed to completely move to the interior of the embryo, leaving much of their apical surfaces exposed to the embryo's exterior.

Arp2/3 is enriched at the cell cortex and is required for stable membrane-cytoskeletal linkages

Before examining specific functions of Arp2/3 in gastrulation, we explored its general functions in cells of the early *C. elegans* embryo by examining its localization and loss of function phenotype in early embryos. The Arp2/3 complex localizes to branched actin at the leading edge of migrating cells and in the cell cortex in other systems (Mullins et al., 1997; Svitkina and Borisy, 1999). However, antibodies previously generated against *C. elegans* ARX-

1/Arp3 and ARX-7/ArpC5 showed only diffuse localization throughout the cytoplasm in embryos (Sawa et al., 2003). We generated affinity-purified polyclonal antibodies against ARX-5, the *C. elegans* homolog of ArpC3, the 21 kDa subunit. We immunostained embryos and found enrichment near plasma membranes, consistent with the expected localization to the cell cortex (Figure 8A-F). This pattern was seen at gastrulation and earlier, and it was eliminated by RNAi targeting *arx-5*. At the time of Ea/p cell internalization, ARX-5 was also present at sites where MS granddaughter cells contact Ea at the cells' apical surfaces (Fig 8C,E), sites that we discuss further below. We saw diffuse cytoplasmic and P granule staining as well, but RNAi targeting *arx-5* eliminated only the cortical signal, suggesting that the cytoplasmic and P granule staining were primarily non-specific background. We conclude that as expected given its known functions, Arp2/3 is enriched at the cell cortex at gastrulation and earlier.

In Arp2/3 RNAi embryos, cells formed membrane protrusions that were previously referred to as blebs (Severson et al., 2002). Blebbing involves detachment of the plasma membrane from the cortical cytoskeleton (Cunningham, 1995) but it is unclear whether the structures described previously reflect such detachments, as they were observed only by DIC microscopy (Severson et al., 2002). Once the membrane-cytoskeleton linkage is broken, blebs continue to expand. F-actin and other components of the contractile cortex then re-assemble under the bleb membrane, and the bleb retracts (Charras et al., 2006). To determine whether Arp2/3 is required for such membrane-cytoskeletal linkage, we first examined the protrusions of Arp2/3-depleted embryonic cells using the plasma membrane marker PH::mCherry. These protrusions formed throughout embryogenesis. Arp2/3-depleted embryos appeared to form membrane protrusions on all of the external cell surfaces (Figure 9C,D), whereas wild-type embryos formed only flattened membrane extensions and apparent membrane tethers (Fig 9A,B).

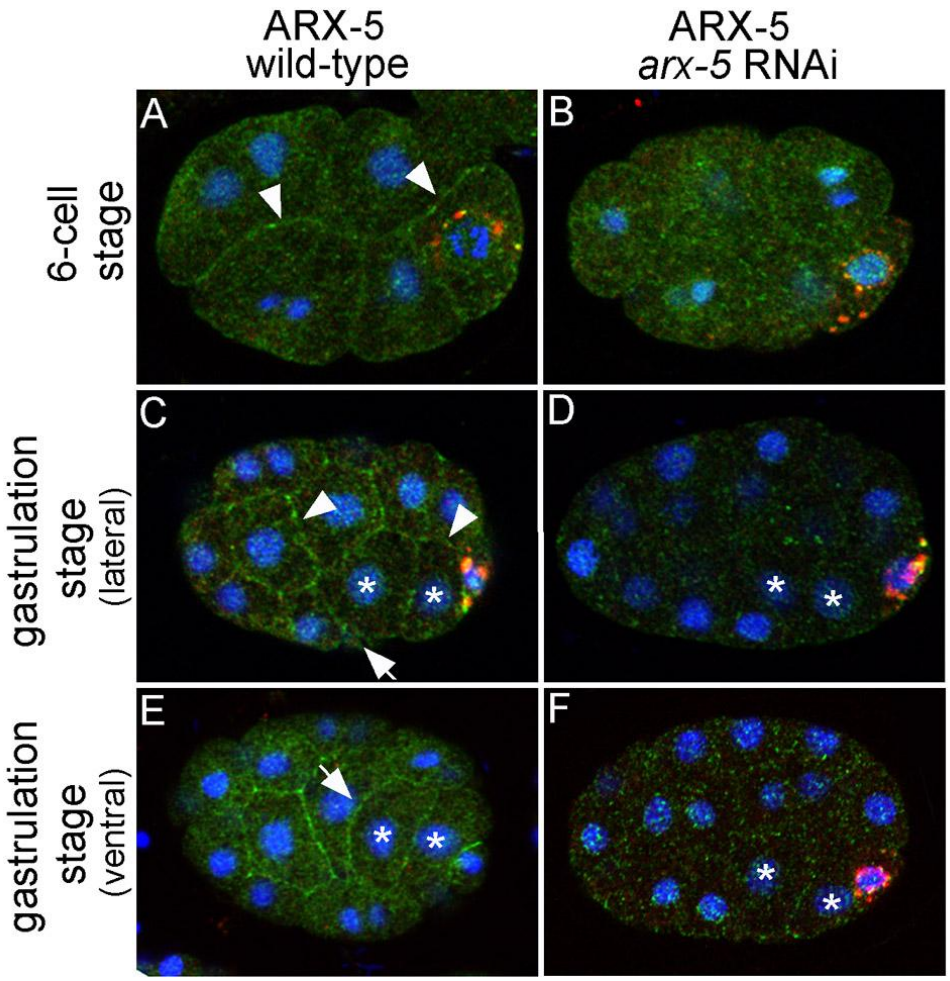
ARX-5
wild-type
ARX-5
arx-5 RNAi
6-cell
stage
gastrulation
stage
(lateral)
gastrulation
stage
(ventral)
A
B
C
D
E
F

Figure 8. The Arp2/3 complex is enriched near cell membranes. (A-F) Embryos immunostained with ARX-5 antibodies (green). (A,B) Embryos at the 6-8 cell stage. ARX-5 appears enriched near plasma membranes (arrowheads). In control *arx-5* RNAi embryos, enrichment near plasma membranes is reduced or absent. (C-F) Lateral views (C,D) and ventral views (E,F) of gastrulation-stage embryos also revealed ARX-5 localization near membranes (arrowheads). ARX-5 was similarly enriched at borders between MSxx and Ea cells (arrow). Cortical staining was absent in *arx-5* RNAi embryos. Antibodies to P granules were used to confirm permeabilization of embryos to immunostaining reagents (red). Nuclei are stained with DAPI (blue).

When we imaged at the mid-plane of Arp2/3-depleted embryos, we found that the rounded protrusions only formed at the contact-free surfaces (Figure 9G,H) and not at surfaces that were in contact with other cells (Figure 9C,D,G,H). Next, to simultaneously image plasma membranes and underlying F-actin dynamics, we crossed the PH::mCherry membrane marker into a strain expressing a GFP-tagged F-actin-binding domain from *Drosophila* moesin (GFP::MOE), which has been used in *Drosophila* and *C. elegans* to specifically mark the filamentous form of actin (Edwards et al., 1997; Motegi et al., 2006). In Arp2/3 RNAi embryos, the apical membrane formed rounded protrusions that lacked cortical GFP::MOE enrichment under the bleb membrane as the bleb expanded (Figure 9I). Once the bleb stopped expanding, GFP::MOE accumulated under the bleb membrane, and the bleb retracted (n=21/21 blebs; Figure 9I,J). Therefore, the cellular protrusions observed in Arp2/3 RNAi embryos have characteristics that suggest that they are *bona fide* membrane blebs. Consistent with the lack of cytoskeletal support observed under growing blebs, we did not observe blebs after fixation and processing for immunostaining (Figure 12, for example). We conclude that Arp2/3 is important in this system for the membrane-cytoskeletal linkages that normally prevents blebbing, possibly through an effect on actin cytoskeletal integrity. Despite the formation of membrane blebs, cell divisions still occurred, and the first developmental defect that we and others observed was failure of Ea/p cell internalization. Therefore, to determine the cellular mechanisms underlying this gastrulation defect, we examined several key factors that regulate Ea/p cell internalization.

Arp2/3-depleted embryos have normal cell fates during gastrulation

Actin-based intracellular motility is important in cell fate specification (Takizawa et al., 1997) and failure to specify endodermal cell fate can prevent gastrulation (Lee et al., 2006). Therefore, we speculated that defective cell fate specification could underlie the gastrulation

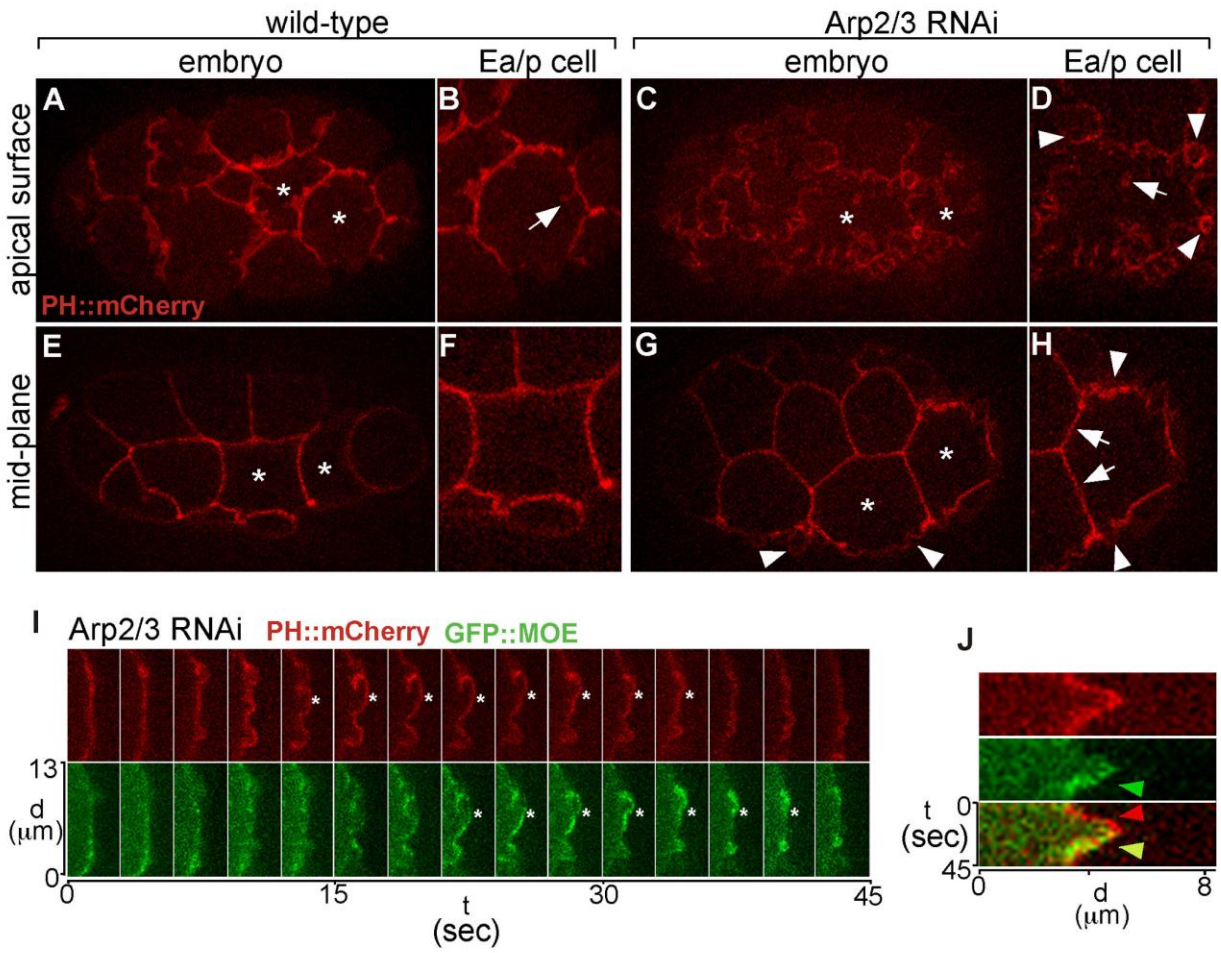
wild-type
Arp2/3 RNAi
embryo
Ea/p cell
embryo
Ea/p cell
apical surface
mid-plane
A
B
C
D
E
F
G
H
PH::mCherry
I
Arp2/3 RNAi
PH::mCherry
GFP::MOE
13
d
(μm)
0
0
15
30
45
t
(sec)
J
t
(sec)
0
45
0
8
d
(μm)

Figure 9: Arp2/3 is required for stable membrane-cytoskeletal linkages at free cell surfaces. (A-H) Ventral views of embryos expressing PH::mCherry plasma membrane marker. (A) A surface view of a wild-type embryo. (B) A higher magnification of the Ep cell. The arrow marks an apparent membrane tether. (C) A surface view of an Arp2/3 RNAi embryo. (D) A higher magnification of the Ea cell with blebs (arrowheads) and apparent inpockets of the surface in the center of the cell (arrow). (E) A mid-plane view of a wild-type embryo. (F) A higher magnification of the Ea cell. (G) A mid-plane view of an Arp2/3 RNAi embryo. Blebs (arrowheads) formed at free apical surfaces. (H) A higher magnification of the Ep cell. Membranes at cell-cell contacts appeared normal (arrows). Blebs (arrowheads) formed only at free apical surfaces (n=37 embryos). (I) Images of an embryo expressing GFP::MOE and PH:mCherry. For PH::mCherry, asterisks mark the membrane bleb. For GFP::MOE, asterisks mark when F-actin accumulated beneath the bleb. (J) A 45-second kymograph of the images in (I), showing individual markers and both markers merged. GFP::MOE was not enriched under the plasma membrane during bleb formation (red arrowhead). GFP::MOE then appeared enriched near the plasma membrane (green arrowhead) and the membrane retracted (yellow arrowheads).

defect of Arp2/3-depleted embryos. Severson et al. (2002) reported that terminally-arrested Arp2/3 RNAi embryos produced some endoderm, but whether this fate was established on time and in the appropriate cells was not examined. We analyzed the expression patterns of two fate markers that are expressed as gastrulation occurs: *end-1::*GFP, a marker for endodermal fate (Calvo et al., 2001), and *ceh-51::*GFP, a marker for MS lineage fate (Broitman-Maduro et al., 2009). In Arp2/3 RNAi embryos, *end-1::*GFP was expressed in the E lineage, as in wild-type (Figure 10A,B). Likewise, we observed *ceh-51::*GFP expression specifically in MS progeny when Arp2/3 function was knocked-down (Figure 10D,E). These results suggest that loss of Arp2/3 does not prevent timely E or MS cell fate specification.

One aspect of normal Ea/p cell fate is the introduction of a G2 phase to the cell cycle in Ea and Ep, delaying division of these cells until they become internalized (Edgar and McGhee, 1988). Because there is evidence that premature division of the Ea/p cells can prevent their internalization (Lee et al., 2006), we examined cell cycle timing after Arp2/3 depletion, measuring the time between Ea/p birth and Ea/p division. In wild-type embryos, Ea/p divided 43.6 ± 4.3 (mean ± s.d.) minutes after they were born (n=9). In Arp2/3-depleted embryos, Ea/p divided 49.2 ± 3.4 minutes after they were born (n=16). Therefore, Ea/p cells did not divide prematurely in Arp2/3-depleted embryos.

Arp2/3-depleted embryos exhibit normal apicobasal polarity

Ea/p cells are apicobasally polarized, with PAR-3 and PAR-6 enriched near apical surfaces and PAR-2 enriched near basolateral membranes (Etemad-Moghadam et al., 1995; Boyd et al., 1996; Hung and Kemphues, 1999; Nance and Priess, 2002). When PAR proteins are experimentally degraded in somatic cells before gastrulation, the Ea/p cells have internalization defects (Nance et al., 2003). The Arp2/3 complex has been implicated in vesicle trafficking

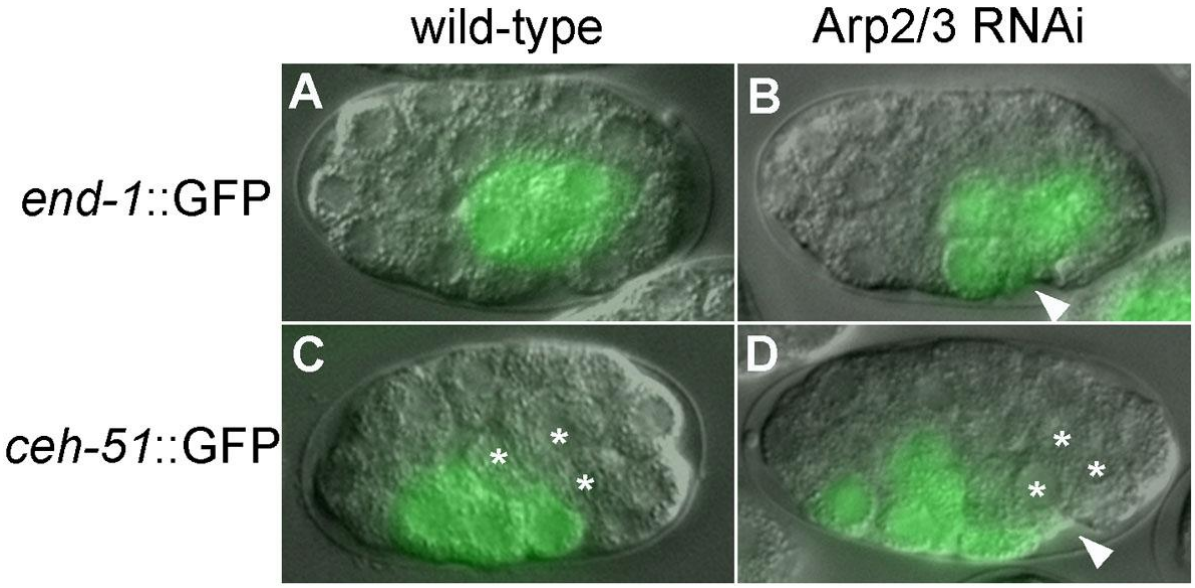
wild-type
Arp2/3 RNAi
A
B
C
D
end-1::GFP
ceh-51::GFP

Figure 10: Arp2/3 RNAi embryos express E and MS fate markers normally. (A, B) *end-1*::GFP, a marker for endodermal fate, was expressed normally in Arp2/3 RNAi embryos as the Ea/p cells divided on the surface (arrowhead, n=28/28). (C, D) *ceh-51*::GFP, a marker for MS cell fate appeared normal as Ea/p cells divided on the surface (n=19/19). 3 of the 4 Ea/p cell descendants are marked by asterisks, as the fourth cell was not in the same imaging plane.

(Fucini et al., 2002; Luna et al., 2002), which could affect apicobasal polarity and PAR protein localization. To determine whether cells in Arp2/3-depleted embryos were properly polarized, we examined the localization of PAR proteins. In Arp2/3 RNAi embryos, PAR-2::GFP localization was indistinguishable from that in wild-type (Figure 11A,B). When we examined the localization of the endogenous apical PAR protein PAR-3, we found that PAR-3 accumulated near the apical cell membranes of Arp2/3 RNAi embryos as in wild-type embryos (Figure 11C,D). Quantification of fluorescence levels across cells confirmed that protein localization profiles in wild-type and Arp2/3 RNAi were similar (Figure 11E). Apicobasal polarization of these PAR proteins in other cells appeared normal as well (Figure 11A-D). We conclude that the Arp2/3 complex is not required for apicobasal polarization of PAR protein distributions.

Apical accumulation and activation of myosin are normal in Arp2/3-depleted embryos

Apicobasally polarized Ea/p cells accumulate the tagged myosin heavy chain NMY-2::GFP at their apical surfaces (Nance and Priess, 2002). We examined NMY-2::GFP-expressing embryos (Nance et al., 2003) to determine whether apical myosin accumulation is affected in Arp2/3-depleted embryos. Wild-type NMY-2::GFP and Arp2/3 (RNAi); NMY-2::GFP embryos at the same stage were recorded side-by-side to facilitate quantification of protein levels in parallel (Figure 12). In both wild-type and Arp2/3-depleted embryos, NMY-2::GFP accumulated apically by ten minutes before MSa/p division (Figure 12A). As the apical surface profiles of the Ea/p cells decreased in length, the apical myosin accumulation could still be seen (Figure 12B,C). In Arp2/3 RNAi embryos, NMY-2::GFP was still enriched apically in the Ea/p cells as the Ea/p cells failed to internalize and instead divided on the surface of the embryo (Figure 12D). Kymographs of wild-type embryos confirmed that NMY-2::GFP was enriched on the apical surface of the Ea/p cells as this surface moved toward the interior of the embryo (Figure 12E). In

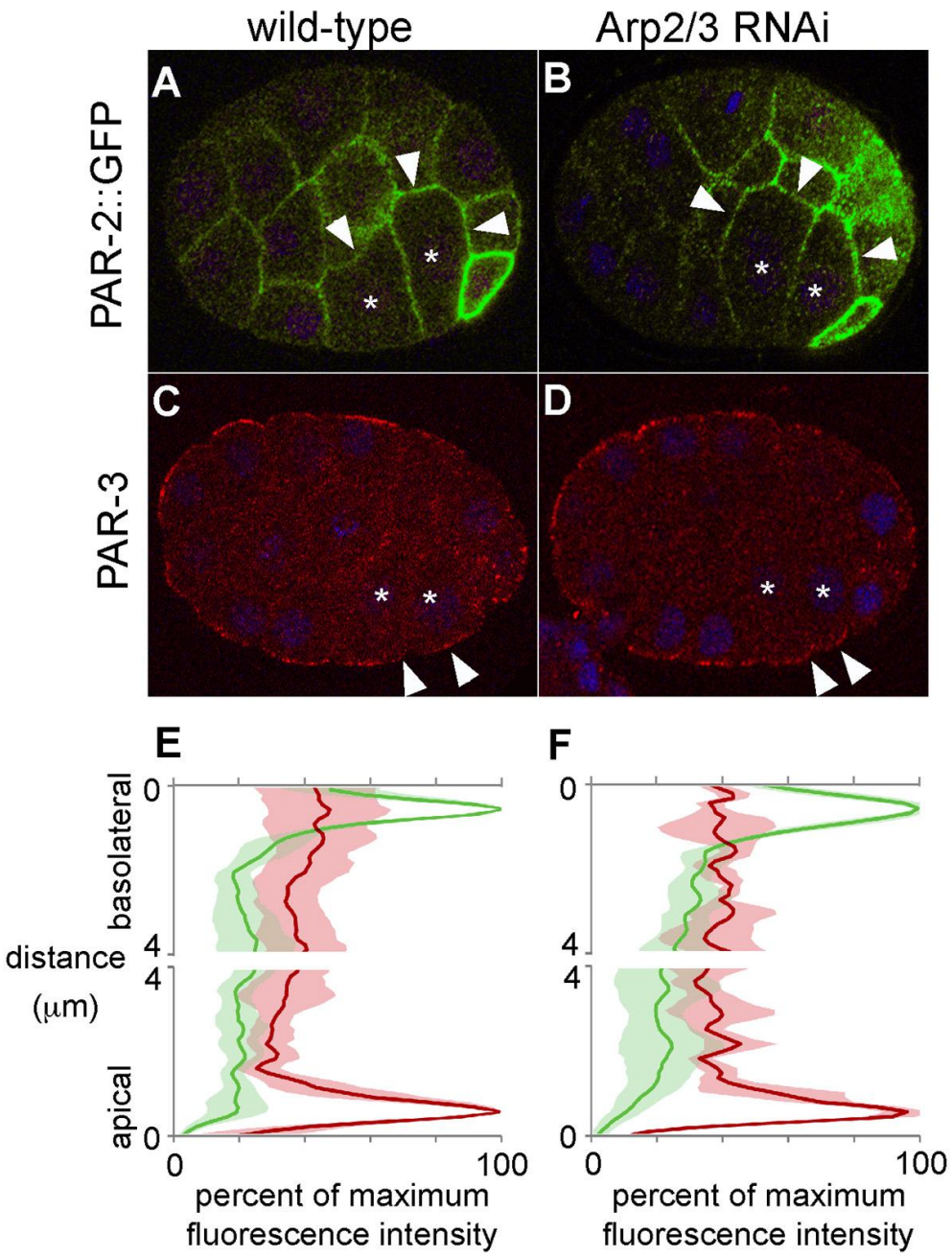
wild-type
Arp2/3 RNAi
A
B
C
D
PAR-2::GFP
PAR-3
E
F
basolateral
apical
distance (μm)
0
4
0
100
percent of maximum fluorescence intensity

Figure 11: Arp2/3-depleted embryos localize apical PAR-3 and basolateral PAR-2 proteins normally. (A,B) Fixed embryos at gastrulation stage immunostained for PAR-2::GFP. In wild-type (n=12/12) and in Arp2/3 RNAi embryos (n=12/12), PAR-2::GFP localized basolaterally (arrowheads). (C,D) Wild-type embryos (n=7) and Arp2/3 RNAi embryos (n=6/6) immunostained for endogenous PAR-3 showed apical accumulation in all cells, including Ea/p (arrowheads). (E) anti-PAR-3 (red, n=7) and PAR-2::GFP (green, n=6) fluorescence intensity levels quantified in wild-type and Arp2/3 RNAi Ea/p cells show peaks of fluorescence intensity at the apical and basolateral membrane, respectively. Shading indicates 95% confidence intervals.

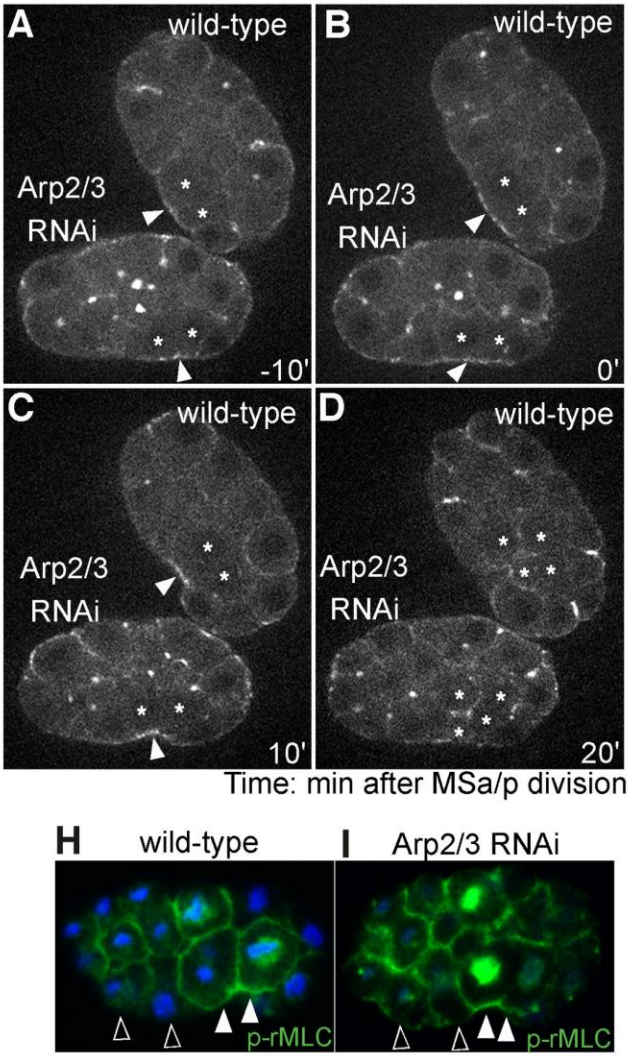
A
wild-type
Arp2/3
RNAi
-10'
B
wild-type
Arp2/3
RNAi
0'
C
wild-type
Arp2/3
RNAi
10'
D
wild-type
Arp2/3
RNAi
20'
Time: min after MSa/p division

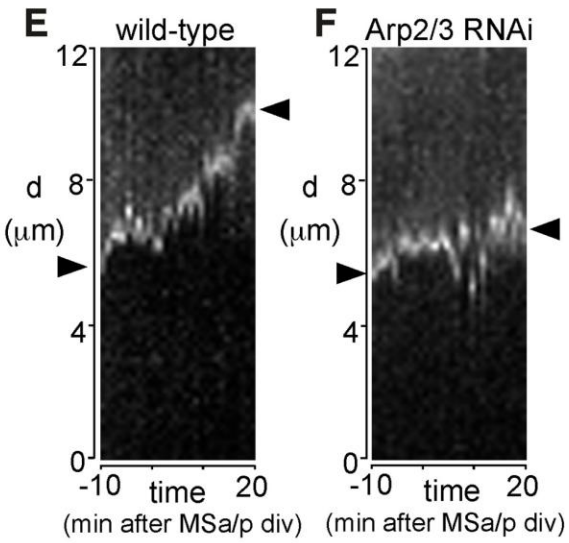
E
wild-type
F
Arp2/3 RNAi
12
d
(μm)
8
4
0
-10
time
20
(min after MSa/p div)

H
wild-type
I
Arp2/3 RNAi
p-rMLC
p-rMLC

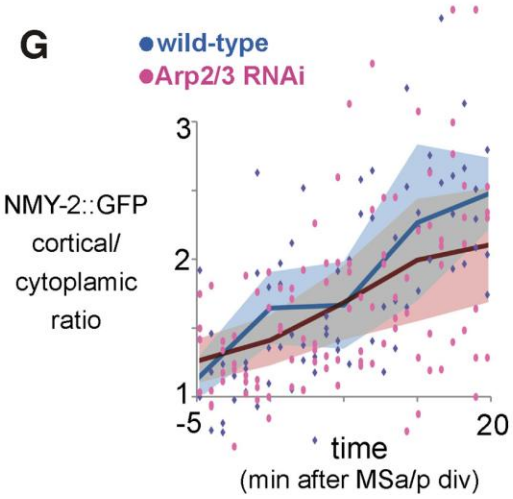
G
wild-type
Arp2/3 RNAi
NMY-2::GFP
cortical/
cytoplamic
ratio
3
2
1
-5
20
time
(min after MSa/p div)

Figure 12: Apical accumulation and activation of myosin is normal in Arp2/3-depleted embryos. (A-D) Wild-type and Arp2/3-depleted NMY-2::GFP embryos of the same age placed side-by-side show apical myosin accumulation (arrowheads). Arp2/3 RNAi embryos accumulated NMY-2::GFP apically in Ea/p (n=21/21 embryos). (E,F) Kymographs of the same embryos over 30 minutes. Arrowheads at the sides of the kymograph mark the initial and final position of the NMY-2::GFP-enriched apical cortex. d is distance in microns from an arbitrary point. (G) Graph of cortical to cytoplasmic ratios of NMY-2::GFP fluorescence intensities over time in wild-type and Arp2/3 RNAi embryos. All measurements from wild-type (n=3) and Arp2/3 RNAi embryos (n=4) were plotted and lines that represent the averages of 5-minute intervals were drawn. Shaded regions indicate 95% confidence intervals. (H,I) Wild-type embryos stained with p-rMLC antibody shows apical p-rMLC in Ea/p (white arrowheads) enriched compared to neighboring cells (black arrowheads) in both wild-type and Arp2/3 RNAi embryos. Nuclear staining is a background signal (Lee et al., 2006).

Arp2/3 RNAi embryos, NMY-2::GFP was enriched similarly near the apical surface as this surface failed to move toward the interior of the embryo (Figure 12F). We quantified cortical NMY-2::GFP levels and found that the cortical-to-central fluorescence intensity ratios rose as expected over time and were statistically indistinguishable between wild-type and Arp2/3-depleted embryos (Figure 12G). We conclude that apical myosin accumulates normally in Ea/p cells in Arp2/3-depleted embryos.

The apically-localized myosin in the Ea/p cells becomes activated by Wnt-dependent regulatory light chain phosphorylation as cell internalization begins (Lee et al., 2006). To determine if Arp2/3 is required to activate myosin II, wild-type and Arp2/3 RNAi embryos were immunostained with an antibody that recognizes the activated (serine-phosphorylated) form of myosin regulatory light chain (p-rMLC). We found that in Arp2/3 RNAi embryos, p-rMLC accumulated on the apical surfaces of the Ea/p cells more so than in other cells, as in wild-type (Figure 12H). These results suggest that apical myosin in Ea/p is activated normally in Arp2/3-depleted embryos.

Three of the six cells surrounding the Ea/p cells form dynamic, F-actin-rich structures

Because gastrulation failed in Arp2/3 embryos despite normal cell fates, cell cycle timings and cell polarity, and with myosin localized and activated normally, we pursued other possible roles for Arp2/3 during gastrulation. Phalloidin staining of fixed, wild-type embryos has not identified any specialized F-actin-rich structures such as filopodia or lamellipodia during gastrulation (Lee and Goldstein, 2003), but it is possible that fixation artifacts could have eliminated such structures. Therefore, we examined F-actin organization in living, wild-type embryos using GFP::MOE. As part of this analysis, embryos were placed on their ventral sides to image the ring of cells that fill the gap left by the internalizing Ea/p cells. This ring of cells is

composed of three of the four MS cell granddaughters (MSpp, MSpa, MSap, but not MSaa), two AB descendants (usually ABplpa and ABplpp), and the single germline precursor cell (P_4). Mid-plane imaging was used to determine the location of the Ea/p cells and neighboring cells. We then imaged at the ventral surface of each embryo where the neighboring cells border the internalizing Ea/p cells. We found that specific cells formed dynamic F-actin-rich structures at their apical borders with the Ea/p cells. Three of the six surrounding cells formed these structures, and tracing cell lineages revealed that these three cells were the three MS descendants that comprise half of the ring (Figure 13A,B). These F-actin-rich structures formed in the same places where flattened structures had been reported previously in fixed embryos by scanning electron microscopy (Nance and Priess, 2002) on the apical sides of MS granddaughter cells where they contacted internalizing Ea/p cells and not on other cells such as P_4 (Nance and Priess, 2002). For this reason, we now interpret the flattened processes first reported by Nance and Priess (2002) as F-actin-rich processes, and we show below that these processes are dynamic in living embryos. The AB descendants of the ring did not form similar F-actin-rich structures at their apical borders with the Ea/p cells (Figure 13A,B). We found similar flattened membrane processes on MSpp, MSpa, MSap in PH::mCherry embryos (Figure 13C). This and the previous SEM reports suggest that these processes are not artifacts of GFP::MOE expression.

We analyzed movies of GFP::MOE embryos to examine F-actin dynamics. F-actin accumulation at the apical sides of MS granddaughters (referred to as MSxx cells) where they contact Ea/p was highly dynamic, with enrichment appearing and disappearing multiple times during Ea/p internalization (Figure 13D-H). Kymographs of MOE::GFP in the MSxx cells confirmed F-actin enrichment and dynamic fluctuations of fluorescence intensity at the apical cell boundary with Ea/p cells (we refer to this as the front of the cell), and weaker and less

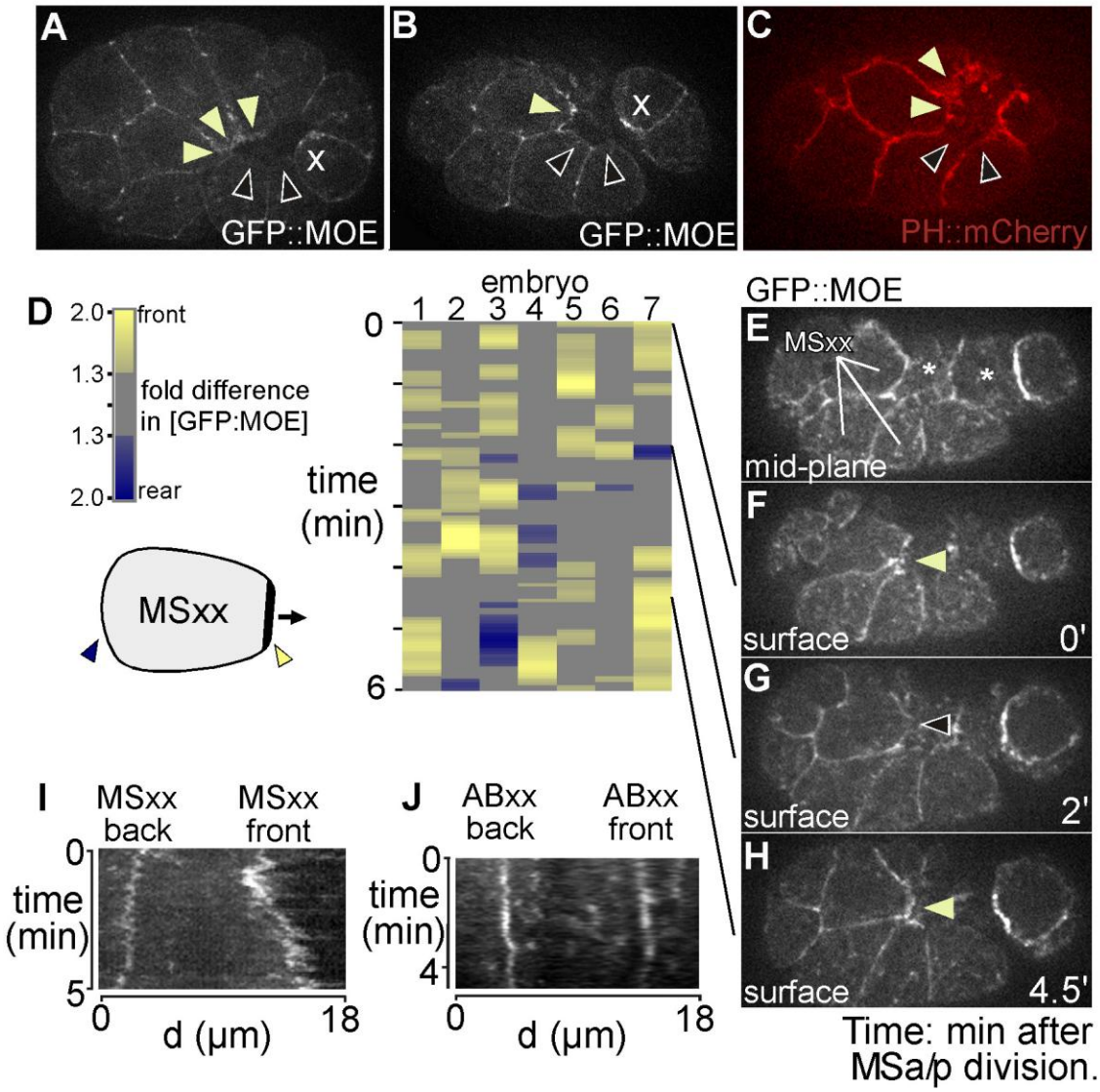
A
GFP::MOE
B
GFP::MOE
C
PH::mCherry
D
2.0
front
1.3
fold difference
in [GFP:MOE]
1.3
2.0
rear
MSxx
embryo
1 2 3 4 5 6 7
0
time
(min)
6
GFP::MOE
E
MSxx
mid-plane
F
surface
0'
G
surface
2'
H
surface
4.5'
Time: min after
MSa/p division.
I
MSxx
back
MSxx
front
0
time
(min)
5
0
d (μm)
18
J
ABxx
back
ABxx
front
0
time
(min)
4
0
d (μm)
18

Figure 13: Three of the six cells surrounding the Ea/p cells produce dynamic, F-actin-rich structures. (A-C) Embryos viewed from their ventral sides. (A,B) GFP::MOE expressing embryos. F-actin-rich structures (yellow arrowheads) formed at the borders of the MS descendants and the Ea/p cells. The AB descendants, ABplpa and ABplpp, did not form these F-actin-rich structures at their borders with the Ea/p cells (black arrowheads). F-actin enrichment at the P_4/Ep cell boundary is marked by an "x". (C) An embryo expressing PH::mCherry showing F-actin-rich processes specifically at the borders of MS descendants and the Ea/p cells and not at the borders of AB descendants and the Ea/p cells. (D) Heatmap representing GFP::MOE accumulation in seven individual embryos. Yellow and blue colors indicate GFP::MOE front to back end ratios above 1.3 fold difference. Front and back ends are defined with respect to direction of extension across the gap as indicated in the diagram. The preponderance of yellow in the resulting heatmap indicates frequent enrichment of GFP::MOE at the front end. (E-H) Representative images from a wild-type GFP::MOE embryo, embryo #7 of the heatmap. (E) Mid-plane view. Ea/p cells are marked by asterisks and the three MSxx cells are labelled. (F-H) GFP::MOE accumulated at the border of MSxx and the Ea/p cells at certain times (yellow arrowhead) and not at other times (black arrowhead). We did not observe GFP::MOE accumulation at the back end of MSxx cells in the imaging plane shown, nor in other planes. (I) Kymograph of a line across an MSxx cell of a GFP::MOE expressing embryo. The front end of MSxx has dynamic enrichment of GFP::MOE. (J) Kymograph of a line across an ABxx cell of a GFP::MOE expressing embryo. The front end of ABxx does not have dynamic GFP::MOE enrichment.

dynamic F-actin localization at the rear MSxx cell boundary (Figure 13I). The apical border between ABxx and Ea/p did not show similar F-actin enrichment (Figure 13J). We conclude that MSxx cells are polarized with respect to F-actin localization and dynamics, unlike the AB progeny that comprise parts of the same ring.

F-actin-rich regions were also present on the P_4 cell where it contacted Ep (Figure 13A-C). F-actin enrichment at the P_4-Ep border differs from that in MSxx cells in that it appears over multiple cell cycles at the borders between endodermal precursors and germline precursors, and it appears in a disc at the entire cell-cell contact region, rather than just at the apical side of this region (Goldstein, 2000).

The F-actin-rich extensions are dependent on the cell fate specification gene *pop-1*

Because F-actin-rich extensions formed specifically on MS granddaughter cells, and not on the other cells of the closing ring, we questioned whether the formation of these structures was dependent on MS cell fate. We transformed mesodermal cell fate using a *pop-1* mutant, in which MS cells are transformed into E cells (Lin et al., 1995). We confirmed the cell fate transformation by cell lineage analysis. In *pop-1* mutants, MSa/p cells divided with cell cycle timing similar to the Ea/p cells (Figure 14D,F). As the Ea/p cells internalized, the MS progeny also began to internalize (Figure 14F,G,J), and neighboring cells began to fill the gap left behind, although the gap was never completely filled (Figure 14J). We did not observe F-actin-rich structures where MS granddaughters contacted Ea/p cells, nor where neighboring cells contacted the internalizing MS cells (Figure 14L). We conclude that the formation of the F-actin-rich structures is dependent on the cell fate specification gene *pop-1*.

The F-actin-rich extensions that form on three MS granddaughter cells are Arp2/3- and PAR-3-dependent

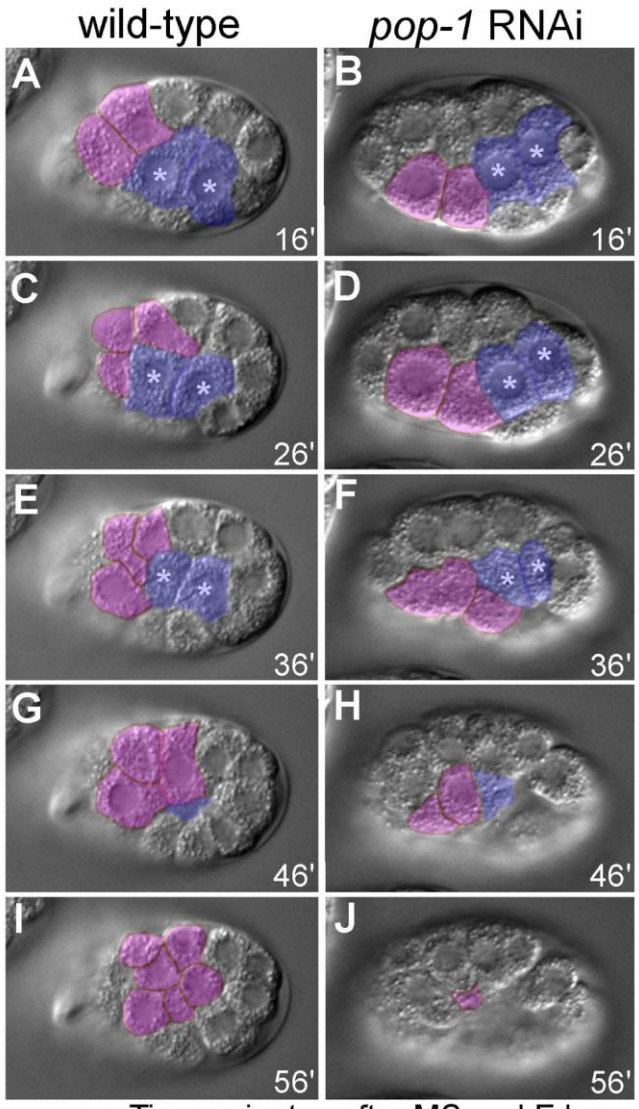
wild-type
pop-1 RNAi
A
B
16'
16'
C
D
26'
26'
E
F
36'
36'
G
H
46'
46'
I
J
56'
56'
Time: minutes after MS and E born.
K
L
MSx
mid-plane
surface

Figure 14: The formation of F-actin-rich extensions is cell fate dependent. Ventral views of embryo with MS descendants color-coded in pink, and E descendants color-coded in blue. Time is indicated as minutes after MS and E are born. (A,C,E,G,I) A wild-type embryo. (A) MSa/p cells have not yet divided, and Ea/p cells are still on the surface. (C,E) MSa/p cells divided and Ea/p cells internalization begins. Only 3 out of the 4 MS descendants are visible in the same plane. (G) By 46 minutes, Ea/p cells are covered by the MS descendants and other neighboring cells. (I) MS descendants have undergone another round of cell division on the surface of the embryo. (B,D,F,H,J) A *pop-1* mutant embryo to show the MS to E cell fate transformation (n=5/5). (D) At 26 minutes, MSa/p cells have not yet divided. (F) By 36 minutes, MSa/p cells begin to divide, but have already started internalizing with the Ea/p cells. (H) At 46 minutes, Ea/p cells and several of the MS descendants have internalized. (I) At 56 minutes, MS and E descendants have internalized, but the neighboring cells have not fully sealed the gap. (K) A mid-plane DIC image of a *pop-1* mutant embryo. MSx is labeled. (L) A surface view of the same *pop-1* depleted embryo expressing GFP::MOE to show the neighboring cell/MSx cell boundary (white arrowhead) and MSx/Ea cell boundary (black arrowhead).

Arp2/3 RNAi embryos have more convoluted membrane conformations specifically at their apical sides, where the plasma membrane bulges and detaches from the underlying cell cortex in blebs (Figure 9). Thus, we predicted that Arp2/3 depletion might interfere with the apical enrichment of F-actin in MS progeny. We analyzed F-actin distribution using GFP::MOE in Arp2/3 RNAi embryos, and observed convoluted membrane conformations as before (Figure 15A-E). Additionally, we found that the MSxx-specific F-actin-rich structures did not form where these cells border Ea (Figure 15B-D, F). Quantification of the front and back MSxx cell boundaries revealed that similar amounts of F-actin were frequently found at front and back ends of MSxx cells (Figure 15F), unlike the more commonly polarized distribution we observed in wild-type. We conclude that Arp2/3 is required, directly or indirectly, for these F-actin-rich structures to form.

The polarized distribution of F-actin to processes in an apical region of the MSxx cells suggested that formation of these processes might depend on apicobasal polarization of MSxx cells. To test whether PAR-based cell polarization is required for formation of the MSxx processes, we crossed GFP::MOE into *par-3 ZF1*, a *C. elegans* strain in which the apical protein PAR-3 becomes degraded in somatic cells after the one-cell stage (Nance et al., 2003). We found that the MS-specific F-actin-rich structures did not form (Figure 16A-F). Instead, the front and back MSxx cell boundaries appeared indistinguishable, each side with varying levels of GFP::MOE and without the apparent front end enrichment we observed in wild-type embryos. Analysis of ARX-5 localization in *par-3 ZF1* mutants revealed that ARX-5 localization was normal, suggesting, as expected, that PAR-3-dependent cell polarity is not required for Arp2/3 cortical localization (Figure 16G). We conclude that PAR-3 is required to form F-actin-rich structures on the apical sides of MSxx cells where they border the Ea/p cells. Together, these

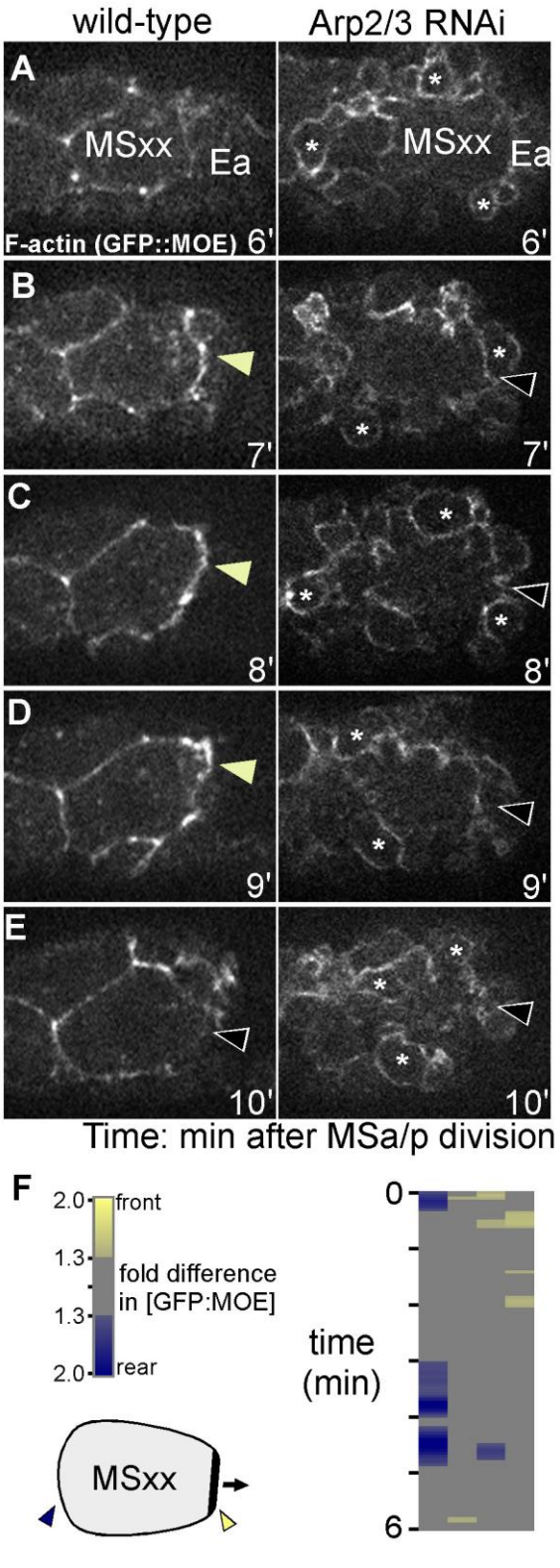
wild-type
Arp2/3 RNAi
A
MSxx
Ea
F-actin (GFP::MOE) 6'
6'
B
7'
7'
C
8'
8'
D
9'
9'
E
10'
10'
Time: min after MSa/p division
F
2.0
front
1.3
fold difference
in [GFP:MOE]
1.3
2.0
rear
MSxx
time
(min)
0
6

Figure 15: The formation of the MSxx specific F-actin-rich structures is Arp2/3 dependent

(A-E) Images from movies of wild-type and Arp2/3 RNAi embryos expressing GFP::MOE. Wild-type embryos formed F-actin-rich structures (yellow arrowheads), whereas Arp2/3 RNAi embryos cell membranes did not (black arrowheads) and instead formed membrane blebs (asterisks, n=6/6). (F) Quantification of GFP::MOE ratios at the front and back MSxx cell boundaries in four Arp2/3 RNAi embryos, with color-coded GFP::MOE ratios as in Fig. 6. The preponderance of gray indicates that ratios are frequently similar in Arp2/3 RNAi embryos.

F-actin (GFP::MOE); *par-3*

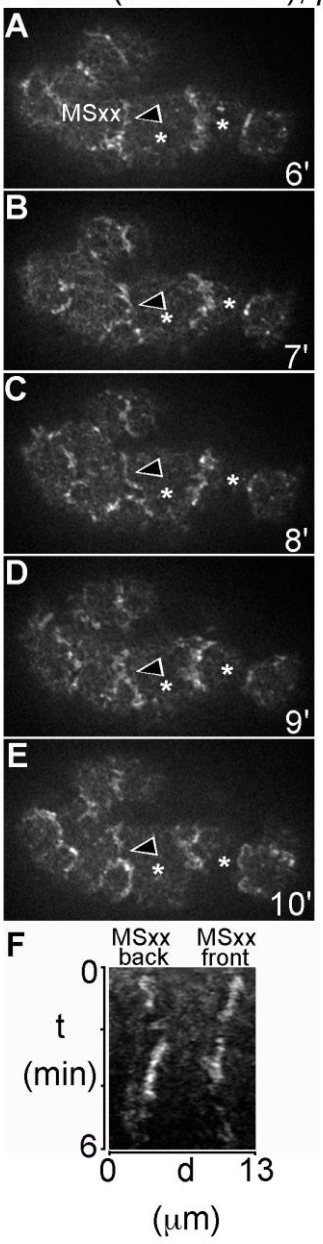

Time: min after MSa/p division

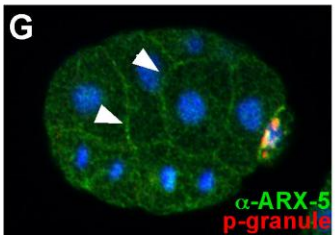

Figure 16: The formation of MS-specific F-actin-rich structures requires the apical PAR protein PAR-3. (A-E) Images from a movie of *par-3 ZF1*; GFP::MOE. An MSxx cell is labeled, and the Ea/p cells are marked by asterisks. Ea/p cells remained in the plane of imaging as expected from an internalization defect reported in *par-3* mutant embryos (Nance and Priess, 2002). An arrowhead marks a boundary between MSxx and Ea cells. F-actin-rich structures did not form here in *par-3 ZF1* (n=7/7). (F) Kymograph of a line across MSxx. The kymograph shows that the MSxx front cell boundary did not transiently accumulate GFP::MOE above levels seen at the back end. (G) Cortical ARX-5 localization (arrowheads) in a *par-3 ZF1* mutant embryo.

results indicate that the dynamic, F-actin-rich structures depend directly or indirectly on Arp2/3 for their formation, as well as on cell polarity and cell fate proteins.

Discussion

We have found that wild-type embryos form dynamic, F-actin-rich structures specifically on mesodermal precursor cells during Ea/p cell internalization. These structures form transiently at the apical borders of MSap, MSpa and MSpp where they contact the internalizing Ea/p cells -- sites consistent with where cell flattenings had been seen previously by SEM (Nance and Priess, 2002) (Figure 17). In Arp2/3-depleted embryos, cell fates, apicobasal cell polarity, myosin localization and myosin activation appeared normal, but plasma membrane association with the cell cortex was perturbed, and the F-actin-rich structures on MSxx cells were absent. Together with previous results (Severson et al., 2002), we conclude that Arp2/3 is required for completion of endoderm internalization in *C. elegans*. We speculate that the F-actin-rich structures lost in Arp2/3-depleted embryos might contribute to completion of gastrulation. Below we discuss this possibility and alternatives. We also discuss roles for such structures in other systems.

The F-actin-rich structures we observed might be specializations for cell crawling, although we have not been able to directly test this hypothesis. Cell surface labeling experiments during gastrulation suggest that these cells do not exhibit surface retrograde flow, as crawling cells often do (Lee and Goldstein, 2003). Furthermore, when MSxx cells were removed and reassociated with Ea/p cells in various orientations, MSxx cells still moved in a direction consistent with the hypothesis that Ea/p apical constriction drives the movement of the MSxx cells, suggesting that MSxx cell polarity is not important for the bulk of MSxx cell movement

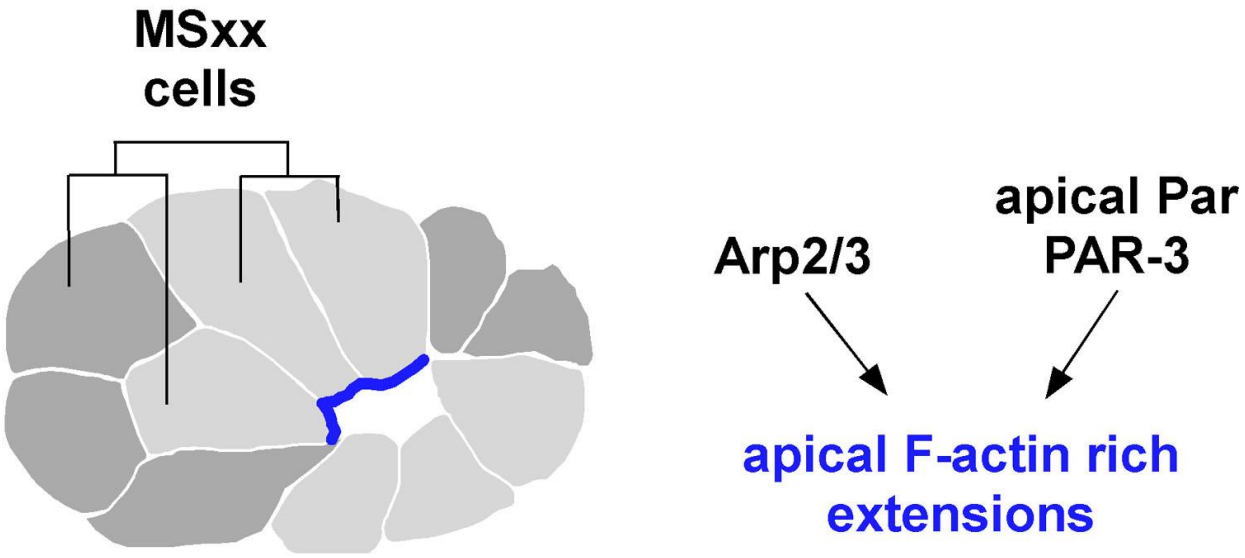
MSxx
cells
Arp2/3
apical Par
PAR-3
apical F-actin rich
extensions

Figure 17: Dynamic, MSxx-specific, F-actin-rich extensions require Arp2/3 and apical PAR protein. Six cells converge in a ring (light grey), filling in the space left by the internalizing E cells (white gap in middle). Three of these cells are MS descendants. F-actin-rich structures formed in MSxx cells that contacted Ea/p cells, at their apical sites of contact (blue). These structures were absent in embryos deficient in either Arp2/3 or the apical marker *par-3*.

(Lee and Goldstein, 2003). However, it is possible that the MSxx cells are motile without surface retrograde flow. There is evidence that some cells can produce lamellipodial protrusions and move by rolling, without retrograde flow (Anderson et al., 1996). Additionally, although the cell manipulation experiments suggest that MSxx cell crawling is not a significant component of normal MSxx cell movement, it is possible that reoriented cells become re-polarized upon reassociation. Therefore, we do not yet know if the F-actin-rich structures are specializations for cell motility. There are a number of precedents for the formation of F-actin-rich structures in cells during morphogenesis. For example, F-actin-rich filopodial extensions form during *C. elegans* ventral enclosure (Williams-Masson et al., 1997). In addition to proposed roles for filopodia in cell motility during ventral enclosure, these actin-rich fingers may play a role in cell-cell adhesion (Raich et al., 1999). In a process termed "filopodial priming", α-catenin is rapidly recruited at sites where contralateral filopodial tips first make contact. This recruitment is thought to allow for rapid cell-cell adhesion as the epithelium seals on the ventral side. Our experiments suggest that proper cell fate is required for the formation of these F-actin-rich structures. Interestingly, while the transformation of MS cells to E cells resulted in the internalization of both groups of cells, we did not observe the formation of F-actin-rich structures on the border of MS and E cells. However, we also never observed complete internalization of Ea/p cells. Whether the F-actin-rich processes on the MSxx cells function similarly to how they function in ventral enclosure to seal the ventral opening during gastrulation is not yet known. However, it is possible that the extensions may function in sealing a gap given the localization of the extensions, on one side of a closing gap.

The combination of actomyosin contractility in internalizing cells with F-actin nucleation in their neighbors in *C. elegans* gastrulation is similar to what is observed in zebrafish

gastrulation (Lai et al., 2008). In this system, Rho signaling regulates actomyosin contractility and neighboring cell migration, controlling cell movements during epiboly and convergent extension. A diaphanous-related formin is required for filopodial-like processes to form in marginal deep cells. Perhaps Arp2/3 is acting redundantly with other actin nucleating proteins in *C. elegans*. If *C. elegans* Arp2/3 were depleted together with other F-actin regulating proteins, such as formins, further defects might occur during Ea/p cell internalization. However, the formins play a role in cytokinesis throughout earlier embryogenesis (Swan et al., 1998), precluding us from carrying out simple double knockdown experiments.

In Arp2/3 RNAi embryos, the F-actin-rich structures that we have detailed do not form. Our Arp2/3 immunostaining studies indicate that Arp2/3 localizes to the cell cortex at the time of Ea/p cell internalization, including at the boundary between MSxx cells and the Ea cell. However, whether the absence of the F-actin structures in Arp2/3 RNAi embryos is due to a direct role for Arp2/3 in the formation of these structures, or whether it is a secondary effect of plasma membrane dissociation from the cell cortex as in blebs, is currently unknown. The Ea/p cell internalization defect seen in Arp2/3 RNAi embryos could also be due in part to defective actin organization in the apically constricting Ea/p cells, independent of Arp2/3's role in the MS cells. Myosin II remains apically localized and activated in Arp2/3 RNAi embryos, but the architecture of the actin network in the apical cortex of the Ea/p cells might be disorganized in ways that are not obvious at the resolution limit of the confocal or spinning disk confocal imaging used (estimated to be about 200nm). Such disorganization could affect the ability of myosin II to contract the apical actin network.

Because the F-actin-rich extensions we observed formed only on MS-derived cells and not on other members of the ring of six cells, and because they formed only on the three MS-

derived cells that contacted Ea/p, we speculate that the structures might be induced in MS progeny by signals or physical cues from Ea/p. Our observation that the apical protein PAR-3 is required for the formation of MSxx-specific extensions suggests that apicobasal cell polarity has a role, either direct or indirect, in spatially regulating F-actin distribution. We do not know whether the absence of MSxx extensions reflects a role for PAR-3 in the Ea/p cells, in the MSxx cells or both. Apicobasal polarity in the Ea/p cells could be important for the Ea/p cells to produce a hypothetical signal to the MSxx cells to form the extensions. The formation of the extensions could also require the normal behavior of internalizing Ea/p cells to produce an effective physical cue. We found that Arp2/3 cortical localization was preserved in *par-3 ZF1* mutants. This was expected given that actin localization as observed by GFP::MOE was also cortical. We also found that Arp2/3 localized to the boundary between MS granddaughters and Ea/p cells in *par-3 ZF1* mutants, although F-actin-rich structures did not form. This suggests that Arp2/3 localization is not sufficient to induce the formation of the extensions, and it provides further evidence that the lack of F-actin-rich extensions in Arp2/3-depleted embryos may be an indirect effect of actin architecture misregulation, and perhaps a result of loss of cortical integrity.

We have shown that the blebs observed in Arp2/3 RNAi embryos (Severson et al., 2002) involve plasma membrane dissociation from the cell cortex. During bleb formation, the plasma membrane protruded without an F-actin-rich cortex. Once bleb growth stopped, GFP::MOE assembled underneath the plasma membrane at the bleb, and the bleb retracted. These dynamics are similar to what have been seen in human cell lines (Charras et al., 2006). However, there are some differences. In human cells, membrane blebs expanded for 5-7 seconds, and remained in a fully expanded state for about 30 seconds. Once F-actin and other contractile machinery

assembled under the membrane blebs, retraction occurred slowly, over the course of one minute (Charras et al., 2006). In Arp2/3 RNAi *C. elegans* embryos, the blebs appeared and disappeared all within 30 seconds, and the rate of retraction did not appear to be slower than the rate of expansion. We do not know if these differences in dynamics reflect differences between systems or differences between normal and Arp2/3-deficient bleb formation. In human cells, membrane blebs can form as a result of detachment of the membrane from the cytoskeleton (Charras et al., 2006). However, ruptures in the cell cortex can also lead to dissociation of the membrane with the cortex, and the flow of cytoplasm into the area results in formation of a membrane bleb (Paluch et al., 2005; Paluch et al., 2006; Sheetz and Dai, 1996). Since Arp2/3 is a major actin regulator, it is likely that the membrane blebs that form in Arp2/3-depleted embryos are a result of loss of microfilament density and the formation of ruptures in the cortex. Indeed, we see little F-actin beneath growing blebs (Fig 9I,J).

Given the pronounced blebbing at free surfaces in Arp2/3 RNAi embryos, we were surprised that many features of the Ea/p cells were normal. Our results suggest that cell fate, PAR protein localization, and myosin localization and activation are not affected by any global changes of the actin cytoskeleton that occur in the absence of Arp2/3, including formation of membrane blebs. The normal apicobasal polarization we observed of PAR proteins and myosin II suggests that any role that Arp2/3 might play in vesicle trafficking in this system must not be essential to regulate localization of these proteins. It is possible that PAR proteins and myosin II are localized by other mechanisms, or that may be localized by Arp2/3-independent vesicle trafficking.

Arp2/3's most well-characterized role is as a regulator of the branched actin network in migrating epithelial cells and growth cones in culture (Pollard, 2007). Additionally, Arp2/3 has

been shown to play many roles during morphogenesis, mostly ascribable to Arp2/3's role in regulating actin architecture (Vartiainen and Machesky, 2004). However, almost all of Arp2/3's previously described roles in morphogenesis were in non-moving cells. Therefore, we sought to bridge what is known about Arp2/3 in tissue culture studies with morphogenesis in developmental systems, to establish roles for Arp2/3 in moving cells during morphogenesis. Our results identify specific cellular roles for Arp2/3 in an embryo during morphogenesis. The results also add a layer to our pre-existing model of *C. elegans* gastrulation. In addition to apical constriction, internalization of the endoderm may involve dynamic, Arp2/3-dependent, F-actin-rich extensions on one side of a closing ring of cells.

Materials and Methods

Strains and Worm Maintenance

Nematodes were cultured and handled as described (Brenner, 1974). Unless indicated, experiments were performed with the wild-type N2 (Bristol) strain. The following mutant and reporter strains were used: KK866 GFP::PAR-2, JJ1473 *unc-119 (ed3)* III; *zuIs45* [*nmy-2*::NMY-2::GFP; *unc-119 (+)*]; referred to here as NMY-2::GFP, JJ1317 *zuIs3* [*end-1*::GFP], OD70 *ItIs44* [*pie-1*::PH domain of PLCγ::mCherry] (PH::mCherry) (Kachur et al., 2008), PF100 *nnIs* [*unc-119(+) pie-1* promoter::*gfp*::Dm-moesin$^{437–578}$ (amino acids 437–578 of D. melanogaster Moesin)] (GFP::MOE) , *unc-32(e189) par-3(it71); zuIs20*(*par-3*::PAR-3;ZF1-GFP) (PAR-3-ZF1) (a gift from Jeremy Nance), LP53 PH::mCherry; GFP::MOE, MS632 *unc-119(ed4)* III; *irIs39* [*ced-51*::NLS::GFP] (Broitman-Maduro et al., 2009), LP54 PH::mCherry; NMY-2::GFP. LP53 and LP54 were constructed by crossing OD70 PH::mCherry males with

PF100 GFP::MOE or JJ1473 NMY-2::GFP hermaphrodites, respectively. All strains were maintained at 20°C, except for the following strains: KK866 PAR-2::GFP, PF100 GFP::MOE, JJ1473 NMY-2::GFP, LP53 PH::mCherry; GFP::MOE, and LP54 PH::mCherry; NMY-2::GFP were maintained at 24°C. Imaging was performed at 20°C–23°C for all strains.

DIC and Confocal Time-Lapse Microscopy

Embryos were mounted and DIC images were acquired as described (McCarthy Campbell et al., 2009). Time-lapse images were acquired at 1 μm optical sections every 1 minute and analyzed with Metamorph software (Molecular Devices). Gastrulation was scored by examination of whether the Ea and Ep cells were completely surrounded by neighboring cells in three dimensions at the time that Ea and Ep divided. If Ea and Ep divided before being completely surrounded, we scored gastrulation as having failed. For measuring apical membranes, the length of the ventral surface was measured in the optical section in which this length was greatest, from the Ea-Ep ventral border to both the Ep-P_4 ventral border and the Ea-MSxx ventral border. Spinning disk confocal images were acquired and processed as described (Lee et al., 2006). To observe the apical boundaries of Ea/p cells during internalization, we filmed the ventral surface of PH::mCherry embryos. Three 2-micron steps were taken every 5 seconds to capture the entire apical surface of the Ea/p cell. To analyze GFP::MOE dynamics, a single plane was acquired every 5 seconds once MSxx cells were born.

RNA Interference (RNAi)

RNAi by injection was performed according to a standard protocol (Dudley et al., 2002), except that a cDNA preparation was used as template to PCR *arx* genes. *arx-1/Arp3* and *arx-2/Arp2* specific primers were used to amplify the entire open reading frame (approximately 1kb).

Double-stranded RNA was injected at a concentration of 100 ng/ml. Embryos were analyzed 22-25 hours later.

Analysis of NMY-2::GFP Accumulation

NMY-2::GFP and Arp2/3 (RNAi); NMY-2::GFP embryos were imaged on a spinning disk confocal microscope as above. Images were captured once each minute after MSa/p division. To analyze NMY-2::GFP levels, a line was first drawn perpendicular to the Ea/p cell cortex. With Metamorph software, these lines were converted into kymographs of maximum pixel intensity over time. NMY-2::GFP levels were quantified by calculating the ratio of cortical to cytoplasmic fluorescence intensities (pixel intensity levels above off-embryo background).

Analysis of Cortical Blebs

GFP::MOE; PH::mCherry embryos were imaged on a spinning disk confocal microscope as above. Single plane images for each of GFP::MOE and PH::mCherry were taken every 3 seconds. Perpendicular linescans were drawn through the membrane blebs with Metamorph software and converted to kymographs.

Analysis of GFP::MOE Distribution

GFP::MOE, Arp2/3 (RNAi); GFP::MOE, and *par-3* ZF1; GFP::MOE embryos were imaged on their ventral surfaces on a spinning disk confocal microscope as above. Images were captured once every three seconds generally starting six minutes after MSa/p cell division. To analyze GFP::MOE levels, a three by three pixel low pass filter was applied, and a line was then drawn along the long axis of each MSxx cell. Lines were converted into kymographs of maximum pixel intensity over time using Metamorph. Linescans along the front and rear MSxx cell boundaries in the kymograph were plotted, and ratios of the GFP::MOE fluorescence intensity between the cell boundaries were determined. These ratios were converted to 5-

timepoint running average heatmaps with colors representing a two-fold higher (yellow) or two-fold lower (blue) difference in GFP::MOE concentration at the front cell boundary as compared to the back using a custom-written BASIC program. Rare ratios beyond two-fold were represented as two-fold.

Immunostaining and Confocal Microscopy

ARX-5 polyclonal antibodies were generated from rabbits expressing the polypeptide KFDTELKVLPLGNTNMGKLPIRTNFKGPAPQTNQDDIIDEALTYFKPNIFFREFEIKGPAD RTMIYLIFYITECLRKLQKSPNKIAGQKDLHALALSHLL (Strategic Diagnostics, Inc). Antiserum was affinity purified to an endpoint titer of 0.35 ng/mL. Immunostaining of embryos for p-rMLC (Abcam) was performed according to previously described protocols (Lee et al., 2006; Marston et al., 2008). Immunostaining embryos for α-GFP (for PAR-2::GFP) (1:100, Invitrogen), α-PAR-3 (1:100, Developmental Studies Hybridoma Bank), α-ARX-5 (1:1000, Strategic Diagnostic, Inc.), and OIC1D4 for P granules (1:200, Developmental Studies Hybridoma Bank) was performed as described (Tenlen et al., 2008). PAR-2::GFP and anti-PAR-3 fluorescence intensity were measured by recording linescans across the Ea/p cell apical and basolateral membranes using Metamorph software. For PAR-3, the Ea/p cell basolateral membrane was identified by determining the localization border of an E-cell specific marker, *end-1*::GFP. Levels were calculated as three-pixel running averages in each embryo, and apical and basolateral peaks were used to align measurements between embryos.

References

Anderson, K. I., Wang, Y. L. and Small, J. V. (1996). Coordination of protrusion and translocation of the keratocyte involves rolling of the cell body. *J Cell Biol* 134, 1209-18.

Boyd, L., Guo, S., Levitan, D., Stinchcomb, D. T. and Kemphues, K. J. (1996). PAR-2 is asymmetrically distributed and promotes association of P granules and PAR-1 with the cortex in C. elegans embryos. *Development* 122, 3075-84.

Brenner, S. (1974). The genetics of Caenorhabditis elegans. *Genetics* 77, 71-94.

Broitman-Maduro, G., Owraghi, M., Hung, W. W., Kuntz, S., Sternberg, P. W. and Maduro, M. F. (2009). The NK-2 class homeodomain factor CEH-51 and the T-box factor TBX-35 have overlapping function in C. elegans mesoderm development. *Development* 136, 2735-46.

Calvo, D., Victor, M., Gay, F., Sui, G., Luke, M. P., Dufourcq, P., Wen, G., Maduro, M., Rothman, J. and Shi, Y. (2001). A POP-1 repressor complex restricts inappropriate cell type-specific gene transcription during Caenorhabditis elegans embryogenesis. *Embo J* 20, 7197-208.

Charras, G. T., Hu, C. K., Coughlin, M. and Mitchison, T. J. (2006). Reassembly of contractile actin cortex in cell blebs. *J Cell Biol* 175, 477-90.

Cunningham, C. C. (1995). Actin polymerization and intracellular solvent flow in cell surface blebbing. *J Cell Biol* 129, 1589-99.

Dudley, N. R., Labbe, J. C. and Goldstein, B. (2002). Using RNA interference to identify genes required for RNA interference. *Proc Natl Acad Sci U S A* 99, 4191-6.

Edgar, L. G. and McGhee, J. D. (1988). DNA synthesis and the control of embryonic gene expression in C. elegans. *Cell* 53, 589-99.

Edwards, K. A., Demsky, M., Montague, R. A., Weymouth, N. and Kiehart, D. P. (1997). GFP-moesin illuminates actin cytoskeleton dynamics in living tissue and demonstrates cell shape changes during morphogenesis in Drosophila. *Dev Biol* 191, 103-17.

Etemad-Moghadam, B., Guo, S. and Kemphues, K. J. (1995). Asymmetrically distributed PAR-3 protein contributes to cell polarity and spindle alignment in early C. elegans embryos. *Cell* 83, 743-52.

Fucini, R. V., Chen, J. L., Sharma, C., Kessels, M. M. and Stamnes, M. (2002). Golgi vesicle proteins are linked to the assembly of an actin complex defined by mAbp1. *Mol Biol Cell* 13, 621-31.

Galletta, B. J. and Cooper, J. A. (2009). Actin and endocytosis: mechanisms and phylogeny. *Curr Opin Cell Biol* 21, 20-7.

Georgiou, M., Marinari, E., Burden, J. and Baum, B. (2008). Cdc42, Par6, and aPKC regulate Arp2/3-mediated endocytosis to control local adherens junction stability. *Curr Biol* 18, 1631-8.

Goldstein, B. (2000). When cells tell their neighbors which direction to divide. *Dev Dyn* 218, 23-9.

Goldstein, B. and Macara, I. G. (2007). The PAR proteins: fundamental players in animal cell polarization. *Dev Cell* 13, 609-22.

Guerriero, C. J., Weixel, K. M., Bruns, J. R. and Weisz, O. A. (2006). Phosphatidylinositol 5-kinase stimulates apical biosynthetic delivery via an Arp2/3-dependent mechanism. *J Biol Chem* 281, 15376-84.

Hudson, A. M. and Cooley, L. (2002). A subset of dynamic actin rearrangements in Drosophila requires the Arp2/3 complex. *J Cell Biol* 156, 677-87.

Hung, T. J. and Kemphues, K. J. (1999). PAR-6 is a conserved PDZ domain-containing protein that colocalizes with PAR-3 in Caenorhabditis elegans embryos. *Development* 126, 127-35.

Kachur, T. M., Audhya, A. and Pilgrim, D. B. (2008). UNC-45 is required for NMY-2 contractile function in early embryonic polarity establishment and germline cellularization in C. elegans. *Dev Biol* 314, 287-99.

Kovacs, E. M. and Yap, A. S. (2002). The web and the rock: cell adhesion and the ARP2/3 complex. *Dev Cell* 3, 760-1.

Lai, S. L., Chan, T. H., Lin, M. J., Huang, W. P., Lou, S. W. and Lee, S. J. (2008). Diaphanous-related formin 2 and profilin I are required for gastrulation cell movements. *PLoS One* 3, e3439.

Le Clainche, C. and Carlier, M. F. (2008). Regulation of actin assembly associated with protrusion and adhesion in cell migration. *Physiol Rev* 88, 489-513.

Lee, J. Y. and Goldstein, B. (2003). Mechanisms of cell positioning during C. elegans gastrulation. *Development* 130, 307-20.

Lee, J. Y., Marston, D. J., Walston, T., Hardin, J., Halberstadt, A. and Goldstein, B. (2006). Wnt/Frizzled signaling controls C. elegans gastrulation by activating actomyosin contractility. *Curr Biol* 16, 1986-97.

Lin, R., Thompson, S. and Priess, J. R. (1995). pop-1 encodes an HMG box protein required for the specification of a mesoderm precursor in early C. elegans embryos. *Cell* 83, 599-609.

Luna, A., Matas, O. B., Martinez-Menarguez, J. A., Mato, E., Duran, J. M., Ballesta, J., Way, M. and Egea, G. (2002). Regulation of protein transport from the Golgi complex to the endoplasmic reticulum by CDC42 and N-WASP. *Mol Biol Cell* 13, 866-79.

Maduro, M. F., Hill, R. J., Heid, P. J., Newman-Smith, E. D., Zhu, J., Priess, J. R. and Rothman, J. H. (2005). Genetic redundancy in endoderm specification within the genus Caenorhabditis. *Dev Biol* 284, 509-22.

Marston, D. J., Roh, M., Mikels, A. J., Nusse, R. and Goldstein, B. (2008). Wnt signaling during Caenorhabditis elegans embryonic development. *Methods Mol Biol* 469, 103-11.

Massarwa, R., Carmon, S., Shilo, B. Z. and Schejter, E. D. (2007). WIP/WASp-based actin-polymerization machinery is essential for myoblast fusion in Drosophila. *Dev Cell* 12, 557-69.

Mathur, J. (2005). The ARP2/3 complex: giving plant cells a leading edge. *Bioessays* 27, 377-87.

May, R. C., Caron, E., Hall, A. and Machesky, L. M. (2000). Involvement of the Arp2/3 complex in phagocytosis mediated by FcgammaR or CR3. *Nat Cell Biol* 2, 246-8.

McCarthy Campbell, E. K., Werts, A. D. and Goldstein, B. (2009). A cell cycle timer for asymmetric spindle positioning. *PLoS Biol* 7, e1000088.

Motegi, F., Velarde, N. V., Piano, F. and Sugimoto, A. (2006). Two phases of astral microtubule activity during cytokinesis in C. elegans embryos. *Dev Cell* 10, 509-20.

Mullins, R. D., Stafford, W. F. and Pollard, T. D. (1997). Structure, subunit topology, and actin-binding activity of the Arp2/3 complex from Acanthamoeba. *J Cell Biol* 136, 331-43.

Nance, J., Munro, E. M. and Priess, J. R. (2003). C. elegans PAR-3 and PAR-6 are required for apicobasal asymmetries associated with cell adhesion and gastrulation. *Development* 130, 5339-50.

Nance, J. and Priess, J. R. (2002). Cell polarity and gastrulation in C. elegans. *Development* 129, 387-97.

Paluch, E., Piel, M., Prost, J., Bornens, M. and Sykes, C. (2005). Cortical actomyosin breakage triggers shape oscillations in cells and cell fragments. *Biophys J* 89, 724-33.

Paluch, E., Sykes, C., Prost, J. and Bornens, M. (2006). Dynamic modes of the cortical actomyosin gel during cell locomotion and division. *Trends Cell Biol* 16, 5-10.

Patel, F. B., Bernadskaya, Y. Y., Chen, E., Jobanputra, A., Pooladi, Z., Freeman, K. L., Gally, C., Mohler, W. A. and Soto, M. C. (2008). The WAVE/SCAR complex promotes polarized cell movements and actin enrichment in epithelia during C. elegans embryogenesis. *Dev Biol* 324, 297-309.

Pollard, T. D. (2007). Regulation of actin filament assembly by Arp2/3 complex and formins. *Annu Rev Biophys Biomol Struct* 36, 451-77.

Pollard, T. D. and Borisy, G. G. (2003). Cellular motility driven by assembly and disassembly of actin filaments. *Cell* 112, 453-65.

Raich, W. B., Agbunag, C. and Hardin, J. (1999). Rapid epithelial-sheet sealing in the Caenorhabditis elegans embryo requires cadherin-dependent filopodial priming. *Curr Biol* 9, 1139-46.

Rouiller, I., Xu, X. P., Amann, K. J., Egile, C., Nickell, S., Nicastro, D., Li, R., Pollard, T. D., Volkmann, N. and Hanein, D. (2008). The structural basis of actin filament branching by the Arp2/3 complex. *J Cell Biol* 180, 887-95.

Sawa, M., Suetsugu, S., Sugimoto, A., Miki, H., Yamamoto, M. and Takenawa, T. (2003). Essential role of the C. elegans Arp2/3 complex in cell migration during ventral enclosure. *J Cell Sci* 116, 1505-18.

Schmidt, K. L., Marcus-Gueret, N., Adeleye, A., Webber, J., Baillie, D. and Stringham, E. G. (2009). The cell migration molecule UNC-53/NAV2 is linked to the ARP2/3 complex by ABI-1. *Development* 136, 563-74.

Severson, A. F., Baillie, D. L. and Bowerman, B. (2002). A Formin Homology protein and a profilin are required for cytokinesis and Arp2/3-independent assembly of cortical microfilaments in C. elegans. *Curr Biol* 12, 2066-75.

Sheetz, M. P. and Dai, J. (1996). Modulation of membrane dynamics and cell motility by membrane tension. *Trends Cell Biol* 6, 85-9.

Somogyi, K. and Rorth, P. (2004). Cortactin modulates cell migration and ring canal morphogenesis during Drosophila oogenesis. *Mech Dev* 121, 57-64.

Stevenson, V., Hudson, A., Cooley, L. and Theurkauf, W. E. (2002). Arp2/3-dependent pseudocleavage [correction of psuedocleavage] furrow assembly in syncytial Drosophila embryos. *Curr Biol* 12, 705-11.

Svitkina, T. M. and Borisy, G. G. (1999). Arp2/3 complex and actin depolymerizing factor/cofilin in dendritic organization and treadmilling of actin filament array in lamellipodia. *J Cell Biol* 145, 1009-26.

Swan, K. A., Severson, A. F., Carter, J. C., Martin, P. R., Schnabel, H., Schnabel, R. and Bowerman, B. (1998). cyk-1: a C. elegans FH gene required for a late step in embryonic cytokinesis. *J Cell Sci* 111 (Pt 14), 2017-27.

Takizawa, P. A., Sil, A., Swedlow, J. R., Herskowitz, I. and Vale, R. D. (1997). Actin-dependent localization of an RNA encoding a cell-fate determinant in yeast. *Nature* 389, 90-3.

Tenlen, J. R., Molk, J. N., London, N., Page, B. D. and Priess, J. R. (2008). MEX-5 asymmetry in one-cell C. elegans embryos requires PAR-4- and PAR-1-dependent phosphorylation. *Development* 135, 3665-75.

Vartiainen, M. K. and Machesky, L. M. (2004). The WASP-Arp2/3 pathway: genetic insights. *Curr Opin Cell Biol* 16, 174-81.

Warren, D. T., Andrews, P. D., Gourlay, C. W. and Ayscough, K. R. (2002). Sla1p couples the yeast endocytic machinery to proteins regulating actin dynamics. *J Cell Sci* 115, 1703-15.

Williams-Masson, E. M., Malik, A. N. and Hardin, J. (1997). An actin-mediated two-step mechanism is required for ventral enclosure of the C. elegans hypodermis. *Development* 124, 2889-901.

Zhu, J., Hill, R. J., Heid, P. J., Fukuyama, M., Sugimoto, A., Priess, J. R. and Rothman, J. H. (1997). end-1 encodes an apparent GATA factor that specifies the endoderm precursor in Caenorhabditis elegans embryos. *Genes Dev* 11, 2883-96.

CHAPTER 3

A MOLECULAR CLUTCH-LIKE MECHANISM REGULATES THE TRANSITION FROM APICOBASAL POLARIZATION TO CELL MOVEMENTS

Summary

How embryonic cells transition from spatial patterning to morphogenesis is a fascinating and incompletely understood topic. In *C. elegans*, the first morphogenetic movement is the internalization of two endodermal precursor cells (Ea/p cells). The current model for how these cells become internalized is that an apically-enriched population of activated non-muscle myosin II motors drives apical constriction, and this may pull a ring of six neighboring cells together covering the free surfaces of the Ea/p cells. We have examined non-muscle myosin II dynamics with diffraction-limited fluorescence imaging to follow movements of myosin foci with respect to the zones where Ea/p cells contact their neighboring cells. We expected to observe narrowing of the contact zones in concert with contraction of the actomyosin network. We were surprised to find instead that centripetal myosin movements preceded narrowing of contact zones, contracting the apical actomyosin network multiple times over before driving significant neighboring cell movements. Later, myosin foci continued to coalesce centripetally and contact zones narrowed in concert. This

suggests that a regulatable link (a clutch) may connect cortical actomyosin contraction to neighboring cell movements. To test this hypothesis, first, we tracked cell surface movements using fluorescent quantum dots. Our results suggest that free surfaces of Ea/p cells move together with cortical actomyosin contraction before neighboring cells move in concert, suggesting that the regulatable link lies between the Ea/p cell apical cytoskeleton and neighboring cells, and hence may be comprised of cell-cell adhesion complex proteins or proteins that link these complexes to the cytoskeleton. Second, we analyzed adhesion-defective embryos and found that coupling of myosin and contact zone dynamics fails. We have also found that during *Drosophila* ventral furrow formation, myosin moves centripetally prior to apical constriction, suggesting that this phenomenon is not unique to *C. elegans.* Together with the finding that similar centripetal myosin movements move apical cell polarity proteins toward the center of the apical surface at earlier *C. elegans* embryonic stages (Munro et al., 2004), our results suggest that the transition from apicobasal cell polarization to cell internalization is governed by a molecular clutch.

The work described in this chapter will form the basis of a manuscript that is in collaboration with Dr. Gidi Shemer and Joseph McCllelan. Gidi Shemer and Joseph McClellan performed the experiments and analyzed the data for Figure 23. Joseph McCllelan calculated myosin rates based on data that I had collected. Gidi Shemer also performed the experiments and analyzed the data for Figures 24, 26, and 27. I have performed experiments and analyzed data for the remainder of manuscript.

Introduction

The ability of cells to move from their initial position to their final position is integral for development. During development, after cells are born, they often need to migrate to the location where they will form specific structures (Friedl and Gilmour, 2009; Weijer, 2009). Impaired migration of these cells often leads to defects during development. Cells can also migrate inappropriately, as in the case of tumour metastasis (Wolf and Friedl, 2006). Thus, the tight regulation of cell movement is crucial for proper development and homeostasis.

Cells can translocate their cell bodies in at least two ways. One method is through the formation of cellular protrusions in the direction of migration propelling the cell forward. This form of migration is observed throughout development, for example, during *Xenopus* neural crest migration, migrating growth cones, and *Drosophila* border cell migration (Christiansen et al., 2000; Hou et al., 2008; Montell, 2003). The coordination of stabilized cell protrusions and the dynamic rearrangement of underlying adhesion complexes that drives this form of motility is best characterized in tissue culture systems (Giannone et al., 2009). Protrusions are generated in part by forces provided by actin polymerization at the leading edge of a cell, and the maturation of adhesions is regulated in part by the tension sensed by adhesion complexes (Crowley and Horwitz, 1995; Ridley et al., 2003). A prevailing model for how actin dynamics and adhesion formation are coordinated is the "molecular clutch" mechanism (Mitchison and Kirschner, 1988). In the molecular clutch model, there is a regulatable link (a clutch) between the retrograde flow of actin and the underlying cell adhesion complexes. When the clutch is engaged, the retrograde flow of actin slows due to its linkage with adhesion complexes, yet actin monomers are still added onto the

fast growing barbed ends of actin filaments. This monomer addition then allows for local protrusions at the leading edge in the form of filopodia and lamellipodia, and the cell advances forward.

Several studies have delved into the identification of clutch molecules (Giannone et al., 2009). In migrating epithelial cells, it was shown that vinculin and talin, proteins that localize to focal adhesions, couple F-actin filaments to the focal adhesions (Hu et al., 2007). Analysis of vinculin and talin movement dynamics at the leading edge of a migrating cell show that vinculin and talin spend a portion of their time with the mobile F-actin, and a portion of their time with the less-mobile focal adhesions. These results suggest that vinculin and talin make up a dynamic interface between F-actin and focal adhesions. During growth cone migration, substrate-cytoskeletal coupling in Aplysia growth cones through ApCAM (a homolog of the vertebrate neural cell adhesion molecule, NCAM) is accompanied by lamellipodial protrusions (Lin and Forscher, 1995; Suter et al., 1998). Additionally, primary neurons plated on N-cadherin-coated substrates reveal that mechanical coupling between N-cadherin and F-actin flow is a major mediator of neurite extension (Bard et al., 2008).

A second method of cell translocation is through a cell shape change. Cell movements require cell shape changes that are dependent on remodeling of the cytoskeleton. One example of a simple change in cell shape is apical constriction, a process in which cells narrow their apical surfaces. Shrinking of the apical side of a cell leads to dramatic cellular rearrangements during development, such as gastrulation, neural tube formation and neurulation (Sawyer et al., 2009). Gastrulation is one of the first morphogenetic movements in animal embryos. In most embryos, the three germ layers -- ectoderm, mesoderm and endoderm -- become positioned during gastrulation. In *Caenorhabditis elegans*, gastrulation

is initiated after two endodermal precursor cells, Ea and Ep (referred to collectively as Ea/p), are born on the surface of the embryo. The Ea/p cells apically constrict, translocating their cell bodies to the embryonic interior where they will continue to divide and develop into the endoderm. This movement is modest, as the distance the cell moves is approximately a single cell diameter. However, this movement is crucial as the inability of Ea/p cells to internalize results in an inviable animal with the endoderm on the exterior (Lee and Goldstein, 2003; Nance and Priess, 2002).

Gastrulation in *C. elegans* is a powerful model system for dissecting mechanisms of cell movements during morphogenesis because it involves a small number of cells and hence can be studied at the level of individual cells. Also, one can readily combine live microscopic imaging with gene function studies. There are several inputs required for apical constriction during *C. elegans* gastrulation. Cell specification is important for proper apical constriction. Mutations in endodermal specification genes such as the GATA factor genes *end-1* and *end-3*, result in gastrulation defects (Lee et al., 2006; Maduro et al., 2005; Zhu et al., 1997). Ea/p cells must be properly polarized. PAR proteins, conserved polarity proteins with homologs in *Drosophila* and vertebrates, localize to specific cell membranes (Sawyer et al., 2009). In the Ea/p cells, PAR-1 and PAR-2 localize basolaterally, whereas PAR-3, PAR-6 and atypical protein kinase C (aPKC) localize apically (Boyd et al., 1996; Etemad-Moghadam et al., 1995; Hung and Kemphues, 1999; Nance and Priess, 2002). Embryos depleted of PAR proteins specifically at gastrulation have defects in Ea/p cell internalization (Nance and Priess, 2002). Apical PAR protein localization allows for the apical accumulation of non-muscle myosin II (NMY-2) (Nance and Priess, 2002). The myosin light chain is then phosphorylated, resulting in activation of myosin (Lee et al., 2006). This activation allows

for actomyosin contractility, which is thought to apically constrict the Ea/p cells and result in their internalization.

The mechanism of actomyosin contraction has been intensively studied. During *Drosophila* gastrulation, the mesodermal cells on the surface of the embryo accumulate myosin and undergo a coordinated apical constriction (Dawes-Hoang et al., 2005; Royou et al., 2004; Young et al., 1991). This constriction leads to the invagination of the mesodermal cells as a sheet of cells, which are then spread along the interior of the embryo. It had previously been thought that a purse-string-like contraction of circumferential actomyosin bundles at the apical surface of ventral furrow cells drives apical constriction in the ventral furrow cells. However, closer examination of myosin II dynamics during ventral furrow formation reveals that individual myosin punctae across the apical surface come together to form bigger myosin complexes, in a process referred to as myosin coalescence (Martin et al., 2009). These myosin punctae appear to drive contraction with a ratchet-like mechanism, incrementally apically constricting the cells with repeated cycles of contraction and pauses. Furthermore, myosin contractions are linked to the adherens junctions, as myosin coalescence causes bending of the membrane toward the coalescence sites. When adherens junctions are impaired, or when linkages between the cytoskeleton and adherens junctions are compromised, the actomyosin network continues to contract, but the apical membrane of the ventral furrow cells does not constrict (Dawes-Hoang et al., 2005; Sawyer et al., 2009).

The mechanism of actomyosin contraction in the one-cell stage *C. elegans* embryo has also been well studied (Munro et al., 2004). Similar to the dynamics of the apical myosin meshwork in *Drosophila* ventral furrow cells, the authors show that a network of F-actin and myosin punctae forms on the cell cortex. Myosin punctae flow towards the anterior end of

the embryo. At the anterior end, myosin punctae coalesce repeatedly. Interestingly, there is no evidence for a ratchet mechanism in the early *C. elegans* embryo, as myosin moves continuously without interruption. The actomyosin contraction observed at the one cell stage is not for apical constriction, but rather, the anterior driven cortical flows of actin and myosin transports anterior PAR proteins, such as PAR-3, PAR-6 and aPKC to the anterior end, establishing polarity (Cheeks et al., 2004; Munro et al., 2004).

We sought to dissect the mechanism of *C. elegans* apical constriction during Ea/p cell internalization. Although activated myosin is known to accumulate apically in Ea/p cells during internalization (Lee et al. 2006), it is not known how myosin transmits the force required for apical constriction. In this study, we report that during *C. elegans* Ea/p cell internalization, myosin II punctae move from the cell periphery toward the cell center (centripetal movements) on the apical surface of the Ea/p cells. Myosin II punctae coalesce and disassemble rapidly. Surprisingly, during the beginning stages of Ea/p cell internalization, these centripetal myosin II movements occur with little constriction of the Ea/p apical surface. Thus, during this phase, myosin II movements are generally uncoupled from the movements of neighboring cell boundaries. The first phase is followed by a second phase in which centripetal myosin II movements are coupled with movement of the neighboring cell boundaries, and the Ea/p cells constrict their apical surfaces. These results suggest that a molecular clutch may mediate the linkage between the contracting cytoskeletal machinery and neighboring cell movements. Further exploration of the identity of the clutch suggests that it may be comprised of cell-cell adhesion complex proteins or proteins that link these complexes to the cytoskeleton. Furthermore, examination of *Drosophila* ventral furrow cells suggests that centripetal myosin II movements are occurring prior to furrow formation.

Together with the finding that similar centripetal myosin movements move polarity proteins at earlier *C. elegans* embryonic stages (Munro et al., 2004), our results suggest that the transition from apicobasal cell polarization to cell internalization is governed by a molecular clutch. To our knowledge, this is the first report of a molecular clutch regulating a developmental process in a multicellular organism. Our results also suggest that the use of a molecular clutch may be a general mechanism used in development to regulate cell internalization.

Results

Ea/p cell internalization is biphasic

To closely examine the dynamics of Ea/p cell internalization, we positioned embryos with their ventral sides facing the coverslip to image the entire Ea/p cell apical surface (Figure 18A). Cell membranes were visualized in embryos expressing an mCherry labeled PH domain of phospholipase C δ (PLCδ), PH::mCherry (Kachur et al., 2008). We made en face tracings of the entire ventral surface of the Ea/p cell that was exposed to the egg shell over time (Figure 18B). We then measured the change in Ea/p average cell radii of wild-type embryos over time and found that Ea/p cell internalization was biphasic (Figure 18C). Ea/p cell surfaces initially constricted slowly, with Ea/p cells remaining on the surface of the embryo. This slow phase occurred for approximately 8 minutes after MSa/p division. This phase was then followed by a faster phase of Ea/p cell constriction as Ea/p cells internalized. The fast phase occurred for approximately 2-3 minutes. Thus, Ea/p cell internalization rate is biphasic with a slow first phase followed by a second fast phase.

There are 2 distinct phases of non-muscle myosin II movement during apical constriction

To closely examine the cytoskeletal network required for apical constriction, we sought to document non-muscle myosin II dynamics during these two phases of Ea/p cell internalization. To simultaneously image non-muscle myosin II movement with respect to cell-cell contacts, we crossed a strain containing tagged non-muscle myosin II, NMY-2::GFP, to a strain containing PH::mCherry (Figure 19A). The PH-mCherry strain was used to visualize the movement of "contact zones", the cell-cell boundaries at which the Ea/p cells contacted neighboring cells. Thus, as Ea/p cells apically constricted, the constriction is visualized as narrowing of the area between the contact zones.

To determine how myosin might generate force for apical constriction, gastrulation-stage wild-type embryos were imaged on their ventral surfaces to analyze the movement of NMY-2::GFP on the apical surfaces of the Ea/p cells. NMY-2::GFP foci were present on all cell surfaces, including Ea and Ep (Figure 19A). We imaged the movement of NMY-2::GFP foci during the first slow phase of Ea/p cell internalization, when Ea/p cells were still on the embryonic surface. We were surprised to find that during this slow phase, NMY-2::GFP punctae were moving centripetally (Figure 19B). The rate of myosin movement was 4.70 ± 0.27 μm/min, and the centripetal movements occurred multiple times over the entire surface of Ea/p cells, with little movement of the contact zones. We observed pockets of myosin coalescence as seen in Munro et al., 2004, where nearby myosin punctae would coalesce at indiscriminate positions on the Ea/p cell apical surface, yet there was a general direction of movement centripetally. As with foci at the one-cell stage, local coalescence of myosin foci

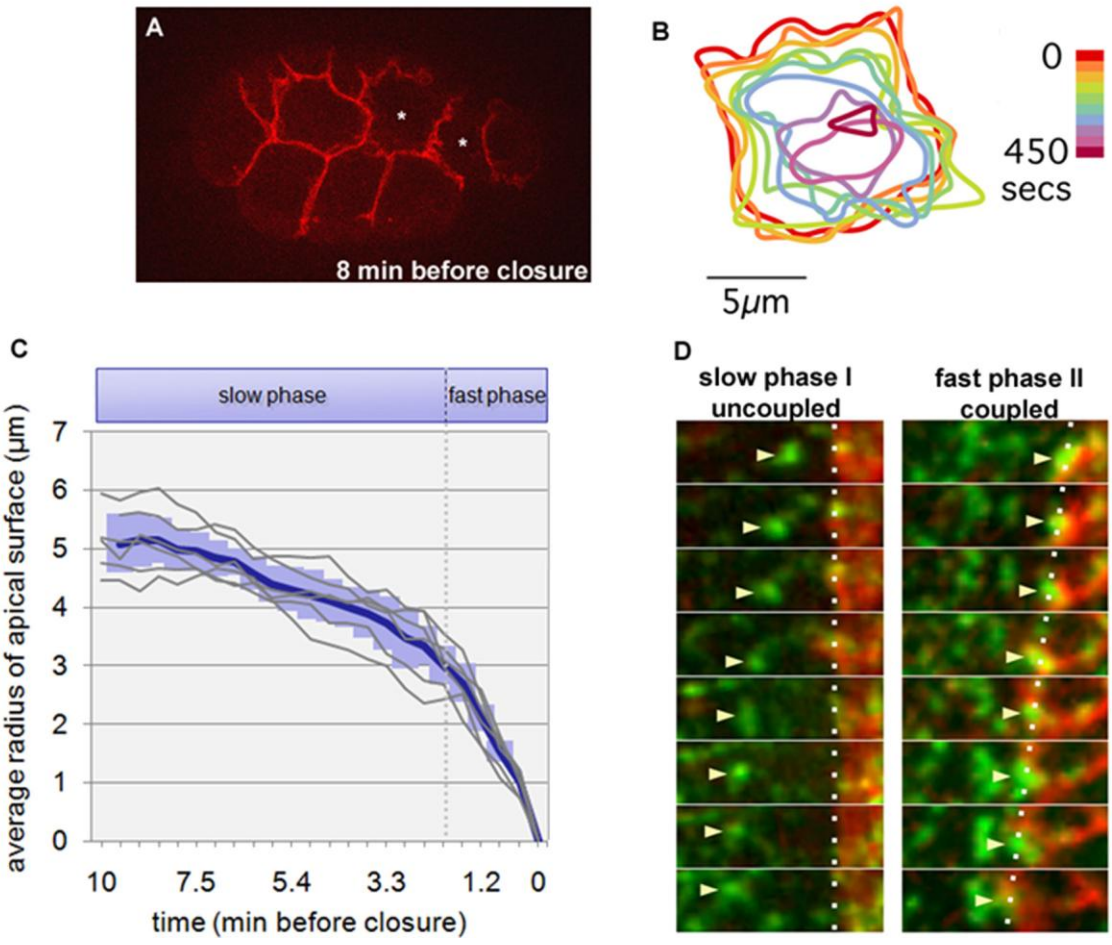
A
8 min before closure
B
0
450
secs
5μm
C
slow phase
fast phase
average radius of apical surface (μm)
7
6
5
4
3
2
1
0
10
7.5
5.4
3.3
1.2
0
time (min before closure)
D
slow phase I
uncoupled
fast phase II
coupled

Figure 18: The rate of myosin movements decreases and the rate of membrane movement increases. (A) Ventral view of embryo expressing the membrane marker PH::mCherry. In this figure, and subsequent figures, Ea/p cells are marked with asterisks unless stated otherwise. (B) The E cell surface was traced over time and merged. Each tracing is colour-coded with respect to time. (C) Plotted in grey is the radius (microns) of the Ea cell over time for 6 embryos. The dark blue line is the average radius, with light blue shading indicating 95% confidence intervals. (D) Representative images of uncoupled myosin (arrow) and contact zone (dotted line) dynamics during phase I (left panel), as well as coupled dynamics during phase II (right panel).

disassembled (Munro et al., 2004). It is likely that the myosin foci disassembled, rather than moved to a different imaging plane, as we imaged two planes that were 0.5 μm apart at the apical surface of the Ea/p cells. When we imaged at a focal plane that was located more basolaterally, we could no longer detect apical myosin. Thus, with our imaging parameters, it is likely that we captured most of the myosin foci dynamics. We conclude that the general movement of NMY-2::GFP foci was uncoupled, or weakly coupled, from the movement of the contact zones during the initial phase of Ea/p cell internalization.

During cortical flows at the one-cell stage, the speed of myosin movement increased from the center of the coalescence site (Munro et al., 2004). That is, the rate of myosin movement was faster the further the punctae were from the coalescence center, and punctae moved slower as the punctae moved closer to the site, as would be expected of a contracting meshwork. We tested whether this phenomenon occurred during Ea/p apical constriction. Myosin punctae that were 0-0.5 μm from the site of coalescence moved at an average rate of 3.05 ± 0.82 μm/min (n=17, average ± 95% confidence interval), whereas myosin punctae that were 1.5-2 μm from the site of coalescence moved at a rate of 5.91 ± 1.71 μm/min (n=2, average ± 95% confidence interval). Thus, similar to myosin dynamics at the one-cell stage, the rate of myosin punctae movement was significantly faster the further away the punctae were from the coalescence site (student's t-test, $p<0.05$).

Kymograph analysis of NMY-2::GFP movements during the initial slow phase of Ea/p cell internalization highlighted the centripetal movements of NMY-2::GFP in an Ea cell, and the apical surface area, defined by the positions of the contact zones, did not shrink appreciably (Figure 19B). Three separate kymographs along different orientations across the Ea cell indicated that there was a radial generally inward movement of NMY-2::GFP toward

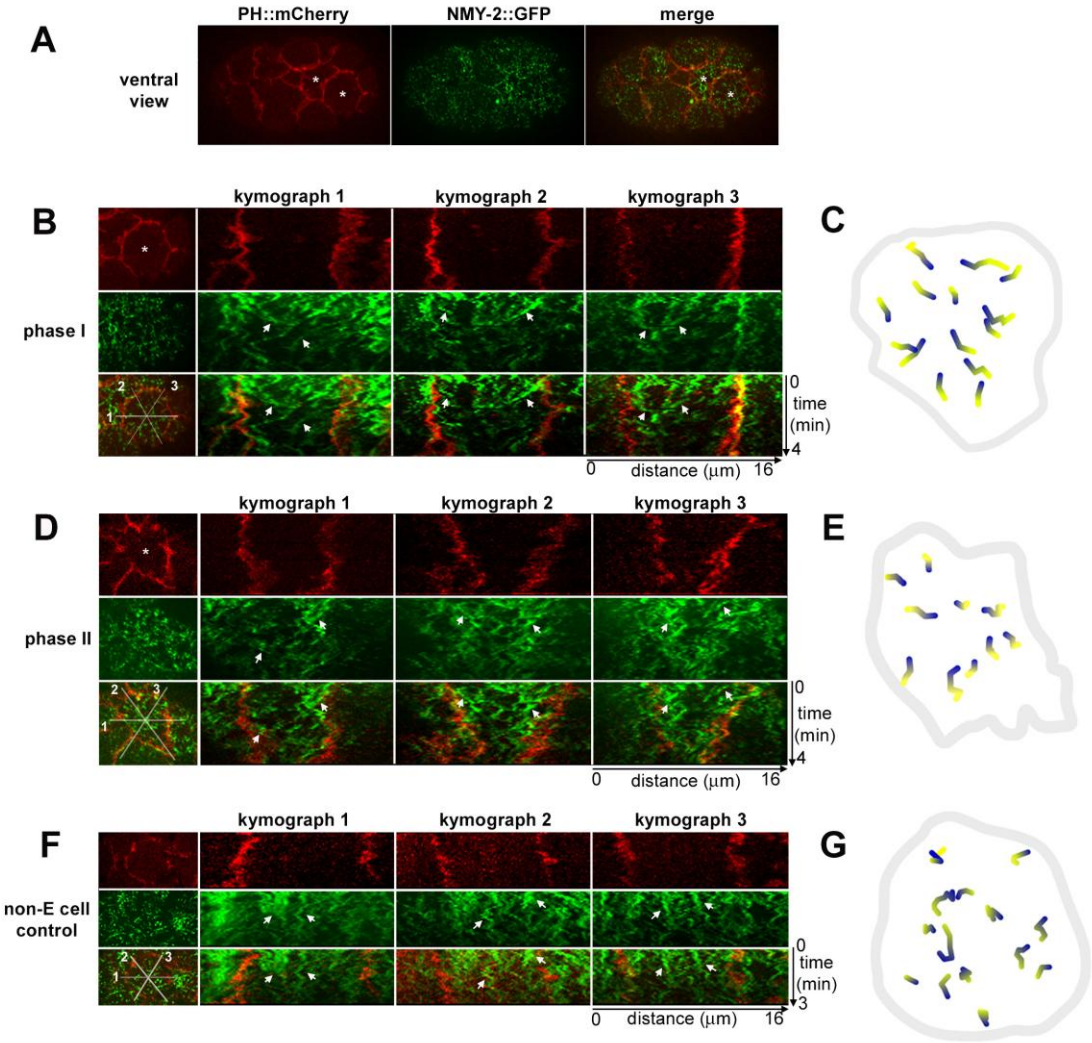
A
PH::mCherry
NMY-2::GFP
merge
ventral view
B
kymograph 1
kymograph 2
kymograph 3
phase I
time (min)
distance (µm)
C
D
phase II
E
F
non-E cell control
G

Figure 19: There are two distinct phases of non-muscle myosin II movement during E cell ingression. (A) Wild-type embryos were imaged on their ventral surfaces to analyze the movement of non-muscle myosin (NMY-2::GFP) relative to the cell-cell boundaries as marked by the PH domain of PLCδ::mCherry (PH::mCherry). The two planes were merged for analysis to allow for the tracking of NMY-2::GFP foci. (B) Kymography of three separate linescans (1, 2, 3) in phase I to show uncoupled dynamics (arrows). (C) Myosin punctae were manually tracked over time with colour indicating time. Yellow is an older time point, fading to blue, which is more recent. (D) During phase II, we also analyzed kymographs of three separate linescans (1, 2, 3). Myosin foci continued to coalesce centripetally (arrows), and contact zones narrowed in concert. (E) Myosin punctae were also manually tracked during phase II. (F) Kymography of a non-E cell reveals no centripetal NMY-2::GFP movement (arrows). (G) Manual tracking of NMY-2::GFP foci in the non-E cell control.

the center of the cell. Each orientation along the Ea cell also showed uncoupled myosin movements from the contact zones, as the contact zones did not narrow at this time. The movement of individual NMY-2::GFP punctae or groups of punctae during the initial phase of Ea/p cell internalization were also manually tracked (Figure 19C). These tracings confirmed that many myosin punctae moved centripetally.

We next analyzed NMY-2::GFP foci and contact zone movement during the second, fast phase of Ea/p cell internalization (Figure 19D). The second phase was determined by the time elapsed from MSa/p division, as indicated by the initial experiments observing changes in the Ea cell radii (Figure 18C). We imaged embryos 8 minutes after MSa/p division to capture phase II myosin and contact zone dynamics. As expected, NMY-2::GFP foci continued to move centripetally. During this phase, as myosin foci moved, contact zones moved in concert, at a similar rate. Kymography along three orientations of the Ea cell also revealed centripetal myosin movements with concurrent movement of the contact zones. Manual tracking of myosin punctae confirmed that many NMY-2::GFP punctae moved centripetally (Figure 19E). Therefore, during the second, fast phase of Ea/p cell internalization, myosin movement generally appeared coupled to the movement of the contact zones. Additionally the rate of myosin movement during the second phase was 4.35 ± 0.22 μm/min, which was statistically significantly slower than that during phase I (student's t-test, $p<0.05$), as might be expected for an ensemble of motors pulling a load (Debold et al., 2005). Taken together, we conclude that there are two phases of myosin movement in the Ea/p cells: A first phase in which most of the myosin movement is uncoupled from the movement of the contact zones, and a second phase in which the myosin movement is then coupled to contact zone movement (Figure 18D).

We next determined whether the biphasic myosin movement was specific to the Ea/p cells, or whether the other cells in gastrulation-stage embryos could be exhibiting these movements as well. Three mesodermal descendants, MSpa, MSpp, and MSap, are part of the ring of neighboring cells that fill in the gap left behind by the internalizing E cells (Lee and Goldstein, 2003). MS granddaughter cells were analyzed similarly to Ea/p cells to document the movement of NMY-2::GFP punctae relative to the contact zones (Figure 19F). Kymographs of myosin movement in the MS granddaughter cells showed a lack of centripetal movement. Often, myosin punctae oscillated and appeared to move in random directions. Manual tracking of these punctae also revealed apparently random myosin movements (Figure 19G). Therefore, it appears that when Ea/p cells are internalizing, the neighboring cells are not undergoing centripetal myosin movements, and that these centripetal movements are specific to the Ea/p cells.

The transition from apicobasal polarity establishment to cell internalization is governed by a molecular clutch

Our results revealing that the movements of myosin foci relative to the contact zones transitioned from an uncoupled to coupled phase suggested that there may be a molecular clutch-like mechanism that regulates the transition. The identification of a molecular clutch regulating cell internalization caused us to question why an embryo would require regulatable coupling between the contracting cytoskeletal network and contact zone movement. The answer may lay in the fact that centripetal myosin movements are already occurring prior to gastrulation (Munro et al., 2004). Endoderm fate is specified at the four-cell stage, when a cell (EMS) divides asymmetrically, generating an anterior mesodermal precursor cell (MS) and a posterior endodermal precursor cell (E). Twenty minutes later, E

and MS divide simultaneously, generating Ea and Ep, and MSa and MSp, respectively. MSa and MSp divide again another twenty minutes later; however, Ea and Ep introduce a gap phase and do not divide for forty minutes. As mentioned previously, actomyosin contractility at the one-cell stage is thought to transport PAR polarity proteins to the anterior end of the embryo, concomitant with anterior-posterior polarity establishment (Munro et al., 2004). Beginning at the late four-cell stage, the somatic cells adopt an apicobasal polarity. The former anterior PAR proteins localize to the free apical surface, whereas the former posterior PAR proteins localize to the basolateral cell surfaces (Etemad-Moghadam et al., 1995; Boyd et al., 1996; Hung and Kemphues, 1999; Nance and Priess, 2002). Munro and colleagues (2004) showed that myosin and an apical PAR protein, PAR-6, moved centripetally toward the apical surfaces of somatic cells. Thus, myosin centripetal movements accompanied apicobasal polarization. Consistent with these findings, our analysis of NMY-2::GFP punctae at early embryonic stages revealed centripetal myosin movements on the apical surface of the EMS cell, as well as when E and MS cells were born (Figure 20). When E divided into Ea and Ep, and MS divided into MSa and MSp, centripetal myosin movements persisted in all these cells (Figure 20). However, when MSa and MSp cells divided into the four mesodermal granddaughter cells, in some cases, we observed centripetal myosin movements, whereas in other cases, we did not observe centripetal myosin movements (Figure 20; Figure 19F). Therefore, we are continuing these studies to determine whether centripetal myosin movements cease upon MSa/p division. Together with the finding that centripetal myosin movements transport polarity proteins to the apical cell surface during early embryogenesis, our results suggest that the molecular clutch may be required to take advantage of a pre-

existing actomyosin contractility network to transition from apicobasal polarization to cell internalization.

Internalizing cells in other systems may also be regulated by a molecular clutch

Our results suggested that myosin movements were uncoupled from the movement of the contact zones at the initial stages of Ea/p cell internalization. Thus, the apical constriction network was already active before the engagement of the clutch, and the engagement of a clutch coupled the movement of myosin to the movement of the neighboring cells. We questioned whether this phenomenon was specific to *C. elegans*, or whether other developmental systems might use a similar mechanism to internalize cells.

Several morphogenetic processes occur through apical constriction of individual cells or a sheet of cells. We analyzed the invagination of the *Drosophila* ventral furrow cells to determine whether centripetal movements of myosin are occurring prior to apical constriction of the cells. The ventral furrow is composed of a strip of cells that is 18 cells wide and 60 cells long. *Drosophila* embryos that were simultaneously expressing a tagged form of MLC, spaghetti squash-mCherry, and a tagged membrane marker, spider-GFP (Martin et al., 2009) were mounted on their ventral surfaces (Figure 21). When apical myosin accumulation was observed in the ventral pocket cells, the cells began to apically constrict approximately 2-3 minutes later (Figure 21A-D). We analyzed myosin dynamics during this 2-3 minute window. A previous study had observed that pulses of myosin coalescence preceded apical constriction by 5-10 seconds, suggesting that actomyosin contraction drives constriction of the membranes, but had not reported on earlier stages (Martin et al, 2009). We found that myosin punctae moved centripetally and coalesced without significant constriction of the

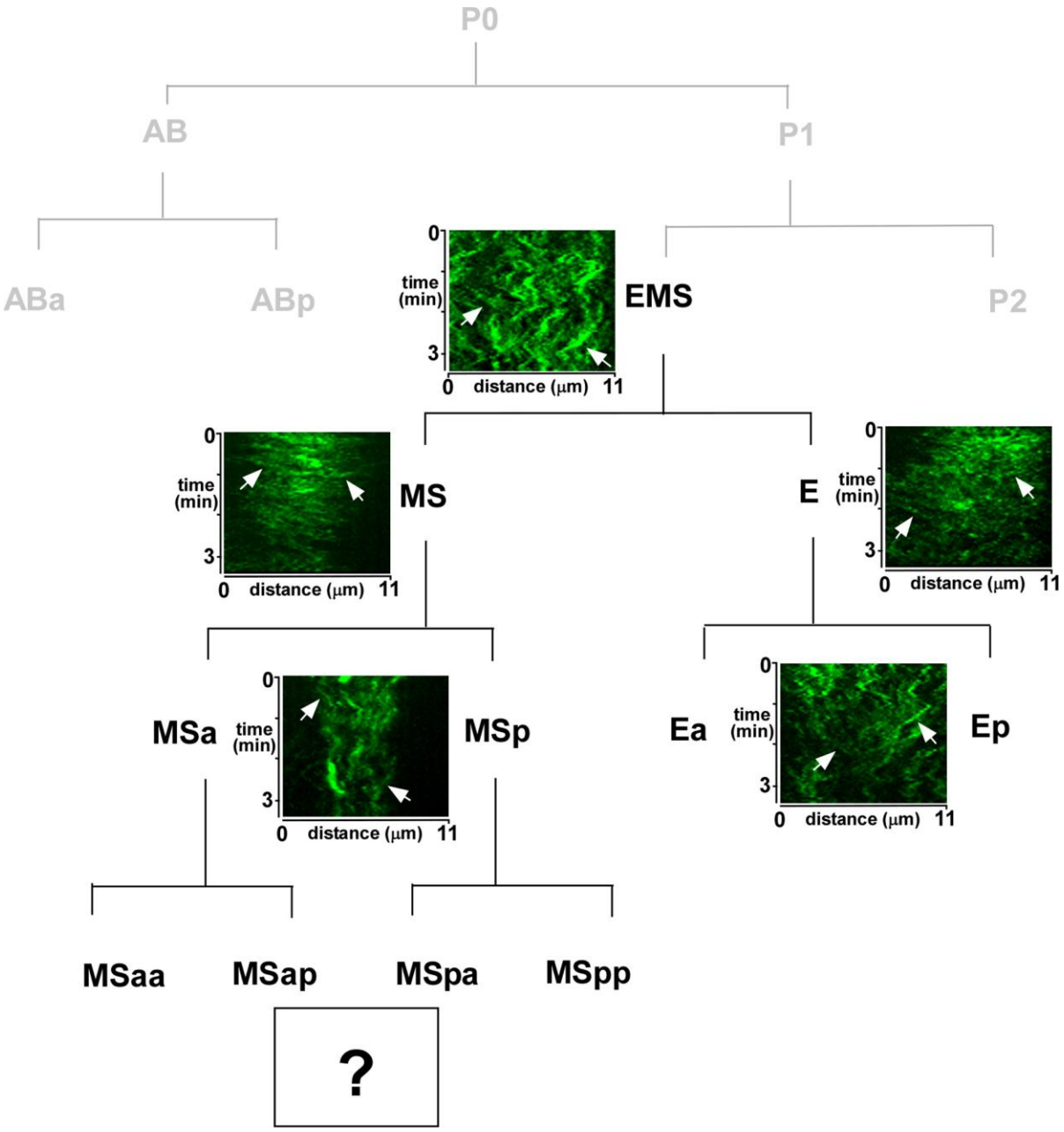
P0
AB
P1
ABa
ABp
EMS
P2
time (min)
0
3
0 distance (μm) 11
MS
E
MSa
MSp
Ea
Ep
MSaa
MSap
MSpa
MSpp
?

Figure 20: Centripetal myosin movements are observed throughout early embryogenesis. A cell lineage is drawn with kymographs drawn next to cells to indicate NMY-2::GFP dynamics at that stage. Arrows point to centripetal myosin movements.

ventral furrow cells. Thus, myosin movement was uncoupled from movement of the neighboring cell membranes (Figure 21E-K). Similar to what we observed in *C. elegans* Ea/p cells, there was a radial movement of myosin to the center of the cells. As myosin moved in centripetally (Figure 21F,G,I,J), the coalesced punctae disassembled (Figure 21H,K). The mesodermal cells then apically constricted, with myosin continuing to move centripetally. Thus, it appears that the actomyosin network was already active in the ventral furrow prior to apical constriction. These results suggest that myosin movements are initially uncoupled from contact zone movements in *Drosophila* mesodermal cell apical constriction, as in *C. elegans* Ea/p cell apical constriction.

The clutch-like link may lie between Ea/p cell cytoskeletal machinery and neighboring cells

Our results in *Drosophila* and *C. elegans* suggested that the movements of myosin foci relative to the contact zones transitioned from an uncoupled to coupled phase, and that there may be a molecular clutch-like mechanism that regulates the transition. We sought to further analyze the molecular clutch during *C. elegans* Ea/p cell internalization because the system involves a small number of cells and hence can be studied at the level of individual cells. Also, one can readily remove the egg shell and vitelline membrane for *in vitro* studies.

We hypothesized that during the uncoupled phase, the regulatable clutch between myosin motors and neighboring cells was disengaged. Therefore, myosin moved freely with little movement of the contact zones (Figure 19B). However, when we observed myosin foci and contact zone movement in concert (Figure19D), we hypothesized that during this phase, the clutch was engaged, and myosin motor activity was linked to the movement of neighboring cells. Thus, we sought to determine which link the clutch could be regulating.

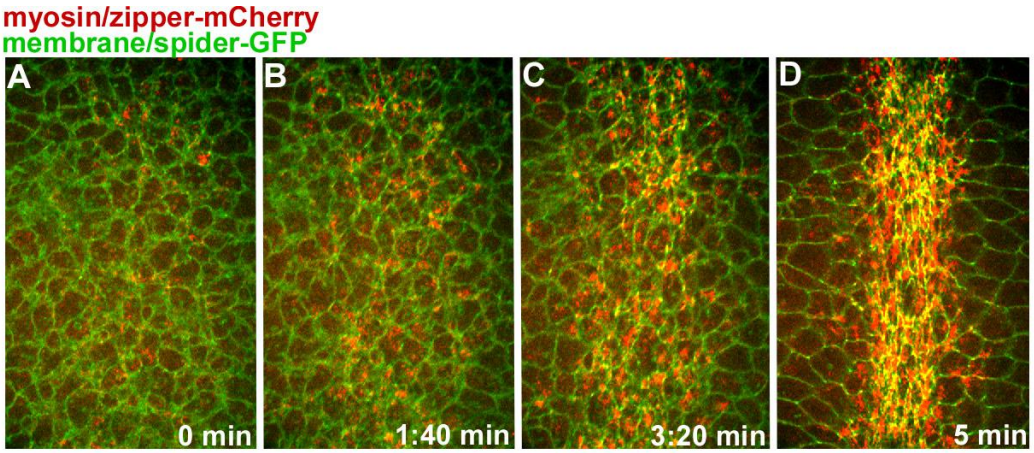
myosin/zipper-mCherry
membrane/spider-GFP
A
0 min
B
1:40 min
C
3:20 min
D
5 min

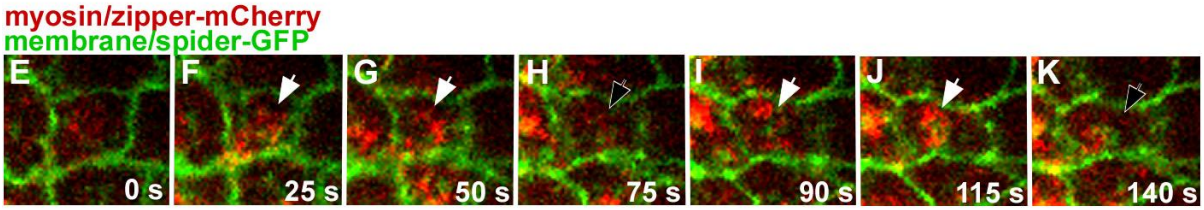
myosin/zipper-mCherry
membrane/spider-GFP
E
0 s
F
25 s
G
50 s
H
75 s
I
90 s
J
115 s
K
140 s

Figure 21: Myosin moves centripetally prior to apical constriction in *Drosophila* ventral furrow cells. (A-K) *Drosophila* embryos expressing mCherry labeled myosin and GFP labeled membrane marker. (A) Ventral furrow cells began to accumulate myosin apically. (C) Within 3 minutes of the initial myosin recruitment, ventral furrow cells began to apically constrict. (D) By 5 minutes, the central furrow cells had apically constricted. (E-K) A timelapse of an individual ventral furrow cell. Myosin coalescence was observed (F,G – white arrow) with little movement of the membrane. Myosin then disassembled (H – black arrow). Another cycle of myosin coalescence was observed (I,J – white arrow) and the coalesced myosin disassembled again (K – black arrow).

One hypothesis was that the clutch regulated the link between myosin and the overlying cell surface. If myosin movement was not linked to the overlying cell surface, then as myosin moved centripetally, the overlying cell surface would not move and thus, the contact zone would not move in concert. A second hypothesis was that the molecular clutch was between the Ea/p cell cytoskeletal machinery and the neighboring cells. This could occur either through cell-cell adhesion between the Ea/p cells and neighboring cells, or cytoskeletal-cell adhesion linkages within the Ea/p cells themselves. If either of these links was perturbed, then as myosin II moved centripetally in the Ea/p cells, the contact zones would not move concurrently. To distinguish between these two hypotheses, we used quantum dots to introduce fiduciary marks on the overlying cell surface to determine whether the overlying surface moved centripetally as myosin exhibited uncoupled phase I movements.

Gastrulation-staged embryos were devitellinized and coated non-specifically with quantum dots (Figure 22A-D). In one successful case, we observed two quantum dots associated with the surface of the Ea cell at early stages of gastrulation (Figure 22B-D). Using DIC images to identify cell-cell boundaries, we found that the contact zones between the Ea/p cells and neighboring cells were not narrowing, which suggested that this embryo was imaged during phase I (Figure 22E). Although the contact zones were not narrowing, the overlying cell surface, marked by quantum dots, still moved toward the Ea/Ep boundary. We are currently continuing these experiments to track surface quantum dots and myosin foci together. Therefore, during phase I, it appears that the link between myosin and the overlying cell surface is intact, and these results suggest that the molecular clutch is disengaged between the E cell cytoskeletal machinery and the neighboring cell membranes.

The regulatable clutch may be comprised of adhesion complex proteins or associated proteins

Our quantum dot experiment suggests that the molecular clutch regulates the link between the Ea/p cell cytoskeletal machinery and the neighboring cell membranes, and that during phase I, this clutch is disengaged. This model predicts that if adhesion was compromised between the Ea/p cells and the neighboring cells, myosin dynamics will fail to become linked to movements of the contact zones: phase II coupled dynamics will be prevented. Based on this model, we began to test candidate adhesion proteins by knocking down their gene expression by RNAi by injection.

Adhesion complexes in *C. elegans* look similar to those in vertebrate and fly systems. Transmission electron microscopy (TEM) reveals a single electron dense structure near the apical surface of epithelial cells, although this single structure is composed of two distinct adhesion complexes (McMahon et al., 2001). The most apical of these two apical complexes is the cadherin-catenin complex, which includes homologues of a classical E-cadherin (HMR-1), β-catenin (HMP-2), α-catenin (HMP-1), and p120 catenin (JAC-1) (Costa et al., 1998; Koppen et al., 2001; Pettitt et al., 2003). It has been shown that *C. elegans* adhesion complexes form later in embryogenesis, after Ea/p cell internalization, as TEM studies have shown a lack of electron dense structures near apical surfaces during early embryogenesis. However, these studies do not preclude a role for adhesion complex proteins during gastrulation movements.

In *Drosophila* and vertebrate systems, when the function of the cadherin-catenin complex was impaired, this resulted in severe defects in cell adhesion (Schock and Perrimon, 2002). We analyzed *C. elegans* embryos depleted of a classical *cadherin/hmr-1* to determine

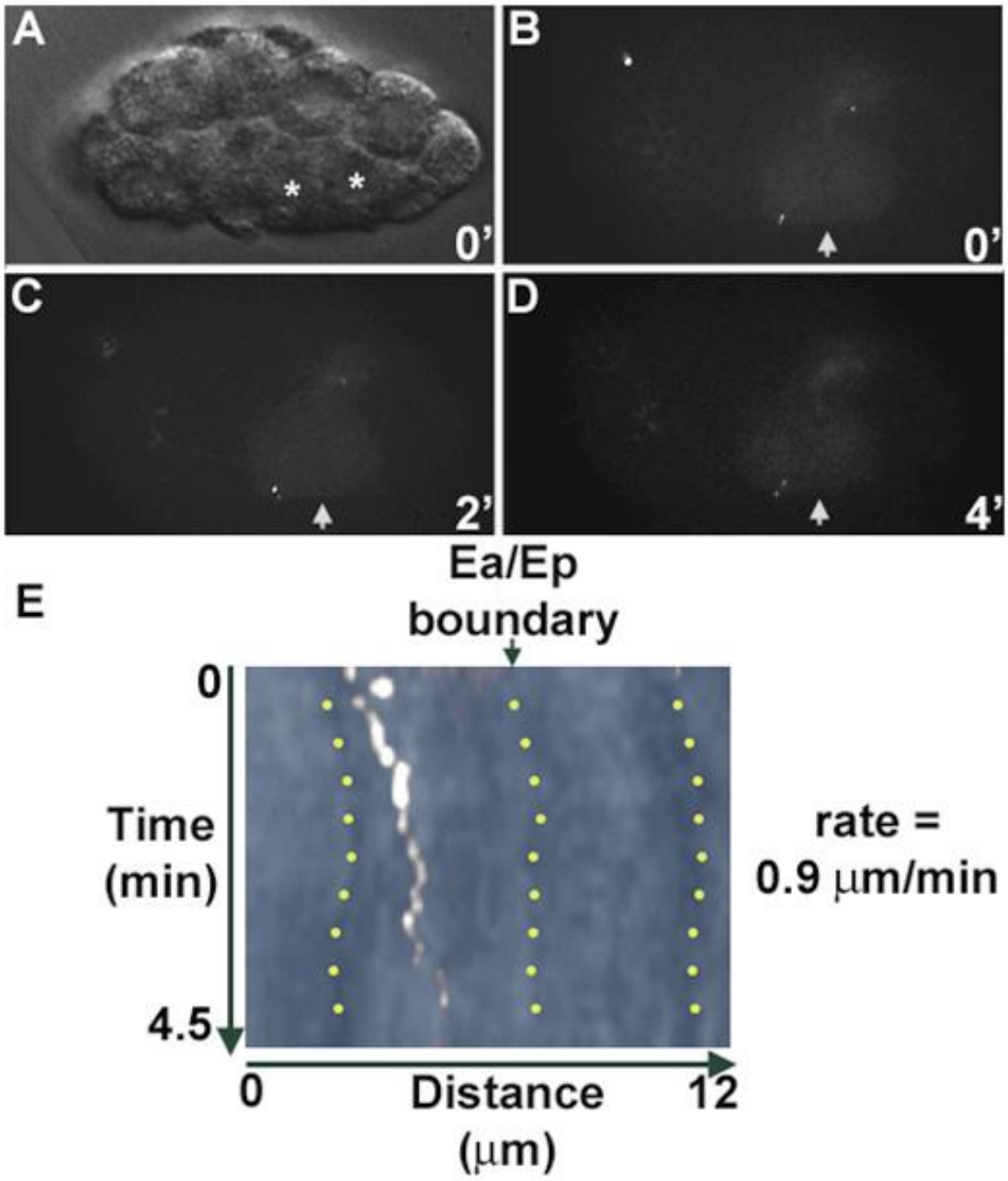
A
0'
B
0'
C
2'
D
4'
E
Ea/Ep
boundary
0
Time
(min)
4.5
0
Distance
(μm)
12
rate =
0.9 μm/min

Figure 22: The clutch-like link may lie between the Ea/p cell cytoskelton and neighbouring cells. Gastrulation-stage embryos were devitellinized and coated non-specifically with quantum dots. (A) Shown is a DIC image of an embryo that was devitellinized just prior to gastrulation (white arrow marks the border between the E cells). (B-D) Still images of a movie of the embryo in (a). Two quantum dots associated with the surface of the E_a cell at early stages of gastrulation. The Ea/Ep border is marked by an arrow. (E) A kymograph of the quantum dot movement over one of the E cells. Yellow dotted lines mark the cell-cell boundaries, and an arrow indicates the Ea/Ep boundary.

whether there were Ea/p cell internalization defects. When we measured the change in Ea/p average cell radii over time with en face ventral tracings, we found that *cadherin/hmr-1* depleted embryos did not reach the same maximum internalization rate as wild-type (Figure 23A). We are also currently analyzing *cadherin/hmr-1* depleted embryos by TEM to determine whether these embryos exhibit any adhesion defects that are not visible by confocal microscopy. However, *cadherin/hmr-1* depleted embryos internalized Ea/p cells normally (Figure 23B). Thus, *cadherin/hmr-1* depleted embryos displayed subtle defects in Ea/p cell internalization, which suggested that adhesion proteins play a role in gastrulation, but that these proteins may be acting redundantly with other players.

Due to the subtle gastrulation defects observed in *cadherin/hmr-1* depleted embryos, we searched for a genetic background that would enhance these gastrulation defects. When we depleted *cadherin/hmr-1* in the genetically sensitized background of a Rac signaling mutant, *Dock180/ced-5*, we found that Ea/p cell internalization failed (57% gastrulation defects, n=49; Figure 23C). *Dock180/ced-5* is part of a family of guanine nucleotide exchange factors (Wu and Horvitz, 1998), and *Dock180/ced-5* functions to activate a Rac GTPase (Reddien and Horvitz, 2000). *cadherin/hmr-1; Dock180/ced-5* mutant embryos also displayed defects in general cell adhesion, as these embryos displayed cell-cell separation defects that were not observed in wild-type embryos (Figure 24A,B). These gaps in the embryo were quantified, and *cadherin/hmr-1; Dock180/ced-5* mutants displayed significantly larger cell separations than in wild-type embryos (Figure 24A,B). We then asked whether the inability of Ea/p cells to internalize in *cadherin/hmr-1; Dock180/ced-5* mutants was due to the prevention of phase II coupling of myosin and membrane dynamics. We placed *cadherin/hmr-1; Dock180/ced-5* mutant embryos expressing NMY-2::GFP and PH::mCherry

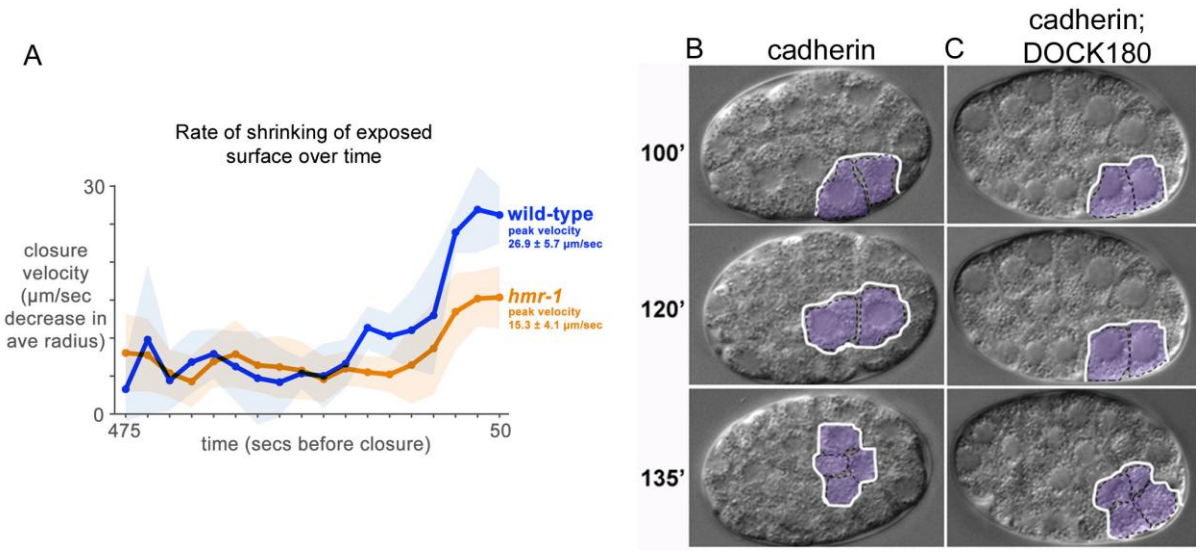
A
Rate of shrinking of exposed surface over time
30
0
closure velocity (µm/sec decrease in ave radius)
475
50
time (secs before closure)
wild-type
peak velocity
26.9 ± 5.7 µm/sec
hmr-1
peak velocity
15.3 ± 4.1 µm/sec
B
cadherin
C
cadherin; DOCK180
100'
120'
135'

Figure 23: Embryos deficient in a classical cadherin *(hmr-1)* and a Dock180 *(ced-5)* have gastrulation defects. (A) *cadherin/hmr-1* RNAi did not reach the same maximum velocity of average radius decrease as in wild-type embryos. Averages are shown, with 95% confidence intervals indicated. (B,C) Time is indicated as minutes after fertilization. (B) *cadherin/hmr-1* RNAi embryos did not have E cell internalization defects (pseudocoloured purple). The E cells were born on the surface and moved to the embryonic interior. Once inside, the E cells divided. (C) When *cadherin/hmr-1* RNAi embryos were placed in a *Dock180/ced-5* mutant background, E cells failed to internalize. The E cells divided on the surface of the embryo (pseudocoloured purple).

on their ventral surfaces to analyze myosin movement relative to the contact zones (Figure 25A). During phase I, *cadherin/hmr-1; Dock180/ced-5* embryos displayed myosin dynamics in Ea/p cells that were similar to wild-type, where myosin rapidly moved centripetally with little movement of the contact zones (Figure 25B). These results were confirmed with kymography along three orientations in the Ea/p cells. However, during phase II, myosin dynamics in *cadherin/hmr-1; Dock180/ced-5* mutant embryos were still un-coupled (Figure 25C). Myosin continued to move centripetally, with little movement of the contact zones. Thus, when embryos are depleted of adhesion complex proteins, the coupling of myosin and the contact zones is prevented.

Given the adhesion defects observed in *cadherin/hmr-1; Dock180/ced-5* embryos, quite surprisingly, many features of Ea/p cells were found to be normal. We examined whether cell fate was properly specified in these mutant embryos by analyzing cell fate reporter constructs for mesodermal cells (*tbx-35*::GFP) and endodermal cells (*end-1*::GFP), and found that cell fate was normal (Figure 26A-D). We observed actin localization by imaging embryos expressing a GFP-tagged F-actin-binding domain from *Drosophila* moesin (GFP::MOE), which has been used in *Drosophila* and *C. elegans* to specifically mark the filamentous form of actin (Edwards et al., 1997; Motegi et al., 2006). *cadherin/hmr-1; Dock180/ced-5* embryos expressing GFP::MOE revealed that F-actin was cortically localized, as in wild-type embryos (Figure 26E,F). Additionally, myosin localization was assessed in Ea/p cells by analyzing NMY-2::GFP localization in laterally oriented embryos. We found that myosin II localized normally in *cadherin/hmr-1; Dock180/ced-5* embryos, with apical NMY-2::GFP accumulation in Ea/p cells (Figure 26G,H). We have not yet

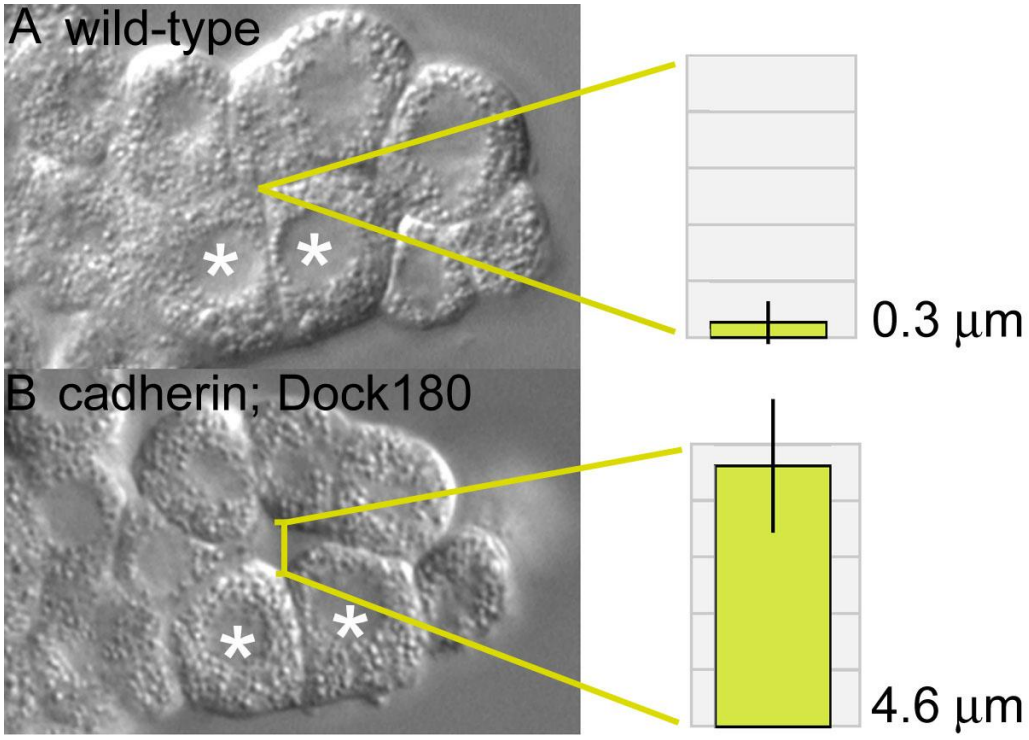
A wild-type
B cadherin; Dock180
0.3 µm
4.6 µm

Figure 24: *cadherin/hmr-1; Dock180/ced-5* mutant embryos display adhesion defects. (A) wild-type devitellinized embryo did not exhibit cell separation defects. (B) Devitellinized *cadherin/hmr-1; Dock180/ced-5* mutant embryos exhibited cell separation defects.

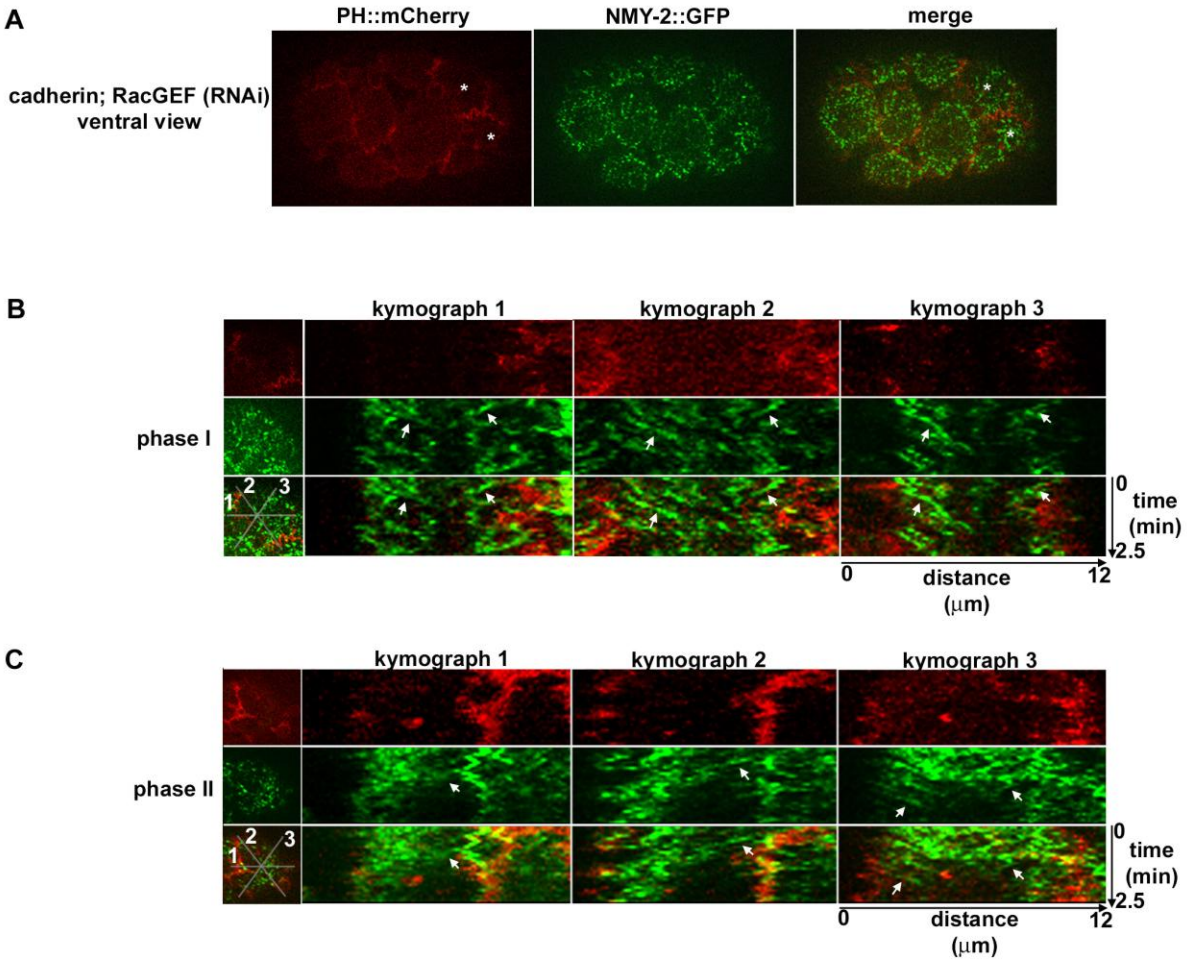
A
PH::mCherry
NMY-2::GFP
merge
cadherin; RacGEF (RNAi)
ventral view
B
kymograph 1
kymograph 2
kymograph 3
phase I
1
2
3
0
time
(min)
2.5
0
distance
(μm)
12
C
kymograph 1
kymograph 2
kymograph 3
phase II
1
2
3
0
time
(min)
2.5
0
distance
(μm)
12

Figure 25: Coupled myosin II and membrane dynamics is prevented in *cadherin/hmr-1; Dock180/ced-5* embryos. (A) Ventral surface of *cadherin/hmr-1; Dock180/ced-5* embryos expressing PH::mCherry and NMY-2::GFP. NMY-2::GFP was present as foci at the surface. (B) Phase I dynamics in *cadherin/hmr-1 (RNAi); Dock180/ced-5* was similar to that seen in wild-type, with uncoupled NMY-2:GFP and contact zone dynamics (arrows). (C) Coupled dynamics in phase II was prevented in *cadherin/hmr-1; Dock180/ced-5*. Instead of NMY-2::GFP punctae moving in concert with the contact zone, NMY-2::GFP movement was uncoupled from the movement of the membrane (arrows).

determined whether phosphorylation and activation of the regulatory myosin light chain was affected in *cadherin/hmr-1; Dock180/ced-5* mutant embryos, although myosin movements (Figure 19) suggest that motor activation occurs as normal. Therefore, from the experiments that we have performed thus far, the Ea/p cell internalization and myosin dynamics defects observed in embryos were likely not due to earlier defects in the embryo and suggest a function for Cadherin/HMR-1; Dock180/CED-5 specifically in coupling contact zone movements to the observed centripetal myosin movements.

To further determine whether the prevention of coupled myosin and membrane dynamics during phase II in *cadherin/hmr-1; Dock180/ced-5* mutant embryos was due to a defect in cell-cell adhesion, we analyzed myosin dynamics in embryos defective in another component of the adhesion complex. We depleted embryos of *α-catenin/hmp-1* and found that Ea/p cells were able to internalize normally (Figure 27A). However, when we depleted *α-catenin/hmp-1* in the genetically sensitized background of *Dock180/ced-5*, we observed defects in Ea/p cell internalization (Figure 27B). The defects observed in *α-catenin/hmp-1*; *Dock180/ced-5* mutant embryos were similar penetrance as that in *cadherin/hmr-1; Dock180/ced-5* mutant embryos (33% Ea/p cell internalization defects, n=21). The similar phenotype observed when knocking down *cadherin/hmr-1* or *α-catenin/hmp-1* further suggested a role for the adhesion complexes in gastrulation movements. We then began to analyze myosin dynamics in *α-catenin/hmp-1; Dock180/ced-5* mutant embryos during phase I and phase II.

Preliminary experiments have shown that depleting embryos of *α-catenin/hmp-1* in the *Dock180/ced-5* mutant background also prevented coupled movements of myosin and the

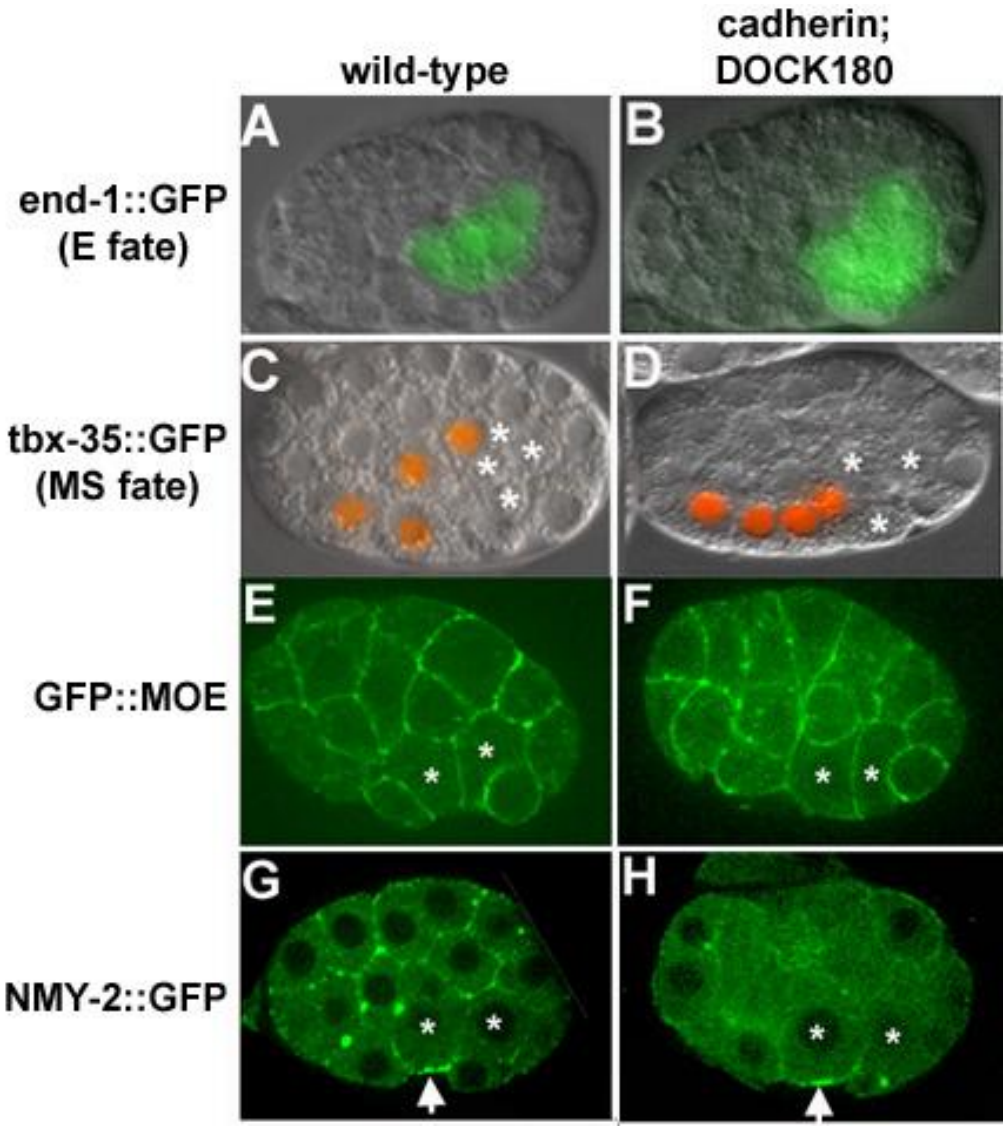
wild-type
cadherin;
DOCK180
end-1::GFP
(E fate)
tbx-35::GFP
(MS fate)
GFP::MOE
NMY-2::GFP
A
B
C
D
E
F
G
H

Figure 26: Cell fate, actin and myosin localization appear normal in *cadherin/hmr-1; Dock180/ced-5* embryos. Embryos were imaged on their lateral sides. (A) *end-1::GFP* was used as a marker for E fate. (C) *tbx-35::GFP* was used as a marker for MS fate. In wild-type, E and MS fate were determined. In *cadherin/hmr-1; Dock180/ced-5*, E (B) and MS (D) fate were as in wild-type. (E) GFP::MOE labels F-actin and was localized cortically in wild-type embryos. (F) As in wild-type, MOE::GFP was also cortical in *cadherin/hmr-1; Dock180/ced-5* embryos. (G) When imaging NMY-2::GFP embryos, myosin II was apically enriched (arrow) in the E cell (asterisks). (H) In *cadherin/hmr-1 (RNAi); Dock180/ced-5* embryos, myosin II was still apically enriched in the E cell (arrow).

contact zones (data not shown). We are currently continuing these studies. Thus, depleting embryos of components of the adhesion complex and *Dock180/ced-5* gives rise to Ea/p cell internalization defects, potentially through preventing the linkage between myosin movement and movement of the neighboring cells.

Discussion

In this study, we found that a molecular clutch may regulate the linkage between the Ea/p cell cytoskeletal machinery and neighboring cells. Our preliminary results using quantum dots to introduce fiduciary marks on the overlying cell surface suggest that the clutch is likely to lie at the adhesions between Ea/p cells and neighboring cells, or between the cytoskeleton and adhesion complexes within the Ea/p cells. Consistent with this hypothesis, when adhesion was affected by depleting embryos of *cadherin/hmr-1* in a genetically sensitized background, the coupling of myosin and contact zone movement and Ea/p cell internalization were impaired. Furthermore, when embryos were depleted of *cadherin/hmr-1* alone, the Ea/p cells did not reach the maximum internalization rate as in wild-type. A previous report had shown that during early embryogenesis, cells were undergoing centripetal myosin II movements as apicobasal polarity was established. Thus, the clutch may be required to regulate the transition from apicobasal polarity establishment to cell movements. We also found that centripetal myosin movements occurred in *Drosophila* ventral furrow cells prior to the contraction of the apical surfaces, suggesting that a clutch may be a general mechanism to regulate cell internalization during development.

Similar to myosin dynamics described by Munro and colleagues at the one-cell stage, in Ea/p cells, myosin punctae coalesced and disassembled rapidly. These dynamics differed from what was previously reported in the *Drosophila* ventral furrow. During ventral furrow formation, when the linkages between the cytoskeleton and adherens junctions were impaired, the actomyosin network continued to contract (Dawes-Hoang et al., 2005; Sawyer et al., 2009). Immunostaining fixed embryos revealed stable clusters of F-actin and myosin at the center of the ventral furrow cells. Thus, it appeared that myosin did not rapidly remodel in *Drosophila*, as it did in *C. elegans*. However, when we imaged myosin dynamics in the ventral furrow cells, we found that myosin coalescence occurs prior to apical constriction, and that the larger myosin foci disassembled before the next wave of coalescence (Figure 21E-K). These observations were also consistent with a previously published report (Martin et al., 2009). Live imaging of myosin movement during ventral furrow formation also revealed that myosin coalescence incrementally constricted the ventral furrow cells (Martin et al, 2009). We reduced the time interval between myosin images to determine whether a similar ratchet like movement was occurring in Ea/p cells. Three-second time interval, as well as 150 ms time interval imaging of myosin dynamics did not reveal cycles of pauses and contraction as seen in *Drosophila* ventral furrow cells (Figure 20; Figure 28). Thus, although some aspects of myosin dynamics are conserved between apical constriction in *Drosophila* and *C. elegans*, there are key distinct differences as well.

Molecular clutches have been identified in migrating cells to regulate the linkage between the actin cytoskeleton and adhesion, allowing cells to move with respect to the underlying substrate (Giannone et al., 2009). Similarly, the molecular clutch during Ea/p

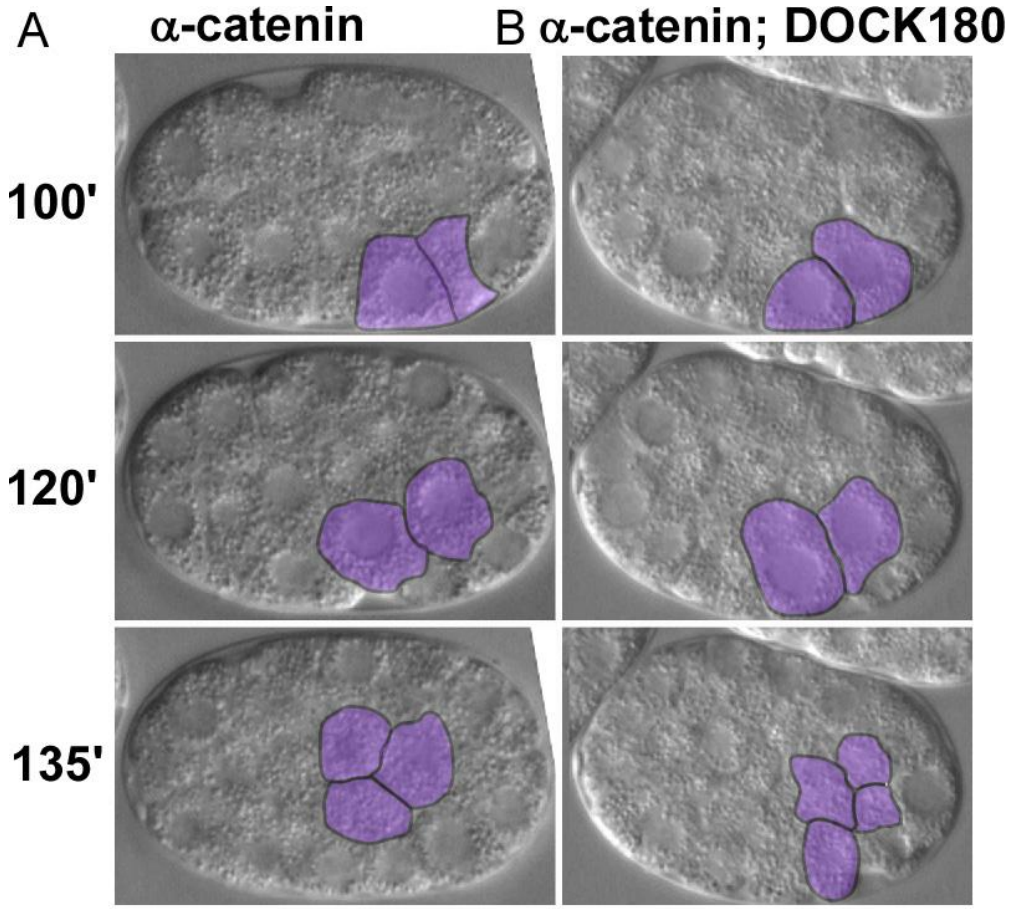
A
α-catenin
B α-catenin; DOCK180
100'
120'
135'

Figure 27: Embryos depleted of *α-catenin/hmp-1* and *Dock180/ced-5* also have Ea/p cell internalization defects. (A) Embryos depleted of α-catenin/hmp-1 still internalized Ea/p cells (pseudocoloured purple) normally. (B) *α-catenin/hmp-1*; *Dock180/ced-5* mutant embryos displayed defects in Ea/p cell internalization. Ea/p cells divided on the embryonic surface (135', pseudocoloured purple). Time is indicated as minutes after fertilization.

internalization also regulates the linkage between actomyosin cytoskeleton and adhesion, allowing cells to move relative to one another. However, we do not currently know whether the clutch resides within the Ea/p cells themselves, or between the Ea/p cells and the neighboring cells. Clutch proteins were identified in migrating epithelial cells by carefully analyzing the movements of proteins that were known to reside at the interface between the cytoskeleton and focal adhesions (Hu et al., 2007). As force-carrying links are identified in *C. elegans*, a similar approach can be undertaken to identify the molecular clutch during Ea/p cell internalization. Proteins that spend a portion of their time at the cell boundaries and a portion of their time moving with myosin are key candidates for clutch proteins. Additionally, proteins that move with myosin and are absent from the boundary during phase I, but then reside at the boundary during phase II, are also key clutch protein candidates.

Our preliminary experiments examining centripetal myosin movements at several stages during development suggested that although all somatic cells were undergoing centripetal myosin movements during early embryogenesis (Munro et al., 2004; this study), centripetal myosin movements may cease in non-endodermal cells during Ea/p cell internalization (Figure 19F,G). These results suggested that myosin movement was regulated spatially and temporally.

Centripetal myosin movements are widely used to transport proteins to specific domains. In addition to establishing apicobasal polarity in *C. elegans* cells, the interface between a T-cell and an antigen presenting cell (APC), termed the "immunological synapse" also exhibit centripetal actin and myosin flow. The formation of the immunological synapse is first initiated by the engagement of the T-cell receptor to the APC. Within seconds of this engagement, actin-dependent microclusters form at the interface and signaling proteins are

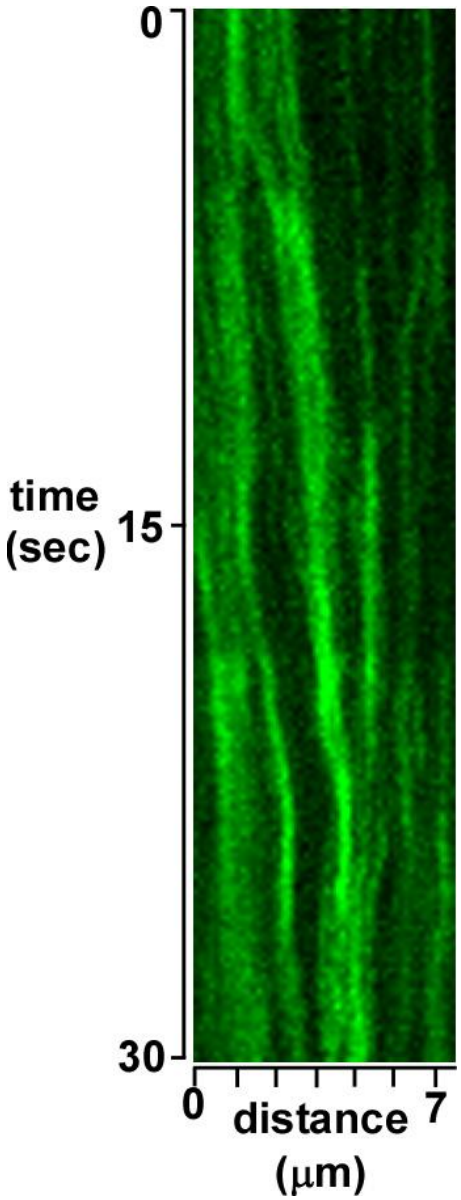
0
time
(sec)
15
30
0
distance
7
(μm)

Figure 28: Myosin continuously moved centripetally and did not appear to undergo pauses of contraction.

Kymograph of myosin coalescence from a movie in which images were taken every 150 ms.

recruited to form the "signalosome" (Bunnell et al., 2002; Campi et al., 2005; Huse et al., 2007). The formation of these microclusters is dependent on myosin IIA activity; depleting cells of myosin IIA results in loss of microcluster formation and immunological synapse destabilization (Ilani et al., 2009). Thus, actomyosin movements are required to transport signaling molecules to the interface between the APC and the T-cell receptor to form a stable immunological synapse. A similar phenomenon could be occurring during Ea/p cell internalization to regulate clutch dynamics. As myosin moves centripetally along the apical surface of the Ea/p cells, proteins may be transported along the basolateral membranes. These proteins could be transported to the apical region of the basolateral membranes of Ea/p cells and neighboring cells, thereby strengthening adhesion between the two cells, engaging the clutch. Currently, we do not have available strains that label discrete punctae along the basolateral membranes to examine the movements of proteins in these membranes. Photobleaching and photoactivation experiments of fluorescently-tagged membrane markers may not be useful techniques to address this hypothesis if rapid diffusion limits the ability to image the movement of a fiduciary mark. Further work focused on building appropriate tools will be required to address this issue.

Our studies examining myosin dynamics in the *Drosophila* ventral furrow suggest that myosin movements are initially uncoupled from contact zone movement. Furthermore, it was also shown that *Drosophila* mesodermal invagination occurs by two phases of apical constriction (Oda and Tsukita, 2001). During the first phase, the cells along the ventral midline reduced their apical surfaces slowly. Then, during the second phase, the ventral

furrow cells accelerated their apical constriction. Thus, taken together, these results suggest that a clutch like mechanism may regulate mesoderm invagination.

To our knowledge, this is the first observation of a molecular clutch that regulates developmental processes in a multicellular organism. Previously recognized molecular clutches function in migrating cells that locomote through the formation of actin-rich protrusions, whereas the clutch we have identified occurs in cells that move by a cell shape change. Previous molecular clutches have a sensitivity to tension in common: Increased tension strengthens the initial contact (Giannone et al., 2009). It is possible that a tension sensing mechanism may function during Ea/p cell internalization. During Ea/p apical constriction, the apical surfaces flatten prior to Ea/p internalization. This flattening may be due to the "reeling in" of excess apical membrane as the actomyosin network contracts. This cell flattening could also create tension along the apical surface and at cell-cell contacts. Such a tension could feasibly strengthen an initial link and reinforce clutch engagement. Future studies delving into this hypothesis and the hypotheses mentioned above will yield an exciting avenue of research.

Materials and Methods

Strains and Worm Maintenance

Nematodes were cultured and handled as described (Brenner, 1974). Unless indicated, experiments were performed with the wild-type N2 (Bristol) strain. The following mutant and reporter strains were used: *MT4417 ced-5(n1812) dpy-20(e1282) IV* referred to here as *ced-5; MS126 unc-119(ed4) III; irIs16 [tbx-35::NLS::GFP]; zuIs45* [*nmy-2*::NMY-2::GFP; *unc-119 (+)*]; referred to here as NMY-2::GFP, JJ1317 *zuIs3* [*end-1*::GFP], OD70

ItIs44 [*pie-1*::PH domain of PLCδ::mCherry] (PH::mCherry) (Kachur et al., 2008), PF100 *nnIs* [*unc-119(+) pie-1* promoter::*gfp*::Dm-moesin$^{437–578}$ (residues 437–578 of *D. melanogaster* Moesin)] referred to here as GFP::MOE, MS632 *unc-119(ed4)* III; LP54 PH::mCherry; NMY-2::GFP. LP54 was constructed by crossing OD70 PH::mCherry males with JJ1473 NMY-2::GFP hermaphrodites, respectively. The NMY-2::GFP; *ced-5*, MOE::GFP; *ced-5* and PH::mCherry; NMY-2::GFP; *ced-5* strains were constructed by crossing *ced-5* hermaphrodites with NMY-2::GFP, MOE::GFP, or PH::mCherry; NMY-2::GFP males, respectively.GFP or mCherry positive F1 progeny were isolated and allowed to self-cross. 30 dumpy and GFP-positive F2 progeny were singled and further screen for NMY-2::GFP homozygosity. Dpy worms were verified as carrying the *ced-5* mutant allele, by detecting apoptotic cells that failed to engulf. All strains were maintained at 20°C, except for the following strains: PF100 GFP::MOE, JJ1473 NMY-2::GFP, and LP54 PH::mCherry; NMY-2::GFP were maintained at 24°C. Imaging was performed at 20°C–23°C for all strains.

DIC and Confocal Time-Lapse Microscopy

Embryos were mounted and DIC images were acquired as described (McCarthy Campbell et al., 2009). Time-lapse images were acquired at 1 μm optical sections every 1 minute and analyzed with Metamorph software (Molecular Devices). Gastrulation was scored by examination of whether the Ea and Ep cells were completely surrounded by neighboring cells in three dimensions at the time that Ea and Ep divided. If Ea and Ep divided before being completely surrounded, we scored gastrulation as having failed. For measuring apical surfaces, the length of the ventral surface was measured in the optical section in which this length was greatest, from the Ea-Ep ventral border to both the Ep-P_4 ventral border and the Ea-MSxx ventral border in laterally-viewed embryos. Spinning disk

confocal images were acquired and processed as described (Lee et al., 2006). To observe apical NMY-2::GFP accumulation or GFP::MOE localization, embryos were mounted laterally and imaged every 1 minutes starting at MSa/p division.

Analysis of Ea/p cell internalization rates

To observe the apical boundaries of Ea/p cells during internalization, we filmed the ventral surface of wild-type or *cadherin/hmr-1* depleted embryos expressing PH::mCherry. Three 2-micron steps were taken every 5 seconds to capture the entire apical surface of the Ea/p cell. The z-planes were then merged and the circumference of each E cell was outlined and the area calculated every 5^{th} time point (every 25 seconds) using ImageJ software. An average radius was calculated based on the area, with the average radius defined as the radius of a circle of the same area. To calculate closure rate, the radius at each time point was subtracted from the average of the prior three time points.

Analysis of NMY-2::GFP punctae movements

To analyze NMY-2::GFP; OD70 dynamics, two planes that were 0.5 μm apart for each fluorophore were acquired every 5 seconds either during phase I (0-8 minutes after the MSa/p cells divided) or during phase II (8-11 minutes after the MSa/p cells divided). The two planes of each fluorophore were merged for analysis, and these films were analyzed with Metamorph software. Lines were drawn across Ea/p cells for both NMY-2::GFP and OD70, and converted to kymographs. Myosin punctae were manually tracked by placing a tracing individual or groups of myosin punctae onto a transparency. The transparency was then used to create drawings using the program Canvas (ACD Systems). Lines were colored with a gradient, with earlier time points pseudo-colored yellow, and the later time points were

pseudo-colored blue. The rates NMY-2::GFP punctae movement was calculated using ImageJ software.

RNA Interference (RNAi)

RNAi by injection was performed according to a standard protocol (Dudley et al., 2002), except that a cDNA preparation was used as template to amplify *cadherin/hmr-1* and *α-catenin/hmp-1* genes by PCR. *cadherin/hmr-1* and *α-catenin/hmp-1* specific primers were used to amplify the entire open reading frame of each gene. Double-stranded RNA was injected at a concentration of 100 ng/ml. Embryos were analyzed 22-25 hours later.

Labelling embryos non-specifically with quantum dots

Gastrulation-stage embryos expressing *end-1*::GFP to mark the Ea/p cells were divitellinized using a standard protocol (Edgar, 1995; Lee and Goldstein, 2003), with the exception that the egg shells were manually removed in egg buffer (Hepes pH 7.2 5mM, NaCl 110mM, KCl 4mM, Mg Acetate 5mM, CaCl2 5mM) instead of Edgar's Growth Medium (EGM; Edgar, 1995). Quantum dots (Invitrogen, Qdot 655 IVT carboxyl quantum dots) were diluted in egg buffer. Devitellinized embryos were then moved to the quantum dot suspension, washed 1X with egg buffer, followed by 2X in EGM. The embryos were then mounted in EGM as described above. Three steps, 1μm apart each of DIC and fluorescent images, were taken every 15 seconds. Movies were analyzed with Metamorph software.

Analyzing cell separation defects

Devitellinized embryos were flattened by using 11.6 μm glass beads (Whitehouse Scientific) as spacers between the coverslip and slide. Coverslips were prepared by pipetting beads that were resuspended in water onto the coverslip. The water was allowed to evaporate leaving only the beads. Devitellinized embryos were placed in 15 μL of EGM on the

prepared coverslip, and the slide was placed on top. This approach resulted in partial flattening of the embryos due to the small size of the beads. The sample was then imaged under Nomarski optics, and the cell separation was measured with Metamorph software.

Imaging *Drosophila* ventral furrow

mat-67; spider-GFP squash-mCherry/TM3 Drosophila embryos (a gift from Adam Martin and Eric Wieschaus) were collected over a 4 hour period. Embryos were devitellinized by 10% sodium hypochlorite treatment for 5 minutes, and mounted on their ventral sides in halocarbon oil. As soon as cells began to apically accumulate squash-mCherry, 3 planes that were 1.5 um apart for each of squash-mCherry and spider-GFP were taken every 5 seconds. The 3 planes of squash-mCherry were merged for analysis and a single plane of spider-GFP was used to mark the cell boundaries. Movies were analyzed with Metamorph and ImageJ software.

References

Bard, L., Boscher, C., Lambert, M., Mege, R. M., Choquet, D. and Thoumine, O. (2008). A molecular clutch between the actin flow and N-cadherin adhesions drives growth cone migration. *J Neurosci* 28, 5879-90.

Boyd, L., Guo, S., Levitan, D., Stinchcomb, D. T. and Kemphues, K. J. (1996). PAR-2 is asymmetrically distributed and promotes association of P granules and PAR-1 with the cortex in C. elegans embryos. *Development* 122, 3075-84.

Brenner, S. (1974). The genetics of Caenorhabditis elegans. *Genetics* 77, 71-94.

Bunnell, S. C., Hong, D. I., Kardon, J. R., Yamazaki, T., McGlade, C. J., Barr, V. A. and Samelson, L. E. (2002). T cell receptor ligation induces the formation of dynamically regulated signaling assemblies. *J Cell Biol* 158, 1263-75.

Campi, G., Varma, R. and Dustin, M. L. (2005). Actin and agonist MHC-peptide complex-dependent T cell receptor microclusters as scaffolds for signaling. *J Exp Med* 202, 1031-6.

Cheeks, R. J., Canman, J. C., Gabriel, W. N., Meyer, N., Strome, S. and Goldstein, B. (2004). C. elegans PAR proteins function by mobilizing and stabilizing asymmetrically localized protein complexes. *Curr Biol* 14, 851-62.

Christiansen, J. H., Coles, E. G. and Wilkinson, D. G. (2000). Molecular control of neural crest formation, migration and differentiation. *Curr Opin Cell Biol* 12, 719-24.

Costa, M., Raich, W., Agbunag, C., Leung, B., Hardin, J. and Priess, J. R. (1998). A putative catenin-cadherin system mediates morphogenesis of the Caenorhabditis elegans embryo. *J Cell Biol* 141, 297-308.

Crowley, E. and Horwitz, A. F. (1995). Tyrosine phosphorylation and cytoskeletal tension regulate the release of fibroblast adhesions. *J Cell Biol* 131, 525-37.

Dawes-Hoang, R. E., Parmar, K. M., Christiansen, A. E., Phelps, C. B., Brand, A. H. and Wieschaus, E. F. (2005). folded gastrulation, cell shape change and the control of myosin localization. *Development* 132, 4165-78.

Debold, E. P., Patlak, J. B. and Warshaw, D. M. (2005). Slip sliding away: load-dependence of velocity generated by skeletal muscle myosin molecules in the laser trap. *Biophys J* 89, L34-6.

Dudley, N. R., Labbe, J. C. and Goldstein, B. (2002). Using RNA interference to identify genes required for RNA interference. *Proc Natl Acad Sci U S A* 99, 4191-6.

Edgar, L. G. (1995). Blastomere culture and analysis. *Methods Cell Biol* 48, 303-21.

Edwards, K. A., Demsky, M., Montague, R. A., Weymouth, N. and Kiehart, D. P. (1997). GFP-moesin illuminates actin cytoskeleton dynamics in living tissue and demonstrates cell shape changes during morphogenesis in Drosophila. *Dev Biol* 191, 103-17.

Etemad-Moghadam, B., Guo, S. and Kemphues, K. J. (1995). Asymmetrically distributed PAR-3 protein contributes to cell polarity and spindle alignment in early C. elegans embryos. *Cell* 83, 743-52.

Friedl, P. and Gilmour, D. (2009). Collective cell migration in morphogenesis, regeneration and cancer. *Nat Rev Mol Cell Biol* 10, 445-57.

Giannone, G., Mege, R. M. and Thoumine, O. (2009). Multi-level molecular clutches in motile cell processes. *Trends Cell Biol* 19, 475-86.

Hou, X. G., Siveter, D. J., Aldridge, R. J. and Siveter, D. J. (2008). Collective behavior in an early Cambrian arthropod. *Science* 322, 224.

Hu, K., Ji, L., Applegate, K. T., Danuser, G. and Waterman-Storer, C. M. (2007). Differential transmission of actin motion within focal adhesions. *Science* 315, 111-5.

Hung, T. J. and Kemphues, K. J. (1999). PAR-6 is a conserved PDZ domain-containing protein that colocalizes with PAR-3 in Caenorhabditis elegans embryos. *Development* 126, 127-35.

Huse, M., Klein, L. O., Girvin, A. T., Faraj, J. M., Li, Q. J., Kuhns, M. S. and Davis, M. M. (2007). Spatial and temporal dynamics of T cell receptor signaling with a photoactivatable agonist. *Immunity* 27, 76-88.

Ilani, T., Vasiliver-Shamis, G., Vardhana, S., Bretscher, A. and Dustin, M. L. (2009). T cell antigen receptor signaling and immunological synapse stability require myosin IIA. *Nat Immunol* 10, 531-9.

Kachur, T. M., Audhya, A. and Pilgrim, D. B. (2008). UNC-45 is required for NMY-2 contractile function in early embryonic polarity establishment and germline cellularization in C. elegans. *Dev Biol* 314, 287-99.

Koppen, M., Simske, J. S., Sims, P. A., Firestein, B. L., Hall, D. H., Radice, A. D., Rongo, C. and Hardin, J. D. (2001). Cooperative regulation of AJM-1 controls junctional integrity in Caenorhabditis elegans epithelia. *Nat Cell Biol* 3, 983-91.

Lee, J. Y. and Goldstein, B. (2003). Mechanisms of cell positioning during C. elegans gastrulation. *Development* 130, 307-20.

Lee, J. Y., Marston, D. J., Walston, T., Hardin, J., Halberstadt, A. and Goldstein, B. (2006). Wnt/Frizzled signaling controls C. elegans gastrulation by activating actomyosin contractility. *Curr Biol* 16, 1986-97.

Lin, C. H. and Forscher, P. (1995). Growth cone advance is inversely proportional to retrograde F-actin flow. *Neuron* 14, 763-71.

Maduro, M. F., Hill, R. J., Heid, P. J., Newman-Smith, E. D., Zhu, J., Priess, J. R. and Rothman, J. H. (2005). Genetic redundancy in endoderm specification within the genus Caenorhabditis. *Dev Biol* 284, 509-22.

Martin, A. C., Kaschube, M. and Wieschaus, E. F. (2009). Pulsed contractions of an actin-myosin network drive apical constriction. *Nature* 457, 495-9.

McCarthy Campbell, E. K., Werts, A. D. and Goldstein, B. (2009). A cell cycle timer for asymmetric spindle positioning. *PLoS Biol* 7, e1000088.

Mitchison, T. and Kirschner, M. (1988). Cytoskeletal dynamics and nerve growth. *Neuron* 1, 761-72.

Montell, D. J. (2003). Border-cell migration: the race is on. *Nat Rev Mol Cell Biol* 4, 13-24.

Motegi, F., Velarde, N. V., Piano, F. and Sugimoto, A. (2006). Two phases of astral microtubule activity during cytokinesis in C. elegans embryos. *Dev Cell* 10, 509-20.

Munro, E., Nance, J. and Priess, J. R. (2004). Cortical flows powered by asymmetrical contraction transport PAR proteins to establish and maintain anterior-posterior polarity in the early C. elegans embryo. *Dev Cell* 7, 413-24.

Nance, J. and Priess, J. R. (2002). Cell polarity and gastrulation in C. elegans. *Development* 129, 387-97.

Oda, H. and Tsukita, S. (2001). Real-time imaging of cell-cell adherens junctions reveals that Drosophila mesoderm invagination begins with two phases of apical constriction of cells. *J Cell Sci* 114, 493-501.

Pettitt, J., Cox, E. A., Broadbent, I. D., Flett, A. and Hardin, J. (2003). The Caenorhabditis elegans p120 catenin homologue, JAC-1, modulates cadherin-catenin function during epidermal morphogenesis. *J Cell Biol* 162, 15-22.

Reddien, P. W. and Horvitz, H. R. (2000). CED-2/CrkII and CED-10/Rac control phagocytosis and cell migration in Caenorhabditis elegans. *Nat Cell Biol* 2, 131-6.

Ridley, A. J., Schwartz, M. A., Burridge, K., Firtel, R. A., Ginsberg, M. H., Borisy, G., Parsons, J. T. and Horwitz, A. R. (2003). Cell migration: integrating signals from front to back. *Science* 302, 1704-9.

Royou, A., Field, C., Sisson, J. C., Sullivan, W. and Karess, R. (2004). Reassessing the role and dynamics of nonmuscle myosin II during furrow formation in early Drosophila embryos. *Mol Biol Cell* 15, 838-50.

Sawyer, J. M., Harrell, J. R., Shemer, G., Sullivan-Brown, J., Roh-Johnson, M. and Goldstein, B. (2009). Apical constriction: A cell shape change that can drive morphogenesis. *Dev Biol*.

Sawyer, J.K., Harris, N.J., Slep, K.C., Gaul, U., and Peifer, M. (2009). The Drosophila afadin homolog Canoe regulates linkage of the actin cytoskeleton to adherens junctions during apical constriction. *J Cell Bio* 186, 57-73.

Schock, F. and Perrimon, N. (2002). Molecular mechanisms of epithelial morphogenesis. *Annu Rev Cell Dev Biol* 18, 463-93.

Suter, D. M., Errante, L. D., Belotserkovsky, V. and Forscher, P. (1998). The Ig superfamily cell adhesion molecule, apCAM, mediates growth cone steering by substrate-cytoskeletal coupling. *J Cell Biol* 141, 227-40.

Weijer, C. J. (2009). Collective cell migration in development. *J Cell Sci* 122, 3215-23.

Wolf, K. and Friedl, P. (2006). Molecular mechanisms of cancer cell invasion and plasticity. *Br J Dermatol* 154 Suppl 1, 11-5.

Wu, Y. C. and Horvitz, H. R. (1998). C. elegans phagocytosis and cell-migration protein CED-5 is similar to human DOCK180. *Nature* 392, 501-4.

Young, P. E., Pesacreta, T. C. and Kiehart, D. P. (1991). Dynamic changes in the distribution of cytoplasmic myosin during Drosophila embryogenesis. *Development* 111, 1-14.

Zhu, J., Hill, R. J., Heid, P. J., Fukuyama, M., Sugimoto, A., Priess, J. R. and Rothman, J. H. (1997). end-1 encodes an apparent GATA factor that specifies the endoderm precursor in Caenorhabditis elegans embryos. *Genes Dev* 11, 2883-96.

CHAPTER 4

DISCUSSION AND PERSPECTIVE

Cell movements are an integral part of development. The movement of the endodermal precursor cells marks the initation of gastrulation in *C. elegans*. In this thesis, I have focused on bridging cell and developmental biology to further understand how cytoskeletal dynamics are regulated in a developmental process. In this Chapter, I will briefly summarize my results, and discuss how these results have contributed to the field of morphogenesis.

During my graduate studies, I have used high resolution imaging to answer questions about cytoskeletal dynamics during development. In Chapter 2, I showed that depleting the Arp2/3 complex prevents the formation of F-actin rich structures on the neighbouring mesodermal descendant cells during Ea/p cell internalization. From this and other results, I hypothesize that these Arp2/3-dependent structures may be cell specializations for cell crawling or rolling mechanisms that may facilitate Ea/p cell internalization. In Chapter 3, upon examining myosin dynamics during Ea/p cell apical constriction, I found that there are two distinct phases of myosin movement, and that the transition between these two phases is hypothesized to be regulated by a molecular clutch. Thus, in this dissertation, I highlighted a role for cytoskeletal dynamics in the neighbouring cells, in addition to describing the dynamics of the actomyosin network within the E cells themselves.

One of many questions that arises from these studies is whether the Arp2/3 complex affects the actomyosin network in the E cells. Since Arp2/3 is a major actin regulator, one would predict that the actin architecture on the apical surfaces of the Ea/p cells will be perturbed in the absence of Arp2/3. Indeed, I have shown that cells bleb when Arp2/3 is depleted (see Figure 9). However, we have been unable to visualize the apical actin meshwork with existing transgenic strains. Surprisingly, preliminary evidence suggests that myosin still moves centripetally in Arp2/3-depleted embryos, although it is unknown whether the Ea/p cell internalization failure is due to lack of coupling between myosin and the contact zones, lack of cortical integrity, or another unknown mechanism.

Is E cell internalization intrinsic to the E cells or do neighbouring cells play a role? The molecular clutch hypothesis suggests that the regulation of cell internalization may be intrinsic within the E cells, for example by upregulating adhesion proteins or activating an unknown factor that links the cytoskeleton to neighbouring cells. This idea is consistent with a previous result in which when some of the neighbouring cells are removed, Ea/p cell apical constriction still occurs (Lee and Goldstein, 2003). However, the engagement of the clutch could also involve extrinsic factors, such as upregulation of adhesion within the neighbouring cells. Futhermore, in Chapter 2, we found that Arp2/3-dependent F-actin-rich structures form on the neighbouring cells, suggesting a role for the neighbouring cells to facilitate Ea/p cell internalization by cell crawling or rolling mechanisms. It is possible that the movement of the neighbouring cells is redundant with Ea/p cell apical constriction, and that removal of the cell crawling/rolling mechanisms still allow for Ea/p cell internalization to occur.

It is clear that the molecules that comprise this clutch need to be identified. Our preliminary evidence suggests that molecules that link the cytoskeleton to the neighbouring

cells, such as classical cadherins and α-catenin, may be components of the clutch. However, identifying the clutch interface, as has been done in tissue culture (Hu et al., 2007), is imperative to understand how the clutch is regulated. As mentioned previously, creating transgenic strains with labeled proteins will aid in the identification of the clutch. Proteins that do not remain at the contact zones and move along with myosin during phase I, but then stay bound to the contact zone during phase II, will be of particular interest.

The hypothesis that a molecular clutch regulates the transition from apicobasal polarity to cell movements brings up several questions. Although we have shown that the actomyosin network contracts prior to apical shrinking in the *Drosophila* ventral furrow, is the contracting network also transporting PAR proteins? Is the network instead acting to reel in excess slack to then drive efficient apical shrinking during ventral furrow formation? Will other systems that use apical constriction to internalize cells, such as *Xenopus* bottle cell formation or neural tube closure, also exhibit an actively contracting network prior to apical shrinking? How does the clutch become "engaged"? Future experiments answering these and other questions will yield more insight into how precisely development is controlled, and how cytoskeletal dynamics regulate developmental processes.

References

Hu, K., Ji, L., Applegate, K. T., Danuser, G. and Waterman-Storer, C. M. (2007). Differential transmission of actin motion within focal adhesions. *Science* 315, 111-5.

Lee, J. Y. and Goldstein, B. (2003). Mechanisms of cell positioning during C. elegans gastrulation. *Development* 130, 307-20.